FUNCTIONAL CHARACTERISATION OF A NOVEL IMMUNE MODULATORY MOLECULE FROM *FASCIOLA HEPATICA*

by

Raquel Alvarado B.Sc. (Hons)

A Thesis Submitted for the Degree of

Doctor of Philosophy in Science

School of Medical and Molecular Biosciences, Faculty of Science,

University of Technology Sydney, Australia.

2014

CERTIFICATE OF AUTHORSHIP/ORIGINALITY

I certify that the work in this thesis has not previously been submitted for a degree nor has it been submitted as part of requirements for a degree except as fully acknowledged within the text.

I also certify that the thesis has been written by me. Any help that I have received in my research work and the preparation of the thesis itself has been acknowledged. In addition, I certify that all information sources and literature used are indicated in the thesis.

Signature of Student: Production Note: Signature removed prior to publication.

Date: 22nd December, 2014

ACKNOWLEDGEMENTS

Science has fascinated me ever since I was a child, therefore I am very grateful to God for not only giving me the opportunity, but also the willingness and strength to pursue my studies in this field that I truly enjoy. I consider myself very fortunate for being able to do this PhD project, which despite being my greatest challenge as a student, has rewarded me with getting to know so many people who have generously shared their knowledge and friendship with me.

To my parents, I thank them for all their love, for listening, encouraging me and always giving me their complete support and to my mum in particular for being my best friend. Without them I would simply not have been able to achieve this goal.

I thank Bronwyn O'Brien, Sheila Donnelly and Mark Robinson, for giving me the privilege of working with them. It was Bronwyn's enthusiastic Immunology lectures that first showed me how interesting this field can be. I really appreciate the direct involvement in the laboratory of Sheila and Mark, who patiently dedicated a lot of their time to teach me new techniques and help me with experiments. I want to thank the three of them for giving me such an interesting project, for teaching me so much, checking my drafts, giving their valuable feedback, for all their guidance and overall for being such excellent supervisors. I'm also very grateful to Joyce To for helping me so much in this project and for teaching me her clever modifications of experimental techniques. To Maria Lund, Andrew Hutchinson and Paddy McCauley-Winter, I thank all their assistance in flow cytometry and their valuable advice. I am very proud to have been part of this research team, whose members were so kind to me and I wish them all very successful futures with the hope that our friendship endures a very long time.

In these years I have also met fellow postgraduate students with whom I have acquired what I would love to be lifelong friendships, and with whom I have shared unforgettable moments. I want to thank them for being so wonderful, especially to Maria Lund, Alex Gale and Rita Rapa for letting me count on them in good and difficult moments.

I would also like to express my gratitude to the UTS technical staff, especially Mike Johnson and Lynne Turnbull for their assistance in microscopy. Also, I thank Ashley Mansell, Anita Pinar and Suat Dervish for their contribution to my project and the science faculty for granting me a postgraduate research scholarship.

PUBLICATIONS ASSOCIATED WITH THIS THESIS

Journal Publications

Mark W. Robinson, **Raquel Alvarado**, Joyce To, Andrew Hutchinson, Stephanie N. Dowdell, Maria Lund, Lynne Turnbull, Cynthia B. Witchurch, Bronwyn A. O'Brien, John P. Dalton and Sheila Donnelly, 2012; A helminth cathelicidin-like protein suppresses antigen processing and presentation in macrophages via inhibition of lysosomal vATPase. FASEB Journal. 26, 4614-4627.

Raquel Alvarado, Bronwyn O'Brien, Akane Tanaka, John P. Dalton, Sheila Donnelly, 2014; A parasitic helminth-derived peptide that targets the macrophage lysosome is a novel therapeutic option for autoimmune disease. Immunobiology. (In press, DOI 10.1016/j.imbio.2014.11.008).

Raquel Alvarado, Joyce To, Anita Pinar, Ashley Mansell, Mark Robinson, Bronwyn O'Brien, John Dalton, Sheila Donnelly, 2014; The *F. hepatica* cathelicidin like peptide (FhHDM-1) modulates the activation of the NLRP3 inflammasome in macrophages. (Manuscript in preparation).

Conference presentations

Raquel Alvarado, Maria Lund, Mark W. Robinson, Andrew Hutchinson, Joyce To, John P. Dalton, Bronwyn O'Brien and Sheila Donnelly, 2012; Presentation entitled: A novel molecule secreted by *Fasciola hepatica* modulates the activity of innate immune cells. 42nd Annual Scientific Meeting of the Australasian Society for Immunology.

Raquel Alvarado, Joyce To, Maria Lund, Mark W. Robinson, Andrew Hutchinson, Bronwyn O'Brien, John P. Dalton and Sheila Donnelly, 2013; Presentation entitled: A novel molecule secreted by the parasite *F. hepatica* modulates the response of macrophage NLRP3 inflammasome. 27th Annual Conference of the European Macrophage & Dendritic Cell Society.

TABLE OF CONTENTS

LIST OF ILLUSTRATIONS

LIST OF TABLES

ABBREVIATIONS

ACEC	Animal Care and Ethic Committee
ADCC	Antibody dependent cell mediated cytotoxicity
AIM2	Absent in melanoma 2
ALUM	Aluminium salts
AMPs	Antimicrobial peptides
APC(s)	Antigen presenting cell(s)
ARC	Animal Resources Centre
ASC	Apoptosis associated speck like protein
ATCC	American Type Culture Collection
Az	Azide
BcR	B cell receptor
BMDMs	Bone marrow derived macrophages
BSA	Bovine serum albumin
CAT	Catalases
Cav-1	Caveolin-1
ChTx	Cholera toxin subunit B
CLIC	Clathrin-independent non-caveolar pathway
CO_2	Carbon dioxide
DAMPs	Damage-associated molecular patterns
DAPI	4'6-diamidino-2 phenylindole, dilactate
DMSO	Dimethyl sulfoxide
DC(s)	Dendritic cell(s)
E. coli	*Escherichia coli*
ELISA	Enzyme-linked immunosorbent assay
ES	Excretory secretory products
FACS	Fluorescence-activated cell sorting (flow cytometry)
FBS	Foetal bovine serum
FhCL1	*Fasciola hepatica* cathepsin L-1
FhES	*Fasciola hepatica* excretory/secretory products
FhHDM-1	*Fasciola hepatica* helminth defence molecule-1
FhHDM-1p2	FhHDM-1 peptide 2
FhPrx	*Fasciola hepatica* peroxiredoxin

Geo Mean	Geometric mean
GPx	Glutathione peroxidase
hCAP18	Human cationic antimicrobial protein 18kDa
HDMs	Helminth defence molecules
HDPs	Host defence peptides
HEPES	4-(2-hydroxyethyl)-1-piperazineethanesulfonic acid
HVS	*Herpesvirus saimiri*
IAPP	Islet amyloid polypeptide
IFNγ	Interferon gamma
Ig	Immunoglobulin
IL	Interleukin
IMDM	Iscove's modified Dulbecco's medium
IPSE	IL-4 inducing principle of schistosome eggs
kDa	Kilo daltons
LBP	LPS-binding protein
LNFPIII	Lacto-N-fucopentaose III
LPS	Lipopolysaccharide
MAPKs	Mitogen-activated protein kinases
MCD	Methyl-β-cyclodextrin
M-CSF	Macrophage colony stimulating factor
MHC	Major histocompatibility complex
MIC	Minimal concentration capable of inhibiting visible microbial growth
MIF	Migration inhibitory factor
MPR	Mannose phosphate receptor
mRNA	Messenger ribonucleic acid
MS	Multiple sclerosis
MSU	Mono sodium urate
MW	Molecular weight
MyD88	Myeloid differentiation factor 88
N/A	Not applicable
Na_2CO_3	Sodium carbonate
Nano-SiO_2	Silicon dioxide (nanoparticles)
NH_4Cl	Ammonium chloride
NPG	N-propyl gallate microscopy mounting media

NLRs	NACHT-leucine-rich repeat receptors
(NOD)-like receptors	Nucleotide-binding oligomerisation domain protein like receptors
OD	Optical density
O/N	Overnight
OPep	Ovalbumin peptide
Ova	Ovalbumin
PAMPS	Pathogen-associated molecular patterns
PBMCs	Peripheral blood mononuclear cells
PBS	Phosphate buffered saline
PC	Phosphorylcholine
PFA	Paraformaldehyde
PGE_2	Prostaglandin E2
PI	Peak I
PII	Peak II
PI 3-K	Phosphoinositide 3 kinase
Prx	Peroxiredoxin
RecFhHDM-1	Recombinant *Fasciola hepatica* helminth defence molecule 1
RELM-α	Resistin-like molecule-alpha
RIPA	Radioimmunoprecipitation Assay Buffer
ROS	Reactive oxygen species
RPMI	Roswell Park Memorial Institute 1640 medium
RP-HPLC	Reversed-phase high performance liquid chromatography
RT	Room temperature
SmCB1	*Schistosoma mansoni* cathepsin B
SDS-PAGE	Sodium dodecyl sulphate- polyacrylamide gel electrophoresis
SEA	Soluble egg antigens
SEMs	Standard errors of the means
sFhHDM-1	Synthetic *Fasciola hepatica* helminth defence molecule-1
SiO_2	Silicon dioxide (nanoparticles)
SOD	Superoxide dismutases
T1D	Type I diabetes
TBS	Tris buffer saline
TcR	T cell receptor
TGF-β	Transforming growth factor beta

TGN	Trans-Golgi network
Th	T helper cells
Tip	Tyrosine kinase interacting protein
TLR	Toll like receptor
TNF	Tumour necrosis factor
TMB	3,3′,5,5′-Tetramethylbenzidine liquid substrate system for ELISA
Treg	T regulatory cells
TRIF	TIR domain-containing adaptor inducing IFN-β
TX100	Triton X 100
vATPase	Vacuolar adenosine triphosphatase
v/v	Volume / volume
w/v	Weight / volume

ABSTRACT

The ability of tissue dwelling helminth parasites to induce chronic long term infections, is enabled by the establishment of T helper 2/ regulatory T cell (Th2/Treg) immune responses within their mammalian hosts. Such responses prevent the expulsion of the parasites, whilst simultaneously avoiding excessive inflammation/fibrosis arising within the host, as a consequence of tissue damage induced by helminth migration. Importantly, helminths excrete and secrete a series of molecules (collectively known as ES products), which not only play major roles in parasite biology, but also exert direct immune modulatory functions, promoting the establishment of Th2/Treg immunity. The trematode, *Fasciola hepatica*, is an excellent model of helminth-mediated immune modulation, because it induces a very rapid switch towards Th2 responses in its mammalian hosts and inhibits Th1 immunity. Fractionation of the ES products of *F. hepatica* has identified three major immune modulatory components: the protease cathepsin L1, the antioxidant peroxiredoxin, and a previously uncharacterised peptide, FhHDM-1.

Structural analysis of FhHDM-1 revealed a close resemblance to the cathelicidin, LL-37, a well characterised mammalian immune-modulating peptide. Therefore, a putative immune modulatory role for FhHDM-1 was explored in this project. Immunofluorescent confocal microscopy demonstrated that FhHDM-1 interacted with macrophage lipid rafts, prior to being actively internalised by cholesterol- and cytoskeletal network-dependent endocytosis, with progressive compartmentalisation of the peptide into early endosomes and endolysosomal vesicles. Flow cytometry studies indicated that, once internalised, FhHDM-1 enhanced the rate of endocytosis of dextran by macrophages. Despite this, FhHDM-1 was found to impair the acidification of macrophage endolysosomes and as a consequence, the efficient processing and subsequent presentation of ovalbumin to T cells was prevented, as assessed by decreased detection of digested fluorescent ovalbumin and reduced IL-2 secretion by transgenic $CD4^+$ T cells. Additionally, FhHDM-1 impaired NLRP3 inflammasome activation by lysosomal disruptive agents in macrophages. This was found to be a consequence of reduced cathepsin B activity (due to FhHDM-1 induced suboptimal lysosomal acidification), which was incapable of stimulating inflammasome complex formation, thus avoiding IL-1β and caspase-1 cleavage.

These findings suggest that by targeting endolysosomal activity, FhHDM-1 limits macrophage function. Therefore, the current study is the first to demonstrate that FhHDM-1 possesses immune modulatory properties, which are directed by a mechanism not previously described for a helminth-secreted cathelicidin-like peptide.

CHAPTER 1 GENERAL INTRODUCTION

1.1. Versatility of the mammalian immune system

Unlike other lower order organisms, mammals possess an intricate and highly specialised immune system, to provide protection against a wide variety of pathogens. The first line of defence against potential threats relies on the surveillance mounted by the innate arm of the mammalian immune system. It comprises, amongst others, a combination of specialized immune cells (including monocytes, basophils and eosinophils), the complement system and immune modulatory peptides. Innate immune cells recognize particular molecular motifs that are commonly expressed amongst pathogens[1, 2]. These pathogen-associated molecular patterns (PAMPs) act as ligands that bind and stimulate their correspondent cellular receptors (e.g. Toll like receptors [TLRs]) initiating a cascade of events that lead to innate immune cell activation. In case of monocytes, once activated they are capable of migrating to diverse tissues and there become antigen processing cells (APCs) by differentiating into either macrophages or dendritic cells (DCs)[3, 4]. Macrophages are the most abundant leukocyte type in mammals, and aside from their important role as APCs (discussed below), these cells have high levels of plasticity. This enables their functions in maintaining tissue integrity (by the recognition of damage-associated molecular patterns [DAMPs] released by neighbouring cells in distress), as well as rapid pathogen killing (by a combined action of nitrogen and reactive oxygen species triggered by recognition of PAMPs; which is very beneficial in the in the control of highly proliferative bacteria), to be fulfilled[5].

Frequently the innate immune system is capable of clearing potential threats by its own account, however when this is not achieved, adaptive immune responses have to take control. The specific adaptive immune responses initiated vary according to the type of pathogen that is infecting the host, and are characterised by the proliferation of specific T cell subsets and their accompanying effector cytokine production[6]. A variety of T cell differentiation lineages have been identified to date, however the principal helper (Th) cell subsets include Th1, Th2 and Th17, which counter regulate each other[6, 7]. Th1 cell expansion with secretion of interferon (IFN) γ is characteristic of immune responses mounted during bacterial and viral infections[6, 7]. The dominance of Th17 cells instead, which secrete interleukin (IL)-17, is characteristic of fungal and extracellular

bacterial infections. However, Th17 cells that co-produce IFNγ can also drive autoimmunity[8-10]. Furthermore, proliferation of Th2 cells featuring secretion of IL-4, IL-5 and IL-13 support the generation of allergies and fibrosis[6, 11, 12]. Modified Th1 and Th2 responses are mounted during chronic protozoan/mycobacterial and helminth infections, respectively. These responses have a regulatory counterpart, which features the proliferation of T regulatory (Treg) lymphocytes (that are capable of suppressing the proliferation of all the other T cell subsets) and secretion of the immunosuppressive cytokines IL-10 and transforming growth factor (TGF)-β[13].

Antigen presenting cells (APCs), including macrophages, are fundamental for the establishment of all adaptive immune responses. Macrophages internalise, process and present pathogenic antigenic peptides to T cells, which, along with secreted cytokines, lead to the proliferation and orchestration of the specific T cell subsets. Macrophage phenotypes are determined by their activating agents and the environment to which they are exposed (e.g. secreted cytokines). Classical activation (in response to IFNγ and tumour necrosis factor [TNF]) results in a pro-inflammatory macrophage phenotype (M1), stimulating Th1 or Th17 cells that are driven towards host defence or autoimmunity[3, 14, 15]. M2 macrophages comprise an alternative phenotype which can be further sub classified according to their stimulant agents (which include IL-4/IL-13, IL-10, glucocorticoids, immune complexes and secosteroid hormones), the surface receptors that they express, and the cytokine milieu that they secrete[16]. Generally, M2 macrophages are regulatory, drive tissue repair by producing unique growth factors/enzymes and induce the development of Th2 immune responses[3, 5, 14, 15, 17].

1.2. Helminth parasites are master regulators of the mammalian immune system

Infection with intracellular pathogens, such as bacteria, induce pro-inflammatory immune responses, which are characterised by Th1 expansion, with concomitant secretion of pro-inflammatory cytokines, such as IFNγ and IL-12. Importantly, macrophages are converted into classical microbicidal phenotypes capable of internalising and degrading the invading organism, and also of producing toxic substances (e.g. reactive oxygen species), which target infected cells and are frequently lethal to the microbes[13, 18].

However, this type of immune response is ineffective against parasitic worms (helminths). In contrast to microorganisms, helminths are multicellular, extracellular pathogens. Thus, they are too large to be internalised by phagocytes for processing and presentation to T cells. Furthermore, direct killing of helminth parasites would require a vast amount of host secreted toxic substances, which would lead to extensive inflammation, and result in detrimental host tissue damage[13, 18]. Therefore, in response to invading helminth parasites, the mammalian host typically develops an anti-inflammatory and regulatory immune response. This response is characterised by the proliferation of Th2 and Treg lymphocytes, eosinophilia, basophilia, mast cell expansion, activation of M2 macrophages, production of parasite-specific immunoglobulin (Ig)E, and at latter stages of infection IgG4 (which counteracts IgE). The associated cytokine milieu primarily consists of Th2 type (IL-4, IL-13 and IL-5) and immune suppressive (IL-10 and TGF-β) cytokines [18-21].

The direct impact that Th2 responses have on the longevity of helminth infections varies between different helminth species. For example, gut-dwelling nematodes are susceptible to the environmental changes that Th2 responses cause to the intestinal epithelium. These changes include production of high amounts of mucus, accelerated epithelial turnover, and intestinal muscle hypercontractability, with all of these phenomena favouring parasite expulsion. Murine studies have demonstrated that these effects are mediated by IL-4 and IL-13 ligation with the IL-4 receptor α on epithelial cells, as the depletion of these cytokines causes a delay in parasite expulsion by the host[21-25]. Contrary to this, Th2 responses are actually protective for certain helminths, promoting chronicity of infection, in tissue-dwelling parasites specifically. This is demonstrated by anti-helminth vaccination studies where a switch towards a Th1 or Th1/Th2 response, makes the host resistant to parasite infection[26-29].

It is estimated that approximately one third of the world's population is currently infected with at least one type of helminth species, and, in the majority of cases, infections with these parasites are asymptomatic or sub-clinically long term chronic[19, 30-32]. The persistence of tissue dwelling parasites is accommodated by the modulation of immune responses, away from mammalian host-protective responses and towards Th2/Treg profiles. However, whether the host, the parasite or a combined participation of both, drives this regulation is still not completely clear. It has been proposed that the

host may activate Th2 immunity in response to parasite infections as a damage limitation strategy, where the harm associated with pathology would result in lesser damage than that induced by excessive defensive Th1 immunity. However, such an extraordinary evolutionary success has been also attributed to the ability of helminth parasites to breach the host defences, utilising immune modulating strategies, which modify the immune response in favour of their survival, supporting chronicity of infection within their mammalian hosts[19, 21, 31, 33, 34].

The priorities for helminth parasites change at different stages of maturation throughout the course of infection. At initiation, the major goal is reaching the parasite's final niche within its host, therefore, during migration, digestion of host tissue is fundamental. Later on, the adult worms in their final habitat focus on feeding, maturation and production of eggs. To deal with these varied challenges, helminths secrete and excrete a collection of molecules (known as excretory/secretory [ES] products), specially designed to meet the relevant requirements associated with their life cycle, and thus vary in abundance as well as composition between different stages of infection[35]. Isolated ES products also display immune modulating properties, often completely mimicking the immune response to live parasites, which strongly suggest that the molecules secreted-excreted by helminth parasites drive/modulate the Th2/Treg immune response of the host[36-40].

The Th2 component of such responses ensures the maintenance of a viable host by limiting immunopathological lesions (resulting from parasite infection/migration), while the Treg counterpart regulates the Th2 response to prevent extensive tissue fibrosis[18, 21, 32]. However, the parasite-induced Th2/Treg immune response can have negative collateral effects on the host, rendering it susceptible to infection with microbial pathogens, protection from which requires pathogen-specific Th1 responses. In addition, the induction of antigen-specific immune responses by immunisation is compromised in populations that are endemic for helminth parasites[20, 30].

Despite this, emerging epidemiological evidence suggest that infection with helminth parasites may actually be beneficial for the host under certain circumstances. An inverse correlation between the incidence of helminth infections and autoimmune diseases has been identified. This phenomenon has been suggested to arise from the Th2/Treg responses to helminth infections regulating the induction of Th17-mediated

autoimmune disease. Furthermore, a similar association has been established in allergic patients, where helminth infections ameliorate the development of allergy-specific inflammatory Th2 immune responses. In this case, the regulatory arm of the helminth response is responsible for this beneficial effect[41-43]. In both scenarios, the stimulation of regulatory immune cell phenotypes, including M2 macrophages, Tregs and regulatory B cells, along with their secretion of immunosuppressive cytokines (IL-10 and TGF-β), are key for the amelioration of disease associated symptoms and pathology[42, 43]. For example, patients with multiple sclerosis (MS), who are simultaneously infected with intestinal helminth parasites (e.g. *Hymenolepis nana*, *Trichuris trichiura* and *Ascaris lumbricoides*) have been reported to present fewer relapses and reduced disability scores when compared to uninfected MS patients. Immunologically, this improvement has been attributable to the activation of regulatory B cells and Tregs[44, 45]. Similar results have been achieved experimentally in allergic mouse models infected with *Heligmosomoides polygyrus* where a reduction in allergy associated pathology has also been characterised by Treg polarisation[42].

Although encouraging, active infection with live helminths still carries the risk of the host developing adverse parasite-associated pathology, making the direct use of helminths for therapeutic purposes unfavourable. Therefore, the identification of the key molecules involved in helminth induced immune regulation, is not only essential for their characterisation and elucidation of their mechanisms of action on specific arms/pathways of the immune system, but is also crucial for determining their potential usage in therapeutic applications against autoimmunity and allergies[46].

1.3. Characterisation of immune modulatory components of helminth excretory/secretory products

The use of proteomics techniques has allowed the identification and analysis of helminth ES products, enabling the subsequent production of individual synthetic molecules in order to investigate their specific biological functions (Table 1.1)[33].

1.3.1. PROTEASES

Cysteine proteases are commonly secreted by helminth parasites[47]. When these enzymes possess a cysteine residue in their active site, they become capable of catalysing the hydrolysis of proteins and oligomeric peptides, resulting in the cleavage of peptide bonds, thus generating peptide fragments[47]. Aside from their general catabolic functions, the secretion of cysteine proteases is critical for the biology of parasites due to their roles in processing (e.g. haemoglobin degradation which is crucial for blood feeding helminths such as *Schistosoma mansoni*), excystment/encystment (important for filarial nematodes), hatching (for example of schistosome eggs), and host cell/tissue penetration (including the larval stage invasion of *Strongyloides stercoralis* and *Necator americanus*). However, this latter function is more associated with helminth secreted serine and metallo-proteases[47].

Supplementary to these biological roles, it has been demonstrated that secreted cysteine proteases also contribute to the immune modulation of host responses during helminth infection. Supporting this premise, incubation of a human basophil cell line with *N. americanus* ES products induced the expression of the cytokines IL-4, IL-5 and IL-13 at an mRNA level and stimulated the secretion of IL-4 and IL-13, thus favouring the establishment of a Th2 response. This effect was not detected when *N. americanus* ES was pre-incubated with protease specific inhibitors, indicating that the activity of these enzymes was responsible for the stimulated cytokine secretion. It was proposed that a potential cleavage of surface basophil receptors, such as CD23 and CD25, by these proteases, induced IgE-independent basophil activation and subsequent release of cytokines[48]. In a similar manner, the *S. mansoni* secreted protease cathepsin B (SmCB1) also induces Th2 responses[49]. This switch towards protective Th2 immune responses seems to be conserved across phyla, given that Th2 immune responses are also triggered by cathepsin L-like proteases from the protozoan *Leishmania mexicana*, where murine infection with mutated forms of this parasite (with genes encoding cysteine proteases being disrupted), resulted in potent Th1 responses that effectively cleared infection[50]. Activation of basophils and induction of Th2 immune responses also commonly occur after exposure to allergens, many of which have been identified as having cysteine protease activity[19, 35, 47, 51]. For example, the cysteine protease Der p1, from the arthropod *Dermatophagus pteronyssinus*, mediates the development of house

dust mite allergy and asthma[47], and was found to stimulate equivalent cytokine profiles in basophils, as those described for *N. americanus* ES[48].

During a typical mammalian immune response, parasite-specific antibodies, produced by the host, coat the helminth, thus enabling its identification by surface Fc receptors on innate immune cells. This leads to the activation of the latter, and mediates antibody dependent cell mediated cytotoxicity (ADCC), that could be detrimental to the parasite[32, 52]. *In vitro* experiments have suggested that proteases secreted by multiple helminth parasites are capable of cleaving immunoglobulins. Therefore, the subsequent reduced availability or impaired interaction between parasite-specific antibodies with Fc receptors, could be a strategy employed by helminths to prevent being attacked by ADCC, which implies an additional immune-evasive/modulatory role for these enzymes[47, 53]. Additional immune regulatory/evasive functions have also been attributed to cysteine proteases that are secreted by protozoans. For example, cysteine proteases secreted by *Trichomonas vaginalis*, degrade the host protective C3 protein, which prevents complement-mediated parasite lysis[54]. Furthermore, calcium-independent metalloproteases, secreted by the helminth *N. americanus*, have been found to degrade eotaxin *in vivo*, which is a potent eosinophil chemoattractant. Therefore, by this means eosinophil recruitment and activation can be prevented by helminths at the site of infection. However, the specific metalloprotease responsible for this function was not purified and its full characterisation has not been reported[55].

1.3.2. PROTEASE INHIBITORS

Certain helminths, such as filarial parasites, have to undergo a series of moulting stages during their life cycle. This involves the shedding of old cuticle in order to expose the underlying new one, in a process performed, in part, by the action of cysteine proteases. However, these events have to be tightly controlled, so that moulting only occurs at the appropriate time of infection. Therefore, the parasite's cuticle is protected from degradation by protease inhibitors that are located on the parasite surface[56].

In addition to this important role during the parasite's life cycle, some protease inhibitors, mainly the cystatins, are constantly secreted by helminths, which is indicative of their importance in parasite maintenance within its host[57]. Cystatins modulate host immune responses, by inhibiting cysteine protease-mediated processing of antigens in APCs (with a subsequent negative impact on T cell activation and

proliferation in response to antigen presentation)[33, 57-59]. This mechanism of action is characteristic of the *Brugia malayi* secreted cystatin homologue, *BM*-CPI-2, which inhibits the activity of multiple cysteine proteases, including cathepsins S, B and L and asparaginyl endopeptidase in host B cells. This inhibition was sufficiently effective to impair processing of tetanus toxin antigen and invariant chain (which is a fundamental event for antigen loading into major histocompatibility complex [MHC] II) in isolated B cell lysosomes; and in living cells, *BM*-CPI-2 prevented the processing and presentation of tetanus toxin by B cells to T cells[57]. Similarly, Onchocystatin (secreted by *Onchocerca volvulus*) also inhibits cathepsin L and S activity and limits antigen driven and polyclonally stimulated proliferation. In addition, Onchocystatin induces IL-10 secretion from human peripheral blood mononuclear cells (PBMCs), and reduces MHCII and CD86 expression on monocytes[59]. The decreased availability of MCHII would prevent the loading of antigenic peptides to this complex, which is necessary for antigen recognition by the T cell receptor (TcR). Furthermore, the co-stimulatory signal arising from interaction between CD28 on the T cell surface and CD86 on monocytes would not be possible. Both of these events are central to efficient TcR signalling and T cell activation[60]. The Av Cystatin (Av17) secreted by *Acanthocheilonema viteae* also stimulates the production of IL-10 and induces a macrophage regulatory phenotype[61]. Furthermore, recombinant Av17 is capable of down-regulating antigen specific and non-specific T cell proliferation, as demonstrated in experiments using sperm whale myoglobin-specific T cell hybridomas and in thymocytes stimulated with anti-CD3 antibodies[62].

Thus, in general, cystatins directly affect several stages of the pathways involved in processing and presentation of exogenous antigens. Adult filarial parasites for example reside in lymphatic vessels. This close proximity to the lymph nodes, would make filariae particularly vulnerable to immune recognition. During infection with the canine filarial parasite, *Brugia pahangi*, lymph node cells were reported to be less responsive to challenge with parasitic-antigens, as compared to peripheral blood lymphocytes. This implies that by preventing the efficient production of parasite antigenic peptides and inhibiting their presentation to T cells by APCs, cystatins could avoid the development of localised anti-parasite immune responses[57, 63].

1.3.3. IPSE/ALPHA-1, OMEGA-1 AND OTHER HELMINTH GLYCANS

During infection with *S. mansoni* a switch towards a Th2 response is coincident with the deposition of eggs in the mesenteric venules of the host [64-66]. Therefore, many investigators are mining the soluble egg antigens (SEA) of this helminth in an attempt to characterise the individual immune modulating molecules. Using this strategy, the glycoprotein IL-4-inducing principle of schistosome eggs (IPSE)/alpha-1 and the ribonuclease omega-1 (both possessing N-glycosylation sites), were identified[66, 67]. IPSE/alpha-1 stimulates basophil degranulation and secretion of IL-4, which induces Th2 differentiation, by crosslinking IgE found in the surface of these cells, independently of antigen[64]. This glycoprotein also prevents the attraction of neutrophils and other inflammatory cells, by binding chemokines, thus inhibiting their interaction with their corresponding receptors[33]. Omega-1 is suggested to initially interact with APCs via C-type lectin receptors, prior to being endocytosed by these cells[67]. In DCs, omega-1 dampens their pro-inflammatory response to challenge with lipopolysaccharide (LPS), as assessed by suppression of IL-12p40, IL-12p70 secretion and prevention of the up-regulation of CD83, CD86, CD40 and CD54, indicating its inhibitory action on TLR-mediated DC activation[65, 68]. However, incubation of DCs with omega-1 alone, resulted in no alteration in the expression of surface co-stimulatory markers but rendered these cells capable of mediating Th2 responses[65, 68]. Omega-1 induced actin cytoskeletal rearrangements that decreased adherence of DCs, and this change in morphology, correlated with their reduced ability to form conjugates with CD4 T cells, impairing the activation of the latter. Therefore, it was proposed that omega-1 could be setting weak TcR signals, thus mimicking the effects of low-dose antigen, which drives Th2 responses. By reducing the encounter of DCs with T cells, helminths would be able to reduce the response of these cells to high dose parasite-derived antigens[65]. Additionally, *in vivo* studies indicate that omega-1 alone can efficiently drive Th2 responses, characterised by Th2 cell proliferation, stimulation of Tregs (via a TGF-β- and retinoic acid-dependent mechanism) and IL-4 expression[68, 69]. Depletion of omega-1 from SEA *in vitro*, significantly reduced SEA's ability to induce Th2 responses, suggesting that omega-1 is the main component that performs this function. However, this phenomenon does not occur *in vivo*, which was a likely consequence of alternative SEA component(s) compensating for the absence of omega-1 (for example IPSE/alpha-1 collaborating by being an alternative source of IL-4)[65].

Additional helminth glycoproteins have also been associated with immune modulatory properties. For example, chitohexaose (secreted by filarial parasites) was shown to induce TLR4-mediated activation of M2 macrophages that secrete high levels of IL-10. This glycoprotein also inhibited the production of the pro-inflammatory cytokines, TNF-α, IL-1β and IL-6, by macrophages upon stimulation with LPS, both *in vivo* and *in vitro*, which resulted in protection against endotoxemia in mice. Chitohexaose was even protective when administered after the onset of endotoxemia, reverting its effects[70]. Similarly, Lacto-N-fucopentaose III (LNFPIII), present in SEA, modulates APC function, stimulating IL-10 production, proliferation of M2 macrophages and driving TLR4-dependent DC-mediated Th2 responses[71-74]. Furthermore, LNFPIII has been found to induce IL-10 and prostaglandin E2 production by B cells[72, 75].

A common feature between these helminth glycans (with the exception of chitohexaose) is the presence of a $Lewis^X$ moiety in their structure. This moiety has been proposed to be directly involved with the immune modulatory roles of these glycans. Although its mechanism of action has not been fully characterised, it has been demonstrated that $Lewis^X$ directly interacts with C-type lectin receptors on APCs, antagonising TLR signalling and inducing phenotypes that are alternative to those stimulated by pro-inflammatory triggers, such as LPS. However, more recent studies have suggested that the activity of IPSE/alpha-1 is independent of this motif, given that its recombinant form is still capable of inducing IL-4 secretion in a concentration-dependent manner. This indicates that although the $Lewis^X$ moiety might be contributing to the immune modulatory functions of certain helminth glycans, its function does not seem to be a global characteristic of this group of proteins[67, 72].

1.3.4. CYTOKINE HOMOLOGUES

Some proteins secreted by helminth parasites have been identified as homologs of mammalian cytokines, which act in an analogous way, interacting with host cell receptors and inducing changes in phenotype and function of immune cells[33]. For example, the macrophage migration inhibitory factor (MIF) homologue secreted by *B. malayi* and *Ancylostoma ceylanicum*, in conjunction with IL-4, promotes the activation of macrophages, which express markers that are characteristic of an M2 phenotype; including the chitinase-like molecule Chi3L3/Ym-1, the resistin-like molecule (RELM)-

α and arginine-metabolising arginase-1. These M2 macrophages have been shown to inhibit the development Th1 responses[2, 19, 20, 33, 76-78] and also to directly induce T cells to acquire Th2 phenotypes and play roles in protecting the host from the potentially dangerous inflammation[19, 37, 78]. Helminths (including *H. polygyrus*) also produce TGF-β homologues, which facilitate the differentiation of Tregs (by direct stimulation of $Foxp3^+$ expression) that secrete the regulatory cytokine, IL-10[20, 31, 33, 77].

1.3.5. ANTIOXIDANTS

Individuals, who are resistant to parasitic infections, generally present elevated production of reactive oxygen species (ROS). ROS result from the reduction of oxygen to water and are produced upon the detection of danger by innate immune cells, such as macrophages, in order to mount an oxidative assault against invading pathogens[79]. Enzymes specialised in the synthesis of free radicals produce superoxide, oxygen radicals, and hydrogen peroxide, which are toxic to helminths[80, 81]. In their defence helminths secrete a series of antioxidants, including superoxide dismutases (SOD), catalases (CAT), glutathione peroxidase (GPx) and peroxiredoxins (Prx), thereby counteracting the damage that excessive oxidation could generate, as well as helping to maintain redox homeostasis[33, 35, 79, 80]. If contact between ROS and the parasite surface is not prevented, lipid peroxides will be produced, inducing cytotoxic carbonyls that cause damage to proteins, nucleic acids and membranes of the parasite, ultimately leading to its death[79]. SODs (abundantly produced by *Nematospiroides dubius* and adult *S. mansoni*) function by accelerating the dismutation of superoxide to hydrogen peroxide, which is subsequently transformed in to water and oxygen by action of CAT (abundantly secreted by microfilariae and adult worms of *B. malayi*). Despite this, CAT is only secreted by certain helminth species and although mammalian GPx can inactivate hydrogen peroxide, helminth secreted GPx mostly interacts with lipid hydroperoxides[82]. Therefore, the majority of helminth driven hydrogen peroxide detoxification is performed by Prxs, which are abundantly secreted by most helminth parasites, including *S. mansoni* and *Fasciola hepatica*, and whose sulphydrilic groups reduce hydrogen peroxide to water and alkyl hydroperoxides to alcohols[79, 82, 83]. Prxs are classified into 1-Cys or 2-Cys according to the number of conserved cysteine residues, with the latter subgroup being represented by *F. hepatica* and *S. mansoni* Prxs (that plays an important role in protecting eggs from attack by host ROS)[79, 83-85].

Helminths can also use antioxidants to directly damage host cells, which otherwise would be potentially harmful to the parasite. Such is the case of *N. americanus* that by secreting SOD but not CAT, increases the production of hydrogen peroxide, leading to the formation of reactive hydroperoxides which are toxic to host immune cells[79]. In addition, helminth secreted antioxidants have been found to act as immune modulators, for example *F. hepatica*, *S. mansoni* and *Haemonchus contortus* produced Prxs, stimulate the *in vivo* alternative activation of macrophages and macrophage *in vitro* secretion of IL-10, which promotes Th2 development while suppressing Th1 responses[37, 86].

1.3.6. ES-62 A PHOSPHORYLCHOLINE (PC) CONTAINING GLYCOPROTEIN

The best characterised helminth secreted molecule to date is ES-62, a phosphorylcholine (PC)-containing glycoprotein, secreted primarily by the adult stage of the rodent filarial nematode, *A. viteae*, accounting for over 90% of this parasite's ES products. The phosphorylcholines, acquired as post-translational modifications and attached to the terminal N-acetylglucosamine (GlcNAc) residues of this glycoprotein, have been identified as its active immune modulatory component, and despite its extreme abundance, the biological significance of this glycoprotein's backbone structure remains unknown. It has been proposed that its functionality may simply be to act as a carrier for the PC groups[87]. In fact, attachment of PC to irrelevant proteins can reproduce the effects of ES-62. Homologues of ES-62 are found in ES products of *B. malayi* (although lacking PC), *B. pahangi, O. volvulus* and *Loa Loa*[38, 87, 88]. Structurally, ES-62 is formed by ~62kDa monomers forming a tetrameric glycoprotein (~240kDa) with 4 potential N-linked glycosylation sites[38]. *In vivo* studies on BALBc mice indicated that subcutaneous administration of ES-62 stimulates a potent Th2 polarisation, characterised by IgG1 production. This was dependent on the presence of PC and proposed to arise as a combined effect of the down-regulation of Th1 antibodies (IgG2) and the activation of IL-10 production by B1 cells[87, 89]. Amongst its numerous immune regulatory functions, ES-62 has been found to desensitise B cell receptor (BcR) ligation by preventing the activation of downstream proliferative pathways, phosphoinositide 3 kinase (PI 3-K) and Ras/Erk MAPK, thus interfering with activation of B lymphocytes and their subsequent proliferation. Despite this, BcR signalling is not completely blocked. For example, BcR-coupled PLC-γ-mediated hydrolysis of diacylglycerol (controller of Ca^{2+} mobilisation) remains unaffected by ES-62[38, 88].

Similarly, ES-62 also disrupts TcR coupling to phospholipase D, protein kinase C, PI 3-K and Ras/Erk MAPK causing T cell anergy to these signalling cascades[90]. Based on these observations it has been hypothesised that phosphorylcholine-containing ES products, which are conserved in filarial parasites, induce lymphocyte hyporesponsiveness during infection[88, 90].

The modulatory effects of ES-62 are not limited to lymphocytes but also affect APCs via direct modulation of TLR responses and MyD88-dependent signalling pathways. This results in the formation of immature APCs that express low levels of co-stimulatory factors and decreased pro-inflammatory cytokine secretion in response to engagement with PAMPs, which are conditions conducive to the establishment of Th2 responses[38]. Consistent with the brief presence of Th1 responses during the early stages of infection with certain helminths, exposure of unchallenged macrophages to ES-62 induces a weak secretion of pro-inflammatory cytokines. However, it has been suggested TLR4 interaction with ES-62 differs from that of LPS and TLR4[91]. Moreover, treatment of DCs and macrophages with ES-62 prior to IFN-γ/LPS stimulation results in modulation of the MyD88 signalling pathway (downstream of MAPK and NF-κB effectors) that suppresses the production of pro-inflammatory cytokines (IL-12, IL-6 and TNF-α). Such TLR4-MyD88 signalling-dependent cytokine production down regulation has been also detected in mast cells and Th17 cells (with decreased IL-17 secretion) when exposed to ES-62[38, 91].

1.3.7. ADDITIONAL ES PRODUCTS THAT ARE IMMUNE MODULATORS

The immune modulatory properties of certain helminth secretions have been linked to their possession of particular motifs or posttranslational modifications, rather than to belonging to an already established group of homologous molecules with known functions. Such is the case for ES-62 with its PC groups[87]. This means that their backbone structures may not be necessarily conserved amongst helminth secretions or have homology to other molecules with similar mechanisms of action. For example, glycosylation of schistosoma (and other helminth) glycoproteins has been attributed to enable their interaction with TLR4, thus modulating APC activation, specially by inducing anti-inflammatory macrophage phenotypes, that favour the development of Th2 responses during helminth infection[3, 17, 33, 67].

Also, the mechanism(s) of action and/or functional significance of certain ES components secreted by multiple helminth species, which are classified in particular molecular groups, remain elusive. For example, galectins, identified amongst the secretions of a variety of helminths, are capable of binding to carbohydrates and their interaction with host immune cells has been recognised[33]. A direct general function has not yet been attributed to these proteins as a group. However, given that host cells possess cytosolic galectins, which are released by dying cells upon pathogen-induced tissue damage and secreted by inflammatory activated host cells (causing immune modulation), it is possible that helminth secreted galectins may be potentially acting as homologues to host DAMPs[33, 92]. Certain helminth secreted galectins have been well studied, such as *Tl*-gal from *Toxascaris leonina*, which is capable of suppressing inflammatory reactions by inducing the expansion of TGF-β/IL-10 producing T cells and preventing the synthesis of Th1 and Th2 cytokines[92]. Also strong chemokinetic effects on eosinophils have been demonstrated by *H. contortus* galectins *in vitro*, which was suggested to mimic the mammalian galectin GAL-9, that has known eosinophil recruitment functions[93]. Both eosinophilia and the stimulation of Treg cells are features of the Th2/Treg immune response during helminth infection; thus, by secreting these types of galectins, helminths could be promoting the establishment of such immune responses.

Another group of secretions are the venom allergen homologues, often found in helminth ES products, for which a general function has not been clearly demonstrated[33]. However, one of these homologues, *Na*-ASP-2, secreted by *N. americanus* has been found to induce the influx of leukocytes (mainly neutrophils and monocytes) to skin pouches, suggesting an *in vivo* chemoattractant role, which was further supported by an in vitro chemotaxis assay[94]. Furthermore, crystal structural studies had predicted *Na*-ASP-2 to be able to bind to chemokine receptors, which correlates with the aforementioned functional findings[95]. The neutrophil inhibitory factor, NIF, secreted by *A. caninum*, is a glycoprotein that also belongs to the family of venom allergen homologues, and it inhibits neutrophil function, including preventing their adherence to the vascular endothelium, phagocytosis, and secretion of hydrogen peroxide by interacting with the receptor CR3 (CD11b/CD18) found in this cells[96, 97].

Additionally, two heat shock proteins, Sra-HSP-17.1 and Sra-HSP-17.2 (secreted by *Strongyloides ratti*) have been shown to have the ability of binding to monocytes and macrophages, stimulating the former to produce IL-10, which is an indication that these heat shock proteins may be contributing to the modulation of host responses[98]. Also, particularly relevant to gut-dwelling helminths nematodes, acetylcholinesterases secreted by these parasites have been suggested to prevent parasite clearance by reducing the abundance of fluids in the gut[33]. Calreticulin, secreted by *H. polygyrus*, is another helminth immune modulator that has been demonstrated to stimulate T cell secretion of IL-4 and IL-10 which promotes Th2 responses[99]. And chitinases, secreted by this same parasite are proposed to decrease parasite-derived chitin levels (which would otherwise stimulate Th2 responses) therefore dampening Th2 immunity[46]. Finally, the helminth lipid-like schistosome Lyso-phosphatidylserine, has been found to induce DC-mediated activation of IL-10 producing Tregs, by interacting with DC TLR2[100].

Table 1.1 Classification of identified helminth ES components and their immune modulatory/evasive effects.

ES product	Specific molecules (when relevant)	Immune modulatory/evasive effects	Secreted by	Ref
Acetylcho-linesterases	Acetylcho-linesterases	May inhibit fluid accumulation in the gut preventing parasite clearance.	Gut-dwelling nematodes	33
Antioxidants	Superoxide dismutases, catalases, glutathione	Antioxidant properties/ protect from host ROS.	*Heligmosomoides polygyrus, Schistosoma mansoni, Brugia malayi*	79, 82, 83
	Peroxiredoxins	Antioxidant properties/ protect from host ROS. Promotes Th2 responses by inducing M2 macrophages and IL-10 secretion.	*S. mansoni* *Fasciola hepatica*	79, 83-85
Calreticulin	Calreticulin	Drives Th2 responses by inducing IL-4 and IL-10 secretion by T cells.	*H. polygyrus*	99
Chitinases	Chitinases	Reduces Th2 responses by decreasing parasite derived chitin levels.	*H. polygyrus*	46
Galectins and galectin-like molecules	Galectins (e.g. *BM*-GAL-1, *Tl*-GAL)	Inhibit Th1 and Th2 cytokine production and stimulates TGF-β and IL-10. Modulates eosinophil migration.	*B. malayi, Toxascaris leonine, H. polygyrus Haemonchus contortus*	92, 93
Glycans	Chitohexaose	Prevents macrophage response to LPS and induces an M2 phenotype by interacting with TLR-4.	*Setaria digitata, Brugia pahangi*	70
	Lacto-N-fucopentaose III (LNFPIII)	In macrophages stimulates IL-10 secretion and an M2 phenotype. Promotes DCs to secrete IL-10 and mediated Th2 responses. Induces IL-10 and prostaglandin E_2 production by B1 cells.	*S. mansoni* eggs	71-74
	(IPSE)/alpha-1	Stimulates basophil degranulation and IL-4 secretion. Sequesters chemokines.	Schistosome eggs	33, 64
	Omega-1	Dampens DC response to LPS, stimulates DC-mediated Th2 proliferation, and induces Foxp3 expression and IL-4 in T cells.		65, 67, 69

Table 1.1 continued…

ES product	Specific molecules	Immune modulatory/evasive effects	Secreted by	Ref
Cytokine homologues	Migration inhibitory factor	Induce M2 macrophages.	*B. malayi, Ancylostoma ceylanicum*	78
	TGF-β	Stimulates differentiation of Tregs and IL-10 secretion.	*B. malayi, H. polygyrus*	33, 101, 102
Heat shock proteins	Sra-HSP-17.1 Sra-HSP-17.2	Stimulate monocytes to produce IL-10.	*Strongyloides ratti*	98
Lipids	Lyso-phosphatidylserine	Induces TLR2 dependent DC-mediated activation of Tregs that produce IL-10.	*S. mansoni, Ascaris lumbricoides*	100
Phosphorylcholine-containing glycoconjugates	ES-62 and its Homologues	Stimulates Th2 polarisation, B cell IgG1 production, IgG2 down regulation and IL-10 secretion. Desensitizes BcR, TcR, TLRs in APCs and down regulates MyD88 dependent cytokine secretion.	ES-62: *A. viteae* Homologues: *B. malayi, Onchocerca volvulus* and *Loa Loa*	38, 87-89, 91, 103, 104
Proteases	Cysteine proteases -Cathepsin L	Stimulate Th2 responses. Degrade TL3, dampening macrophage response to LPS stimulation. Cleavage of immunoglobulins.	*Fasciola hepatica*	53, 105
	Metalloproteases	Inactivate eotaxin which prevents eosinophil recruitment.	*Necator americanus*	55
Protease inhibitors	Cystatins and homologues (e.g. Av-17, Bm-CPI-2, onchocystatin)	Inhibit cysteine protease activity of APCs reducing antigen processing and by default presentation. Stimulate macrophage regulatory phenotype and IL-10 secretion which inhibit T cell responses. Reduce MHCII and CD86 expression on monocytes.	*A. viteae, O. volvulus, Clonorchis sinesis, H. plygyrus, B. malayi*	46, 57-59, 61
Venom Allergen homologues	*Na*-ASP-2	Induce monocyte and neutrophil chemotaxis.	*N. americanus*	94
	NIF	Inhibit neutrophil functions.	*Ancylostoma caninum*	33

1.4. *Fasciola hepatica*: A model of helminth-induced immune-modulation

Fasciola hepatica is an economically and medically important helminth parasite that causes fasciolosis (liver fluke disease), in its mammalian host[106, 107]. All mammals become orally infected after ingestion of *F. hepatica* metacercariae, which excyst in the duodenum. The excysted juvenile worms then penetrate the intestinal wall, cross the peritoneal cavity and migrate through the liver parenchyma before reaching their final niche in the bile ducts, where flukes mature and produce vast numbers of eggs[32, 37, 39, 108].

Importantly, this parasite infects a wide array of mammalian hosts, and therefore provides an ideal model to study the mechanisms of helminth-mediated immune modulation. Within a laboratory setting, mice are commonly used as an infected host and respond with the same immune response as naturally infected sheep, cattle and humans[29, 106, 107, 109]. In addition, unlike many other helminth parasites, the induction of Th2 immune responses is not dependent upon the deposition of eggs or the maturation to adulthood. Instead *F. hepatica* displays a remarkable ability to induce a very rapid switch (within 12h post infection) towards a Th2 immune response within all its mammalian hosts, to the point that indications of Th1-associated immunology are almost completely absent[37, 109]. This Th2 response is characterised by the activation of M2 macrophages, which respond inefficiently to pro-inflammatory stimuli[37, 110]. By 7 days post-infection, levels of IL-4, IL-5 and IL-13 are significantly increased, indicating that a potent Th2 response is fully established[37, 107]. At the chronic stages of infection with *F. hepatica* (about 21 days post infection in the murine host), macrophages secrete IL-10 and TGF-β, DCs acquire an immature phenotype characterised by the secretion of IL-10, and $Foxp3^+$ Tregs become recruited and their expansion is stimulated[111]. The Tregs control the potency of the parasite-specific Th2 response (this regulation being mostly mediated by action of IL-10) as well as preventing the development of Th1 and Th17 responses[107, 111].

During the entire course of infection, *F. hepatica* secretes and excretes a series of molecules termed *F. hepatica* excretory/secretory (FhES) products that mediate immune modulation. Murine studies have indicated that administration of FhES alone, replicates the main features of natural infection with the helminth, namely the

suppression of Th1 responses and the stimulation of a parasite-specific Th2 immune response[37, 39, 86, 105, 112]. Furthermore, proteomic analysis indicates that the profile of FhES is relatively simple when compared to the ES of other helminth parasites (such as the complex ES of *Trichuris suis*, which has been found to be composed of 1288 molecules, from which 120 have been proposed as possible immune modulators), making the identification of key immune regulatory molecules responsible for driving the switch towards the Th2 response, characteristic in *F. hepatica* infection, more attainable[108, 113].

The constituent molecules of FhES have been extensively analysed and individual components tested for immune modulatory ability[37, 39, 105, 108, 114, 115]. Fractionation of FhES products by size exclusion chromatography, obtained after culture of adult worms *in vitro*, revealed two major protein peaks, termed PI (>200 kDa) and PII (60-20 kDa). Peritoneal injection of these fractions into mice resulted in the stimulation of M2 macrophages and parasite-specific Th2 responses by PI, and inhibition of Th1 immune responses by PII[86]. Subsequent separation of the fractions by one-dimensional gel electrophoresis, followed by in-gel trypsin digestion and mass spectrometry analysis, indicated that PII, which accounts for 80% of FhES, was composed of cathepsin L cysteine proteases (FhCLs) from which cathepsin L1 (FhCL1) was the most abundant; whereas PI, was primarily composed of the antioxidant enzyme, peroxiredoxin (FhPrx), and a more abundant, previously uncharacterised peptide, termed FhHDM-1[37, 86, 108, 115]. Homologues of these three molecules have been identified within the ES products of other helminth species, including the liver flukes *Clonorchis sinensis* and *Opisthorchis viverrini*, the lung fluke, *Paragonimus westermani*, and the blood flukes *S. mansoni and Schistosoma japonicum*[39, 86, 115]. However, the aforementioned parasites preferentially secrete cathepsin F, as opposed to cathepsin L, with the exception of the *Schistosoma spp.*, which despite also secreting cathepsin F, predominantly expresses cathepsin L[116]. Based on this evolutionary conservation, the abundance of these molecules within FhES, and the *in vivo* effects that administration of the individual FhES fractions (PI and PII) that contain them induced, suggested that these molecules are likely important immune modulators.

1.4.1. FhCL1

FhCLs constitute the most abundant secretions of *F. hepatica*, with multiple phylogenetic clades being differentially expressed throughout the diverse stages of infection. These include FhCL1, FhCL2 (both expressed at the immature and mature stages of the parasite), FhCL3 (present during penetration of the host intestinal wall by the infective larvae), and FhCL5 (expressed during the mature stage), FhCL1 being the major clade expressed by the adult parasite[108, 116]. In terms of helminth survival, fluke cathepsin Ls play major roles in parasite migration and feeding, given that these enzymes degrade host interstitial matrix proteins and haemoglobin. These essential functions explain why cysteine proteases are abundantly secreted by the majority of helminth parasites[47]. However, FhCL1 in particular has also been shown to play a role in the evasion and modulation of host immune responses. FhCL1 cleaves host IgG, which prevents the binding (and therefore identification) of the antibody coated helminth by Fc receptor bearing macrophages, which would lead to activation of immune cells and ADCC, to destroy the parasite[53].

Additionally, mice given a systemic injection of FhCL1 were unable to mount a bacterial-specific protective immune response when exposed to *Bordetella pertussis* or the whole cell pertussis vaccine, indicating that FhCL1 inhibits the development of Th1 responses[105-107, 112]. A more detailed analysis of the potential mechanism used by FhCL1 showed that the enzyme cleaved TLR3 in murine macrophages, inducing its degradation within endosomes. This resulted in the inactivation of the MyD88-independent TRIF-dependent signalling pathway in response to TLR4 and TLR3 stimulation[105]. It was proposed that such modulation of macrophage signalling pathways would in turn make these cells more susceptible to switching towards an M2 phenotype by other parasite molecules or cytokines, therefore supporting the establishment of a Th2 environment[117-119].

During the migrating stages of infection with many helminths, including *F. hepatica*, perforation of host intestinal epithelium can cause the dissemination/translocation of luminal bacteria and their toxins into the circulation, which can escalate to fatal septic shock[105, 115]. However, sepsis is not common during helminth infections, and is proposedly prevented by the action of helminth ES components (specifically FhCL1)[105]. By preventing the excessive inflammatory response associated with disseminating intestinal bacteria, FhCL1 would not only

protect the host from sepsis but would also avoid elimination of the parasite by the potent Th1 response.

The importance of FhCL1 in the modulation of immune responses has been further highlighted in vaccination studies. Vaccination of livestock with recombinant FhCL1, in combination with mineral oil based adjuvants, induced significant protection (48.2%) in cattle experimentally challenged or exposed to pastures contaminated with liver fluke. Protected animals presented high titres of FhCL1 specific IgG1 and IgG2 (with IgG1 only being detected in control groups), which are representative of a Th1 type immune response. Furthermore, macrophages from immunised, protected cattle expressed lower levels of Arg1, indicating an impaired stimulation of M2 macrophages[120, 121].

1.4.2. FHPRX

Secretion of FhPrx is most abundant during the juvenile and adult stages of the *F. hepatica* life cycle[37, 86]. Apart from its ability to protect the parasite from reactive oxygen species (by detoxification of hydrogen peroxide), immune modulatory properties have been attributed to this enzyme. Intraperitoneal injections of recombinant FhPrx to mice were found to stimulate the activation of M2 macrophages (characterised by increased Fizz1 and Arg1 gene expression). This occurred independently of the enzyme's antioxidant activity, as an inactive recombinant version of FhPrx, where the active site Cys residue was replaced by Gly, retained the ability to induce M2 macrophages[37, 86]. *In vitro* incubation of unchallenged RAW 264.7 macrophages with this antioxidant also induced increased expression of Arg1, secretion of IL-10 and prostaglandin E_2 (PGE_2), characteristic of an M2 phenotype, suggesting that FhPrx directly induces the activation of M2 macrophages[37]. The FhPrx-induced M2 macrophages displayed an increased production of TGF-β, which aids the orchestration of Th2-type immune responses[37, 86]. Incubation of FhPrx-activated M2 macrophages with naïve $CD4^+$ T cells induces the polarisation of the latter, towards a Th2 phenotype and stimulates subsequent secretion of anti-inflammatory cytokines (IL-4, IL-5 and IL-13)[86]. Given that these effects are independent of the antioxidant function of FhPrx and that they were replicated by a murine Prx homologue, it was proposed that a yet unknown shared motif could be interacting with host receptor molecules. This mechanism is likely to be generically conserved amongst helminths, due to the high

sequence similarities between Prxs secreted by other helminth parasites and the Th2 responses (involving M2 macrophage activity) that they trigger[86].

Similar to the actions of FhCL1, neutralisation of parasite-secreted Prx via immunisation, or by delivery of neutralising antibodies, inhibited the development of Th2 responses in mice, during a challenge infection with *F. hepatica*. In addition, vaccination of sheep with recombinant FhPrx also induced protection levels of 52% after challenge with *F. hepatica*[86]. These outcomes clearly support a role for Prx in the modulation of immune responses, which occur during infection and more specifically in the induction of Th2 immune responses[86, 122].

1.4.3. FhHDM-1

The previously uncharacterised peptide, FhHDM-1, is secreted during all stages of infection. Robinson *et al*. were the first to determine the complete sequence of the secreted mature form of FhHDM-1, and, in its native conformation, this peptide was found to have a size of 8 kDa[115]. In low pH environments FhHDM-1 presents a high degree of oligomerisation, which explains its identification within the high molecular mass fraction (>200 kDa) of ES components (PI) and has been proposed as a possible mechanism that protects this peptide from proteolysis in the acidic gut of the parasite[115]. Most recently, haem-binding properties have been attributed to FhHDM-1[123]. Adult *F. hepatica* flukes are obligate blood feeders and during the digestive process, haemoglobin is degraded by FhCLs resulting in the release of potentially toxic free haem, which is subsequently regurgitated by the parasite[108, 123]. It was suggested that FhHDM-1 could thus possibly function as a chaperone capturing the free haem for detoxification purposes or for its transportation to different organs, however these theories are yet to be proven[123].

Initial studies of the primary sequence of FhHDM-1 (Figure 1.1 B) did not reveal the presence of known functional motifs that could predict the potential roles of the peptide. However, secondary structural analysis by CD spectroscopy revealed that the C-terminal hydrophobic region of this peptide has an amphipathic α-helix conformation (Figure 1.1 A). This structure closely resembles that of the secondary structure of the human cathelicidin, LL-37, which belongs to the family of host defence peptides (HDPs)[115].

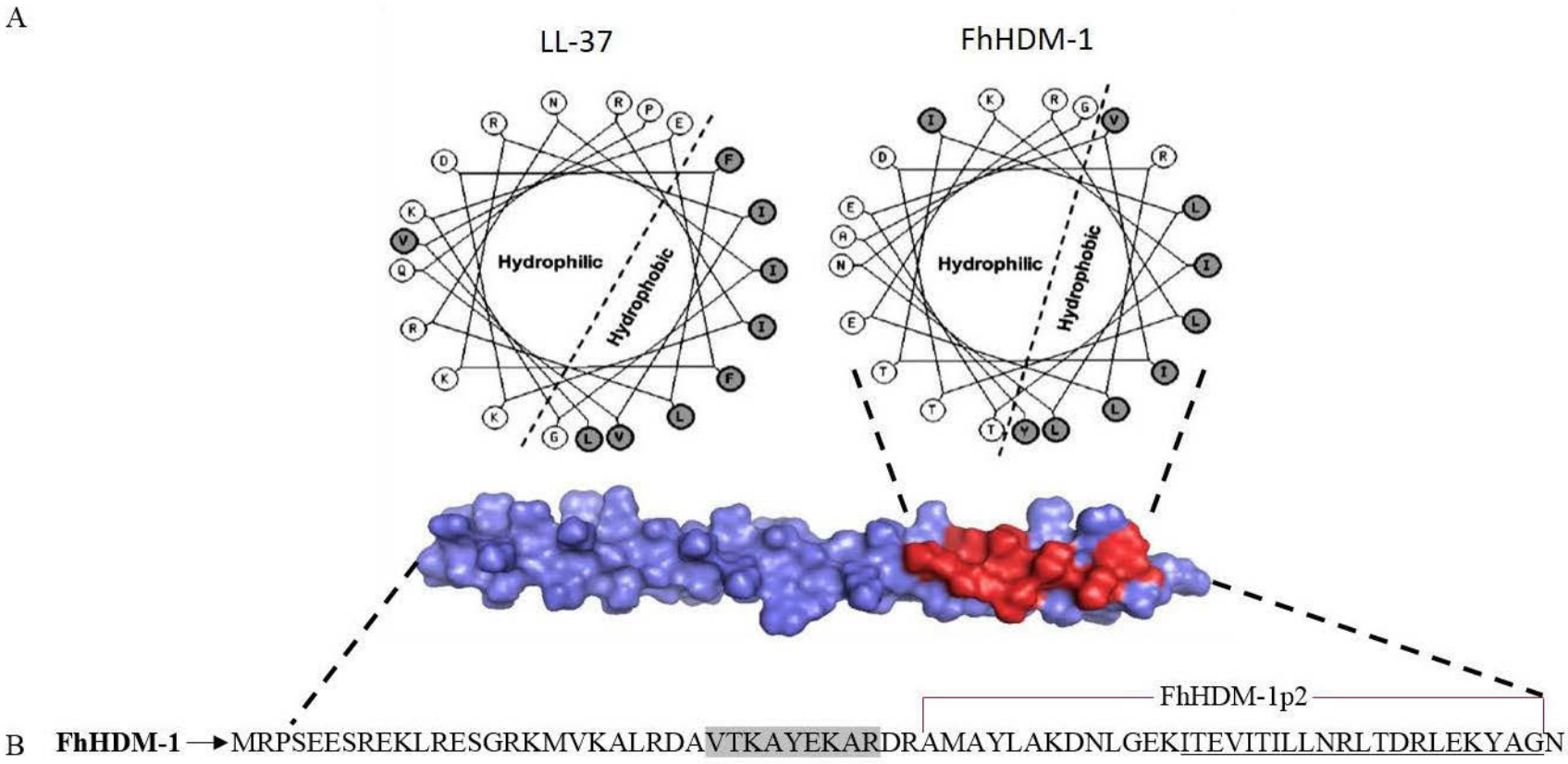

Figure 1.1 Characterization of FhHDM-1 and structural homology to LL-37. A. Helical wheel analysis of the conserved C-terminal hydrophobic regions of LL-37 and FhHDM-1 indicate high structural similarity between these peptides[115]. Directly below, model structure of FhHDM-1 (hydrophobic phase shown in red)[124]. B. Primary sequence of FhHDM-1 (with 34 residue C-terminal fragment; FhHDM-1p2), amino acids comprising the putative cholesterol binding motif are boxed in grey and the hydrophobic regions underlined[114, 115].

[Production note: Figure 1.1 was adapted from references [114, 115, 124]]

1.5. FhHDM-1 is a helminth-derived peptide with homology to the mammalian cathelicidin defence peptides

Eukaryotic organisms produce an evolutionary conserved group of short (12-50 amino acids, at least 50% of which are hydrophobic), amphipathic, positively-charged peptides that are known as antimicrobial peptides (AMPs)[125-127]. AMPs are primarily synthesised by cells of the innate immune system (such as macrophages and DCs) and are released in response to cellular stimulation by pathogens and/or pro-inflammatory triggers, presented during infection and tissue damage[115, 128]. These peptides are generated/activated upon the cleavage of their precursor proteins and have been associated with broad spectrum antimicrobial properties[125, 129]. In addition, some AMPs are efficient immune modulators and these have been additionally called host defence peptides (HDPs)[125, 129-131]. A range of different functions have been attributed to these HDPs, such as, chemotaxis, mimicry and/or regulation of chemokine and cytokine secretion, induction of angiogenesis, promotion of wound healing, and polarisation of adaptive immune responses[125, 132]. AMPs/HDPs have a wide variety of primary sequences; therefore, these peptides are classified according to their secondary structure[115]. The two major groups, with important roles in immune defence, are the cathelicidins and defensins (characterised by linear α-helical or β-sheets [stabilised by intra-molecular disulphide bridges] structures, respectively)[131]. Many HDPs (specially the cathelicidins) exert their immune-regulatory effects directly on APCs, via preventing their full maturation and/or ability to orchestrate adaptive immune responses (such as by modulating cytokine secretion)[130, 133, 134].

The most widely studied HDP is LL-37, which is the only human cathelicidin identified to date. This peptide is derived from the cleavage of its precursor protein, human cationic antimicrobial protein 18kDa (hCAP18), which releases the 37 residue C-terminal peptide[131]. Increased levels of LL-37 are produced in response to injury, infection and during a range of immune-mediated diseases, which has led to suggestions of a role in combating disease and assisting the immune system[124, 131]. LL-37 is expressed (at varying concentrations) in multiple cell types, including neutrophils, macrophages and mucosal epithelial cells. This cathelicidin is capable of modulating and neutralising the response of innate cells to pathogen associated ligands, such as LPS

(a property also shared with other mammalian HDPs, including bovine BMAP-28, sheep SMAP-29, and mouse CRAMP)[135]. LL-37 also acts as a chemoattractant for T cells and mononuclear cells (neutrophils and DCs), and induces mast cell degranulation[115]. Aside from its immune modulatory properties, LL-37 is an antimicrobial peptide that is reported to kill at least 45 bacterial species[136]. Its antimicrobial activity is attributed to its C-terminal helix, and a mechanism by which, the acid phospholipid head groups on bacterial membranes (which are negatively charged) are bound by electrostatic forces to the positively charged amino acids of the peptide. Accumulation of LL-37 causes a positive curvature strain that leads to a series of translocations, which form pores within membranes causing increased permeability, and ultimately bacterial death[136]. Low concentrations of LL-37 preferentially target the negatively charged cell surfaces of bacteria, which distinguishes them from most eukaryotic membranes (that possess essentially neutral surfaces)[137].

LL-37 activation results from the cleavage of hCAP18 by proteinase 3, in the neutrophil azurophil granules[131, 138]. Similarly, FhHDM-1 is also proteolytically cleaved by the co-secreted FhCL1, resulting in the release of a bioactive 34-residue C-terminal peptide fragment (termed FhHDM-1 peptide 2 [FhHDM-1p2]) containing the amphipathic helical region (Figure 1.1 B). This suggests that full length FhHDM-1 may behave as a precursor molecule[115]. However, full-length FhHDM-1, as well as FhHDM-1p2, are capable of suppressing the secretion of pro-inflammatory cytokines by macrophages stimulated with LPS. This inhibition has been attributed to the high binding affinity between FhHDM-1 and LPS (dependent upon the peptide's intact amphipathic helix), which results in sequestration of the bacterial ligand, thus disabling its interaction with LPS-binding protein (LPB) found on the macrophage surface[115]. Furthermore, delivery of FhHDM-1 to mice affords protection against the development of inflammatory responses associated with LPS-induced sepsis[115].

These findings indicated that FhHDM-1 not only resembled LL-37 structurally, but also shared functional similarities[115]. FhHDM-1 also shares multiple similarities (namely, possessing a predicted N-terminal signal peptide, amphipathic α-helical secondary structure and a highly conserved hydrophobic C-terminal portion) with other helminth secreted molecule sequences, indicating an evolutionary conservation amongst trematode pathogens of clinical significance, including *C. sinensis*, *O. viverrini*, *P.*

westermani, *S. mansoni and S. japonicum*[135]. These FhHDM-1 homologues include SmHDM-1 and SmHDM-2 (both secreted by *S. mansoni*)[135]. Thus, a novel family of helminth-produced HDP homologues, termed helminth defence molecules (HDMs), has been revealed, which has been suggested to result from helminths mimicking and exploiting HDP function[115].

A detailed comparison of helminth C-terminal HDM peptides and a panel of similar length, well-studied mammalian HDPs, reported by Thivierge *et al*., demonstrated biochemical similarities between both peptide families, including a net positive charge (+3 to +9; with the exception of FhHDM-1p2 that had a charge of 0), having a percentage of hydrophobic residues between 34 to 44, and an estimated potential to bind to other peptides (Boman index) ranging from 1.34 and 3.11. Furthermore, helical wheel analysis indicated that they all acquire an amphipathic α-helical structure[135].

It was also revealed that SmHDM-2p58 is a very potent LPS inhibitor, almost as efficient as BMAP-28, however the other tested *S. mansoni* HDM peptides did not possess this strong affinity, suggesting that this feature may not be common amongst the HDM family[135]. The bactericidal activity of C-terminal HDM peptides (FhHDM-1p2, SmHDM-1p2 and SmHDM-2p58) was compared to that of mammalian HDPs (CRAMP, SMAP-29 and BMAP-28) against a group of gram negative and positive bacteria, by measuring the minimal concentration capable of inhibiting visible microbial growth (MIC). The tested HDPs were very efficient at killing both bacterial types tested (MIC<8μg/mL). However, the HDM peptides, at all the tested concentrations, were incapable of performing bactericidal activity against any of the bacteria tested. Using a similar approach, the investigated HDPs were parasiticidal against *Cryptosporidium parvum* and *Cryptosporidium hominis* sporozoites, BMAP-28 being the most efficient at 2.5μM and LL-37 displaying the lowest overall efficiency of the group. Contrary to this, the HDM peptides presented no parasiticidal activity, even at the highest concentrations tested[135].

At high concentrations, LL-37, and most mammalian HDPs, haemolyse red blood cells, mediated by their pore forming capabilities. In contrast, the *S. mansoni* HDM peptides did not cause red blood cell lysis at any of the tested concentrations and FhHDM-1p2 displayed only low level cell cytotoxicity (11.4%) when used at the

highest concentration (256μg/mL), which was much lower than the 70% lysis caused by BMAP-28 at the same concentration. Consistent with these findings was the demonstration of pore formation in the membrane of macrophages mediated by HDPs, but not by HDM peptides. This absent/lower cytotoxicity was hypothesised to be associated with the lower abundance of positive charges on the polar face of the HDM peptides, as compared to the HDPs tested[135].

With respect to their modulatory properties, the tested HDPs (even at low concentrations of 0.5μM) were capable of preventing TNF secretion by macrophages stimulated with LPS and IFNγ. However, HDMs were only capable of mimicking this effect when used at much higher concentrations (10-50μM) that in case of HDPs would be cytotoxic. But at these concentrations, HDMs were even more efficient than HDPs. HDPs as well as HDMs (with a lower potency) increased IgG1 production by B cells when exposed to LPS and IL-4 (a favourable environment for Th2 responses) and suppressed generation of IgG2 when exposed to LPS and IFNγ (Th1 biased environment) although again, HDMs were less efficient[135].

The conservation of biochemical and modulatory properties of HDPs by trematode secreted C-terminal HDM peptides, with a lack of bactericidal or parasiticidal abilities, suggest that HDMs are likely more specialised towards immune regulation.

1.5.1. A PROPOSED MECHANISM OF ACTION FOR FHHDM-1

Flow cytometry studies have elucidated a binding preference of FhHDM-1 to macrophages, of both murine and human origin, above other immune cell types (Lund, M. and McCauley-Winter, P. unpublished data). Apart from having general homeostatic roles including elimination of cellular debris and recycling, macrophages have important immunological functions. These cells are specialised in the internalisation, processing and presentation of antigenic material, and thus form an important link between innate and adaptive immune responses[17, 139-141]. Therefore, by selectively binding to macrophages, FhHDM-1 could potentially exert a profound effect in terms of immune regulation. Preliminary localisation studies indicated that a recombinant version of FhHDM-1 (RecFhHDM-1) interacted with primary human macrophages, presenting a peripheral distribution beneath the plasma membrane region. This was further supported by western blot analyses of membrane fractions, obtained from FhHDM-1 treated macrophages, where an interaction between the peptide and soluble

plasma membrane components was identified. Furthermore, the initial binding/association between FhHDM-1 and macrophages was found to be independent of surface macrophage proteins, as trypsinization did not abolish binding[114, 142]. Certain HDPs reportedly influence immune cell function by interacting with and/or penetrating cellular membranes. Once internalised, these peptides bind to intracellular molecules, which result in modulation of specific pathways[129, 143]. Global proteomics analysis of primary human macrophages treated with RecFhHDM-1 revealed a down-regulation of proteins associated with lysosomal function, including lysosomal membrane proteins, hydrolases and vacuolar ATPase subunits[142]. Further exploration into these findings suggested that FhHDM-1 down-regulates ATPase activity in endo-lysosome enriched membrane preparations[114].

Therefore, the hypothesis of the current study was that, similar to the mammalian HDPs, FhHDM-1 has intracellular targets, which impact upon the biological activity of macrophages. Accordingly, this study aimed to investigate if and how FhHDM-1 was internalised by macrophages and the subsequent effects on macrophage function. Elucidating the mechanism of action of FhHDM-1 will not only expand our understanding of the immune modulatory properties that this peptide is likely to have during *F. hepatica* infection, but will also determine potential therapeutic applications for FhHDM-1 in diseases where immune modulation would be a beneficial outcome.

CHAPTER 2 GENERAL MATERIALS & METHODS

Table 2. 1 General materials and reagents.

Product	Supplier
Glycine	AMRESCO (Ohio, USA)
Phosphate buffered saline (PBS)	
Tris	
Triton X100 (TX100)	
Sodium chloride (saline)	Baxter Healthcare (Illinois, USA)
Water for irrigation	
ELISA cytokine detection kits	BD Biosciences (North Ryde, Australia)
Mouse M-CSF	eBiosciences (California, USA)
Ficoll PaqueTM Plus	GE Health Care (Uppsala, Sweden)
DMEM	Life technologies-GIBCO® (California, USA)
Heat inactivated FBS	
HEPES	
IMDM	
Penicillin/Streptomycin	
RPMI 1640	
TrypLe^{TM} Express	
Auto MACS running buffer	Miltenyi Biotec (Bergisch Gladbach, Germany)
MACS Whole blood CD14+ Micro Beads human	
Tissue culture plastic ware	Nunc Thermo Scientific (Roskilde, Denmark) & BD Biosciences (Falcon)
2-Mercaptoethanol	SIGMA-ALDRICH (Missouri, USA)
Bovine serum albumin (BSA)	
Dimethyl sulfoxide (DMSO)	
Lipopolysaccharides (*Escherichia coli*)	
Paraformaldehyde	
Sodium azide (Az)	
Sodium bicarbonate ($NaHCO_3$)	
Sodium carbonate (Na_2CO_3)	
Tween 20	

2.1. Production of RecFhHDM-1, sFhHDM-1 and anti-FhHDM-1 antibody

Endotoxin-free recombinant FhHDM-1 (RecFhHDM-1) was prepared by expressing the native full-length peptide (lacking the N-terminal signal peptide and with the addition of a C-terminal His_6-tag) in *Escherichia coli*, as previously described[115]. The resultant recombinant peptide (9.2 kDa) was then purified and desalted using the Profinia protein purification system (BioRad, California, USA), and endotoxin was removed by RP-HPLC[115].

While these studies were in progress, a synthetic derivative analogue of FhHDM-1 (sFhHDM-1) became available, which was synthesised by GL Biochem (Shanghai, China). This synthetic equivalent of RecFhHDM-1 was identical to its recombinant counterpart in amino acid sequence, with the exception of a methionine that was absent in the N-terminal region, and the lack of the His_6-tag in the C-terminal. Due to these differences, sFhHDM-1 was slightly smaller (7.8 kDa) as compared to RecFhHDM-1.

A rabbit anti full-length RecFhHDM-1 polyclonal antibody was produced by Auspep (Victoria, Australia) and was used for detection of FhHDM-1, in both synthetic and recombinant forms.

For cellular analysis, an Alexa 488 conjugate of sFhHDM-1 was prepared. The Alexa 488 amine reactive probe (Life Technologies), supplied as 1mg lyophilised sample, was resuspended in 100µL DMSO to yield a 10mg/mL working solution. According to the manufacturer's instructions, the peptide solution was required to have a 10-fold molar excess of dye; therefore to 1428.75µL of FhHDM-1 (1mg/mL in water for irrigation; Baxter Healthcare) a 1/10 dilution of 1M sodium bicarbonate was added to reach pH 8 and to this solution, 100µL of dye was added slowly with simultaneous vortexing. This mixture was incubated overnight (O/N) on a spinning wheel at room temperature (RT) and protected from light, to allow conjugation to proceed. The labelled FhHDM-1 was transferred into two eppendorf tubes, which were capped with dialysis tubing (3500MW cut-off) and the solution was dialysed against saline for 24h at 4°C on a magnetic stirrer, with solvent changes occurring at 3h, 6h, and O/N.

2.2. Cell culture

2.2.1. STERILITY

All cell culture and primary macrophage isolation procedures were performed in a class II biological safety hood. Media and plasticware were sterile and aseptic technique was applied in all instances.

2.2.2. CELL LINES

2.2.2.1. RAW264.7 MACROPHAGES

Murine RAW264.7 macrophages (obtained from the American Type Culture Collection [ATCC], Virginia, USA) used in experiments were of low passage number (between 19 and 22) and were maintained in Roswell Park Memorial Institute (RPMI) 1640 medium supplemented with 10% v/v heat inactivated (HI) foetal bovine serum (FBS). Cells were cultured at 37ºC/5% CO_2. Microscopy was utilised to determine confluency and when this reached 80-90% (which occurred approximately every 3 days), cell monolayers were washed twice with cold sterile PBS, scraped into fresh medium/FBS and split 1 in 8. Sufficient medium was added to maintain a total volume of 20mL per 175cm^2 tissue culture flask.

2.2.2.2. ASC MACROPHAGES

ASC macrophages (immortalised macrophages stably transfected with a construct overexpressing cerulean-tagged murine apoptosis associated speck like protein [ASC] and NLRP3-Flag) were kindly donated by Dr V. Hornung (University of Bonn, Germany). Cells of a low passage number were used for experiments and were maintained in DMEM supplemented with 10%v/v HI FBS and 20mM HEPES buffer. Cells were cultured at 37ºC/5% CO_2. When cell monolayers reached 80% confluency, they were washed twice with cold sterile PBS, 5mL of TrypLe^{TM} Express was added, and cells were incubated for 5min at 37ºC/5% CO_2 to allow detachment. Flasks were tapped to achieve complete cell detachment, and 20mL of media was added to stop trypsin activity. Cells were split 1 in 5 and sufficient medium was added to maintain a total volume of 20mL per 175cm^2 tissue culture flask.

2.2.3. PRIMARY CELLS

2.2.3.1. MURINE BONE MARROW-DERIVED MACROPHAGES (BMDMS)

2.2.3.1.1. Isolation of bone marrow cells

BALB/c or C57BL6 mice (6-8 weeks old; Animal Resources Centre [ARC], Perth, Australia) were sacrificed by CO_2 asphyxiation and sprayed with 70% ethanol. Femurs and tibias were dissected and the bone marrow was flushed with media (RPMI 1640 medium supplemented with L-Glutamine, 10%v/v HI FBS and 50µM 2-mercaptoethanol) into a petri dish using a 21-gauge syringe. Single cell suspensions were obtained by aspirating the Petri dish contents using a 19-gauge syringe and cells were transferred to a 50mL falcon tube. Cells were collected by centrifugation (400*g*, 5 min). All animal procedures were performed in accordance with approvals from the UTS Animal Care and Ethic Committee (ACEC; ARA numbers 2012-080A and 2013-075 for BALB/c and C57BL/6 mice, respectively).

2.2.3.1.2. Differentiation of Bone Marrow-Derived Macrophages

Cells were counted, resuspended, and plated at a concentration of $2x10^7$/10mL in media (RPMI 1640 medium supplemented with L-Glutamine, 10%v/v HI FBS, 50µM 2-mercaptoethanol, 50ng/mL macrophage-colony stimulation factor [M-CSF; eBiosciences]). Cells were incubated at 37ºC/5% CO_2. On the third day, 10mL of fresh medium, supplemented with 50ng/mL M-CSF, was added to each dish. BMDMs were harvested on the sixth day by decanting media, washing twice with PBS (RT), and scraping cells into fresh medium. Routinely, the cell populations were >95% $CD11b^+$, as determined by labelling with CD11b MicroBeads (Miltenyi Biotec) and flow cytometry analysis using PE Cy7-anti-mouse CD11b clone M1/70 antibody (BD Pharmingen, North Ryde, Australia; Section 2.4).

2.2.3.2. HUMAN MONOCYTE ISOLATION AND MACROPHAGE DIFFERENTIATION

Under aseptic conditions, 25mL of buffy coat blood (Red Cross, Sydney, Australia) was transferred to two 50mL falcon tubes and diluted 1 in 2 with RPMI 1640. Ficoll (15mL) was added to three 50mL falcon tubes. Using a serological pipette, 35mL of the diluted blood was slowly transferred into each of the tubes containing Ficoll, ensuring that two distinct layers were retained. Tubes were centrifuged (400*g* for 30 min, RT), ensuring that the acceleration and de-acceleration were sufficiently slow to avoid mixing of the layers. After centrifugation, the samples separated into the

following layers: serum (top layer), white blood cells, Ficoll and red blood cells (bottom layer). The white blood cells from each of the three tubes were transferred into a new 50mL falcon tube using a plastic pasteur pipette, ensuring the surrounding Ficoll and serum layers were not collected. White blood cells were washed three times with RPMI 1640 and collected after each wash by centrifugation (400*g*, 7 min, RT). Then, 25mL of autoMACS running buffer (supplemented with 1%v/v FBS) was added and a cell count was performed using a Neubauer counting chamber. Cells were centrifuged once more (400*g*, 7 min, RT), and the pellet was resuspended in running buffer (80µL per 10^7 cells). CD14+ MicroBeads (Miltenyi Biotec) were also added (20µL per 10^7 cells) and the cells were incubated for 15 min/4ºC, washed with running buffer (1-2mL per 10^7 cells), and collected by centrifugation (400*g*, 7 min, RT). The pellet was resuspended in running buffer (500µL per 10^8 cells).

Magnetic separation was performed using an AutoMACS pro-separator unit (Miltenyi Biotec), according to the manufacturer's instructions. The separated cells (monocytes) were counted, centrifuged (400*g*, 7 min, RT) and resuspended in Iscove's Modified Dulbecco's Medium (IMDM) supplemented with 2% v/v human serum (to a concentration of $1x10^6$ cells/mL) and seeded into plates or flasks, according to experimental requirements. Cells were incubated at 37ºC/5% CO_2 for 6 days to allow differentiation of monocytes into macrophages.

2.3. Immunofluorescence Confocal Microscopy

Macrophages were seeded in 35mm Fluorodish cell culture dishes (World Precision Instruments, Florida, USA) at a density of 10^6 cells in RPMI medium, supplemented with 10% v/v FBS and 2% v/v penicillin/streptomycin, and allowed to adhere for at least 1h (37ºC/5% CO_2). Samples were treated according to the specific experimental protocols (which involved incubation with 10µg/mL RecFhHDM-1, at 37ºC/5% CO_2 for 45min, unless otherwise specified). Then cells were washed and fixed with 4%w/v paraformaldehyde for 30min/RT. When internal staining was required, cells were permeabilised using 0.1% v/v Triton X 100, followed by quenching of excess aldehyde with 100mM glycine. This was followed by blocking with 2%v/v FBS and 0.1%v/v Tween20 O/N. Samples were incubated with appropriate primary antibodies, diluted in blocking solution, for 1-2h at RT. Cells were then washed and incubated with

appropriate Alexa Fluor 568 or Alexa Fluor 488 conjugated secondary antibodies, diluted 1:1000 in blocking solution for 1h at RT. Cells were also stained for actin/plasma membrane detection using 1:60 Phalloidin Alexa Fluor 647, and 3% DAPI was used to identify nuclei. Details of the antibodies and dyes used for microscopy studies appear in Table 2.2. Samples were mounted in antifade n-propyl gallate (NPG) antifade mounting solution (Section 2.3.1), and then viewed using a Nikon A1 confocal scanning laser microscope (Nikon, New York, USA), which was set up using unstained and control samples to stablish threshold fluorescence detection levels. Presented images, analysed using NIS Elements software (Nikon), correspond to optical sections through the centre of macrophage cells.

Table 2.2 List of antibodies and dyes used for confocal microscopy experiments.

Antibody (Ab) or Dye	**Concentration**	**Supplier**
Polyclonal rabbit anti-RecFhHDM-1 antibody	1:1000	Auspep (Victoria, Australia)
Monoclonal mouse anti-caveolin-1 [7C8] antibody	1:500	Abcam (Cambridge, England)
Polyclonal rabbit anti-giantin (Golgi apparatus marker) antibody	1:500	
Polyclonal rabbit anti-Rab5 (Early endosome marker) antibody	1:1500	
Monoclonal mouse anti-tubulin antibody	1:100	Life Technologies
4',6-Diamidino-2-Phenylindole, Dihydrochloride (DAPI)	3% (v/v)	Molecular Probes® Life Technologies (California, USA)
Alexa Fluor 647 phalloidin	1:60	
Goat anti-mouse and goat anti-rabbit Alexa Fluor 568 highly cross-adsorbed antibodies	1:1000	
Goat anti-mouse and goat anti-rabbit Alexa Fluor 488 highly cross-adsorbed antibodies	1:1000	
LysoTracker Red DND-99	60nM	
MitoTracker Red FM	50nM	
Recombinant Cholera Toxin Subunit B conjugated to Alexa Fluor 594	4µg/mL	
Monoclonal anti penta-his tag BSA free antibody	1:2000	Qiagen (Limburg, Netherlands)

2.3.1. NPG ANTIFADE MOUNTING MEDIA PREPARATION

In a 50mL falcon tube, 5mL of 0.2M TRIS (pH 8.5), 43mL of glycerol and 2.5g of n-propyl gallate (Sigma) were added. The tube was wrapped in foil to protect it from light and spun on a spinning wheel O/N at 4°C to allow contents to dissolve. The resultant NPG solution was stored at 4°C until use.

2.4. Flow Cytometry

Samples used for flow cytometric studies contained 0.5-1x10^6 cells per Eppendorf tube (as described in Sections 2.2.3.1.2 and 4.2). For all experiments, an unstained or isotype control, as well as single colour controls for each dye, were included. Samples were kept at 4°C at all times (unless otherwise specified). Cells were collected by centrifugation (400*g*, 5min) and washed twice with FACS buffer (PBS, 1% BSA, 2% FBS, and 0.05% Az). Then, each sample to be stained was resuspended in 20µL of this buffer with 1µL of Fc block, and incubated for 5min at RT. After this, samples were supplemented with 50µL FACS buffer and 1µL of the corresponding antibody, and incubated for 20min/4°C protected from light. Cells were then washed twice with 700µL FACS buffer, resuspended in 500µL FACS buffer, and transferred to flow cytometry tubes. To assess cell viability, 1µM SYTOX blue dead cell stain (Molecular Probes) was added per sample immediately before flow cytometric analyses using the BD LSR II Flow Cytometer System (BD Biosciences).

2.5. ELISAs

Levels of various secreted cytokines were detected in cell culture supernatants using appropriate ELISA kits, following the manufacturer's instructions. Briefly, 96 well plates were coated O/N with primary antibody diluted in coating buffer (0.84g $NaHCO_3$ and 0.356g Na_2CO_3). Then, plates were washed three times with 0.1% Tween 20/PBS and blocked with assay diluent (PBS, 10% FBS at pH7) for 1h/RT. This was followed by three washes, prior to the addition of standards and samples (which were incubated for 2h/RT). Plates were washed five times and incubated with working detector (detector antibody plus 1 in 250 of Sav-HRP reagent diluted in assay diluent, 1h/RT; except for TNF and IL-1β assays where detector antibody and Sav-HRP reagent were added in independent incubations). Plates were washed seven times and

Tetramethylbenzidine (TMB) Liquid Substrate System (Sigma) was added until colour developed, the reaction was stopped with 2 N H_2SO_4 (Sigma). Absorbances were read at 450nm with a 570nm correction, using the Tecan 'Infinite® M200 Pro' Quad-monochromator multifunction plate reader (Tecan, Mannedorf, Switzerland). Obtained optical density values were analysed using GraphPad Prism software (GraphPad Software Inc., California, USA).

2.6. Statistical Analysis

The arithmetic mean readings of triplicate samples +/- the standard errors of the means (SEMs) were utilized to construct graphical representations of experimental data presented in this thesis. Statistically significant differences amongst sample treatments were determined using the GraphPad Prism software version 6 and applying the most appropriate statistical test(s) according to the characteristics of each experiment (described in specific methods sections of each chapter and/or corresponding figure legends). In general, when only two groups of repeated measures were being compared, student t-tests were applied, and a $p \leq 0.05$ was considered significant. When three or more groups of repeated measures were compared, initially an ordinary one-way ANOVA test was applied to validate the presence of a significant difference(s) amongst the sample groups being analysed. This was followed by a Dunnett's post-test, to further assess the significance of the effects that a given treatment had on the mean of a sample group when compared to the mean of the experimental control group.

CHAPTER 3 CHARACTERISATION OF THE INTERACTION BETWEEN FHHDM-1 AND MACROPHAGES

3.1. Introduction

In addition to their bactericidal activity, mammalian cathelicidins play important modulatory roles in innate immunity, in certain instances resulting in the inhibition of pro-inflammatory responses directed by both macrophages and DCs[125, 134, 136, 144-147]. In order to exert their immune-modulatory activity, cathelicidins must first be internalised[148]. Although the mechanism(s) by which this occurs is yet to be fully elucidated, studies suggest that this process is mediated by the binding of these peptides to putative surface receptors[149] and/or via atypical endocytic pathways[148, 150], followed by interaction with intracellular receptors (for example GAPDH in case of LL-37[143]).

The observed binding preference of FhHDM-1 to macrophages (Lund, M. and McCauley-Winter, P. unpublished data), the electrostatic interaction/localization of the peptide with non-protein components of the plasma membranes of these cells, in addition to the structural homology between this peptide and the human cathelicidin, LL-37, makes it plausible that analogous to LL-37, FhHDM-1 requires internalisation by macrophages to be able to putatively modulate the intracellular signalling pathways of these cells[114, 142].

Further, it has been reported that FhHDM-1 binds to phospholipid membranes modelled *in vitro*, in a manner dependent upon the amphipathicity of the alpha-helical structure, as demonstrated by the use of a mutated version of the peptide, in which the hydrophobic phase had been abolished[114]. The amphipathic alpha-helical structure shared by FhHDM-1 and cathelicidins, is also typical of a class of molecules known as 'carrier peptides'[151, 152]. The amphipathic helix enables carrier peptides to anchor to cellular membranes via rearrangement of their hydrophobic amino acid side chains, towards the outer membrane face. This facilitates their interaction with membrane lipids, whilst simultaneously isolating their hydrophilic side chains towards the peptide's core regions[153]. After this anchoring to the plasma membrane of the target takes place, subsequent internalisation of carrier peptides (containing the cargo that they transport), occurs via endocytosis[152, 154]. Therefore, their structural homology suggests

that, in a similar way to carrier peptides, the amphipathic alpha-helical region of FhHDM-1 could potentially lead to the internalization of this peptide by macrophages.

Understanding the processes of initial cellular interaction, subsequent internalisation, and ultimate intracellular localisation of FhHDM-1 will be critical to determining the mechanisms by which FhHDM-1 may putatively modulate the function of macrophages. More broadly, this information may also enhance our understanding of the mechanisms of action of mammalian cathelicidins, which are structurally homologous to FhHDM-1.

3.2. Specific methods

3.2.1. CHOLESTEROL BINDING ASSAY

As previously described by Hutchinson *et al.*[155], a PolySorp 96 well ELISA plate (Nunc Thermo Scientific) was coated with 10µg cholesterol (100µL of 100µg/mL stock prepared using 70% ethanol; Avanti Polar Lipids, Alabama, USA), or an equivalent volume of 1% w/v BSA in PBS as a control for binding specificity. After drying O/N under N_2 gas, wells were blocked with 100µL of 1% w/v BSA/PBS for 1h at 37°C, and then washed three times using 200µL of 0.1% w/v BSA/PBS. Doubling dilutions of FhHDM-1 in 0.1% w/v BSA/PBS (ranging from 0-20µg/mL) were prepared and aliquots (100µL) were added to wells previously coated with cholesterol or BSA, in triplicate, and incubated for 2h at 37°C. The plate was washed, 100µL of rabbit anti-FhHDM-1 polyclonal antibody (1:1000 in 0.1% w/v BSA/PBS) was added to the wells, and the plate was incubated for 75min at 37°C. The plate was then washed and incubated with 100µL of anti-rabbit alkaline phosphatase conjugated antibody (Sigma), diluted 1:10000 in 0.1% w/v BSA/PBS, for 45min at 37°C. The plate was washed and 200µL of pNPP substrate (Sigma) was added and absorbances were read after 1h at 405nm in a Tecan 'Infinite® M200 Pro' Quad-monochromator multifunction plate reader. The obtained data was represented in graphical format using arithmetic mean optical density readings +/- the standard errors of the means (SEMs). In order to detect a statistically significant pattern in change in variance between the corresponding binding curves of FhHDM-1 to cholesterol or to control BSA, a Linear Mixed Model with a Residual Maximum Likelihood algorithm (RELM) was applied, and a $p \leq 0.05$ was considered significant.

3.2.2. IMMUNOFLUORESCENT CONFOCAL MICROSCOPY

3.2.2.1. CO-LOCALISATION OF FHHDM-1 WITH LIPID RAFTS

RAW264.7 macrophages (10^6 cells) were untreated (for cholera toxin binding controls) or incubated with RecFhHDM-1 (10µg/mL) in media at 37°C/5% CO_2 for 45min. Lipid rafts were stained using cholera toxin subunit B Alexa 594 conjugate, which binds to glycosphingolipids, at a concentration of 4µg/mL for 20min at 4°C. Cells were then fixed and stained with anti-penta-his tag monoclonal antibody (1:2000), anti-mouse Alexa 488-conjugated secondary antibody (1:1000), and 3% DAPI was used

for identification of nuclei. Staining of the untreated control with the primary and secondary antibodies was used to assess their specificity towards the identification of the His-tag of RecFhHDM-1. Images were analysed using a 100x objective in the Nikon A1 confocal microscope (Nikon, New York, USA) and NIS software (Nikon). This experiment was also performed using primary human macrophages. The only experimental parameters differing in this instance were that the incubation with RecFhHDM-1 was for 2h (as opposed to 45min) and images were analysed using a Delta Vision OMX 3D-structured illumination microscope, version 3 (OMX 3DSIM; Applied Precision Inc., Washington, USA). Images were reconstructed using IMARIS version 7 software (Bitplane Scientific, Zurich, Switzerland). Table 2.2 provides further information regarding the antibodies and dyes used in these experiments.

3.2.2.2. INHIBITOR STUDIES

RAW264.7 macrophages (10^6 cells) were treated with the following inhibitors at 37ºC/5% CO_2: cytochalasin D (2µg/mL, 30min) (Sigma) to block polymerisation of actin filaments; nocodazole (2µg/mL, 30min) (Sigma) to inhibit microtubule polymerisation; or methyl-β-cyclodextrin-MCD (1mM, 30min) (Sigma) to deplete cholesterol[148, 150]. The samples were then treated with 10µg/mL RecFhHDM-1 (without inhibitor removal) and incubated for a further 45min at 37ºC/5% CO_2. Uptake controls were included in the absence of inhibitors by incubating cells with FhHDM-1 at 4°C or 37°C. Samples were then prepared for confocal microscopy (as described in Section 2.3) and analysed using a 100x objective in the Nikon A1 confocal microscope and NIS software. RecFhHDM-1 identification was achieved using a 1:1000 dilution of anti-RecFhHDM-1 polyclonal antibody and microtubules were detected using anti-tubulin antibody diluted 1:100. Macrophages from a vehicle (PBS) only control were also stained to assess antibody specificity for RecFhHDM-1 His tag detection. Table 2.2 provides further information regarding the antibodies and dyes used in these experiments.

3.2.2.3. CO-LOCALISATION OF FHHDM-1 WITH ORGANELLE MARKERS

3.2.2.3.1. Localisation of FhHDM-1 with caveolae, Golgi and mitochondria

RAW264.7 macrophages ($7x10^5$ cells) were left untreated (for organelle staining controls) or incubated with RecFhHDM-1 (for localisation with caveolae) or sFhHDM-1 conjugated with Alexa 488 (for localisation with Golgi and mitochondria) at a

concentration of 10µg/mL, 37°C/5% CO_2 for 45min. For mitochondrial staining, simultaneous incubation with 50nM MitoTracker 568 in media was performed[156]. Cells were then prepared for microscopy, as outlined in Section 2.3 and analysed using a 100x objective in the Nikon A1 confocal microscope and NIS software. The primary antibodies used were as follows: anti-RecFhHDM-1 polyclonal antibody (1:1000), anti-caveolin-1 monoclonal antibody (1:500) for caveolae detection, and anti-giantin polyclonal antibody (1:500) for Golgi detection. Omission of primary antibody controls were included for these experiments and in case of FhHDM-1 antibody detection, untreated controls were also stained with anti-RecFhHDM-1 and anti-rabbit Alexa 488 antibodies, to ascertain their specificity. Table 2.2 provides further information regarding the antibodies and dyes used in these experiments. As stated in Section 2.1 sFhHDM-1 started being synthesised while the current study was in progress. Therefore, from this point onwards, this synthetic version of the peptide was included in experiments to enable comparisons with RecFhHDM-1, and once its functional homology was well stablished, sFhHDM-1 was preferentially used due to its higher degree of purity and availability.

3.2.2.3.2. Temporal localisation of FhHDM-1 with early endosomes

RAW264.7 macrophages ($7x10^5$ cells) were incubated with sFhHDM-1 conjugated with Alexa 488 (10µg/mL) for a period of 5, 15, 30 and 45 min, at 37°C/5% CO_2, fixed, and prepared for microscopy, as detailed in Section 2.3, followed by analysis using a 100x objective in the Nikon A1 confocal microscope and NIS software. Anti-Rab5 polyclonal antibody (1:1500) was used for the detection of early endosomes. Treatment with vehicle only and the omission of this primary antibody provided negative and antibody specificity controls, respectively. Furthermore, an untreated control was also stained for detection of resting endosomes. Table 2.2 provides further information regarding the antibodies and dyes used in these experiments.

3.2.2.3.3. Temporal localisation of FhHDM-1 with late endosomes/lysosomes

RAW264.7 macrophages ($7x10^5$ cells) were incubated with 60nM of LysoTracker 568 for 1h at 37°C/5% CO_2. Cells were then incubated with sFhHDM-1-Alexa 488 conjugate (10µg/mL) in media for a period of 15, 30 or 45min (37°C/5% CO_2), fixed, and prepared for microscopy (Section 2.3), followed by analysis using a 100x objective in the Nikon A1 confocal microscope and NIS software. Table 2.2

provides further information regarding the antibodies and dyes used in these experiments.

For quantitation purposes, the experiment was repeated by incubating BALB/c BMDMs (Section 2.2.3.1) with sFhHDM-1-Alexa 488 conjugate (10µg/mL) or *E. coli* (K-12 strain) BioParticles-Alexa Fluor 488 conjugated (as positive control; 12µg/mL) (Molecular Probes) for 30min only, followed by three washes with PBS (RT). These samples, as well as an untreated control sample, were stained with 60nM of Lysotracker for 30 min, at 37°C/5% CO_2 and washed twice. Then 1mL of phenol-free RPMI media supplemented with 10% v/v FBS was added to each cell culture dish. Sample treatments and staining were staggered so that immediate live cell imaging on the Nikon A1 confocal microscope could be performed. An average of 150 cells were imaged per sample treatment. Co-localisation was performed visually by the presence of intracellular yellow/orange fluorescence. Arithmetic mean values for percentage of cells presenting Lysotracker, sFhHDM-1-Alexa 488 or *E. coli*-Alexa 488 fluorescence, detected per field of view, +/- SEMs were used for graphical representation of data.

3.3. Results

3.3.1. FhHDM-1 BINDS TO CHOLESTEROL AND INTERACTS WITH LIPID RAFTS

It has been reported that RecFhHDM-1 co-localised with the plasma membrane of macrophages, most likely via interaction with non-protein components[114, 142]. Cholesterol is an abundant lipid present in cellular plasma membranes[157] and FhHDM-1 contains the cholesterol binding motif, L/V-[X]1-5-Y-[X]1-5-R/K, spanning residues V45TKAYEKAR53[114]. Therefore, a cholesterol-binding assay was performed to determine if sFhHDM-1 was capable of associating directly with this lipid. An ELISA plate coated with a cholesterol monolayer was utilised to detect the binding of serially diluted sFhHDM-1. Threshold binding levels, attributable to non-specific binding of sFhHDM-1 to BSA, were established (Figure 3.1 A). The binding of sFhHDM-1 to cholesterol was found to be both specific and concentration dependent, until saturation was reached at a sFhHDM-1 concentration of 5µg/mL. Furthermore, RELM statistical analysis indicated that the difference between the obtained binding curves (sFhHDM-1 to cholesterol versus sFhHDM-1 to BSA) was statistically significant ($p= 0.021$).

Lipid rafts constitute micro domains in the plasma membrane, which are rich in cholesterol and glycosphingolipids[158]. Given the capacity of sFhHDM-1 to bind cholesterol, confocal microscopy was employed to determine if FhHDM-1 interacted directly with lipid rafts within the plasma membrane of RAW 264.7 macrophages. Cells were incubated with RecFhHDM-1 for 2h and an antibody, specific for the His-tag in the C-terminal of RecFhHDM-1, was utilised for its visualisation. Cholera toxin-Alexa594, which binds specifically to the glycosphingolipid ganglioside, GM-1[159], was used for lipid raft identification. RecFhHDM-1 was found to co-localise with cholera toxin, indicating that binding was occurring in the subregion of lipid rafts within the macrophage membrane (Figure 3.1 D). Furthermore, analyses by super resolution OMX microscopy revealed that the co-localisation between RecFhHDM-1 and lipid rafts also occurred when RecFhHDM-1 was incubated with primary human macrophages (Figure 3.1 F), thereby confirming the interpretation of confocal microscopy studies (Video 3.1, supplementary data), and corroborating the localisation pattern observed for murine macrophages.

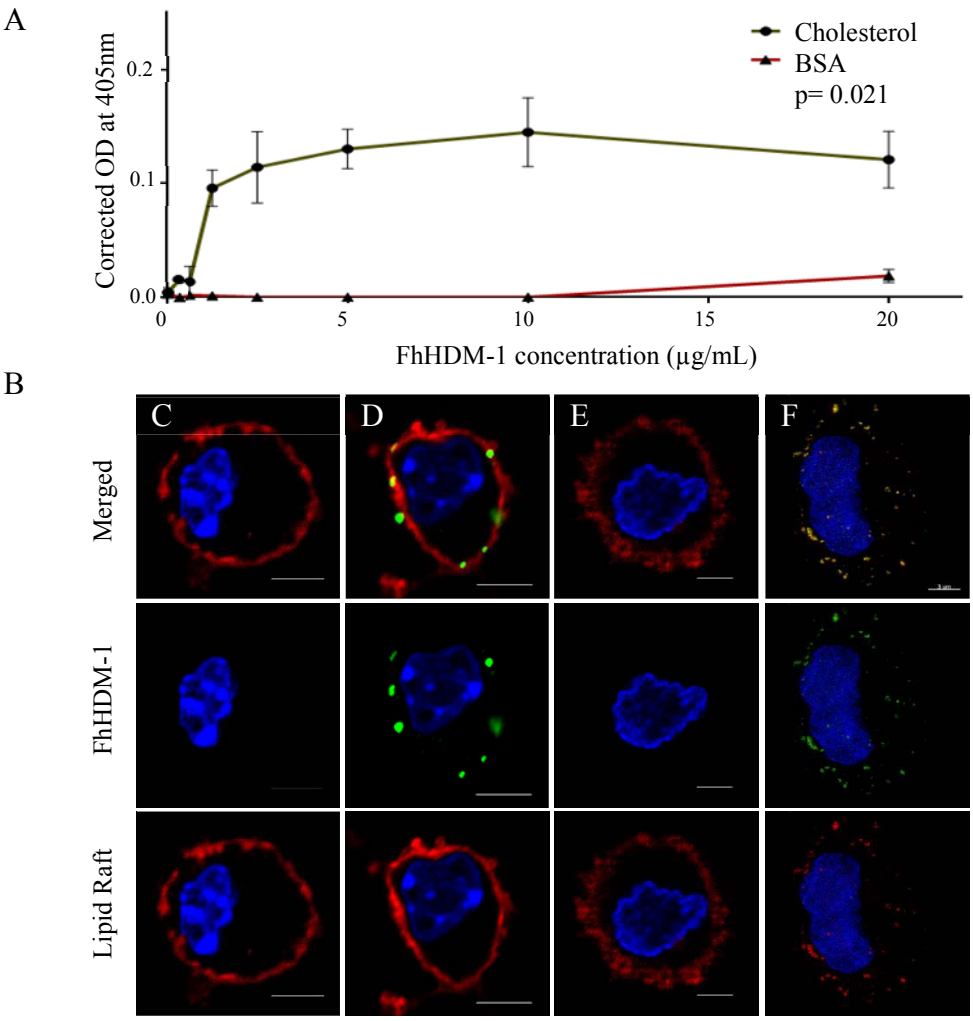

Figure 3.1 FhHDM-1 binds to cholesterol and co-localises with lipid rafts in the plasma membranes of macrophages. A. Triplicate cholesterol or BSA coated wells of an ELISA plate were incubated with two fold dilutions (from 0 to 20µg/mL) of sFhHDM-1. Binding was detected using anti-RecFhHDM-1 and alkaline phosphatase conjugated antibodies. Graphical representation of optical densities (OD) means +/- SEM (statistically analysed using RELM) are provided. B. Representative single plane (C-E) or 3D collapsed (F) immunofluorescent images, obtained by confocal or OMX super resolution microscopy, respectively, of murine RAW264.7 (C & D) and primary human (E & F) macrophages. Macrophages were incubated with RecFhHDM-1 (D & F), which was identified by His tag detection, using an Alexa 488 (green) conjugated antibody (D & F; yellow fluorescence in top panels corresponds to co-localisation). Untreated samples (C & E) were also fully stained and acted as controls for antibody specificity. Cells were stained with cholera toxin subunit B (red) and DAPI (blue) to identify lipid rafts and nuclei, respectively. (Scale bars: C-E: 5µm; F: 3µm). The presented data is representative of two individual experiments for each, A & B.

3.3.2. FhHDM-1 IS ACTIVELY ENDOCYTOSED BY A CYTOSKELETAL-DEPENDENT MECHANISM

To determine whether FhHDM-1 was subsequently internalised after its interaction with plasma membranes, murine macrophages were incubated with RecFhHDM-1. Localisation of RecFhHDM-1 (using an antibody raised against full-length RecFhHDM-1[115]) revealed that within 45min RecFhHDM-1 localised to the cytoplasmic region of macrophages, resulting in a granular pattern of intense fluorescence (Figure 3.2). The intracellular distribution of RecFhHDM-1 was closely associated with both actin and microtubules, suggesting that these cytoskeletal networks were involved in RecFhHDM-1 transportation within the cytoplasmic region.

To determine if the observed uptake of FhHDM-1 was an active or a passive process, macrophages were incubated with RecFhHDM-1 at 37ºC or 4ºC, respectively (Figure 3.3 B & C). Immunofluorescence staining using anti-RecFhHDM-1 antibody indicated that at 37ºC FhHDM-1 was localised to the cytoplasmic region, where it formed aggregates of bright fluorescence, which were not observed at 4ºC. When localisation studies were performed at this lower temperature, most of the fluorescence was detected in close proximity with the plasma membrane, which was visualised by phalloidin staining, confirming specific binding without internalisation. Taken together, this data indicated that RecFhHDM-1 internalisation was attributable to an active process.

Internalisation of extracellular molecules by macrophages typically occurs by endocytosis, a mechanism by which internal membranes are formed using plasma membrane constituents, resulting in the uptake of extracellular contents within regions of the phospholipid bilayer[160]. Endocytic pathways are classified as being either clathrin-dependent or clathrin-independent (also known as alternative endocytosis). While the former pathway has been well studied, many aspects of the latter are yet to be elucidated. The alternative endocytic pathways can be further sub-classified to include caveolae-dependent endocytosis, the clathrin-independent non-caveolar (CLIC) pathway, phagocytosis, and macropinocytosis amongst others[160]. Phagocytosis is the most common pathway by which macrophages effectively internalise larger molecules, such as pathogens and apoptotic bodies[160, 161]. However, clathrin-dependent endocytosis accounts for the internalisation of a significant proportion of smaller molecules[160].

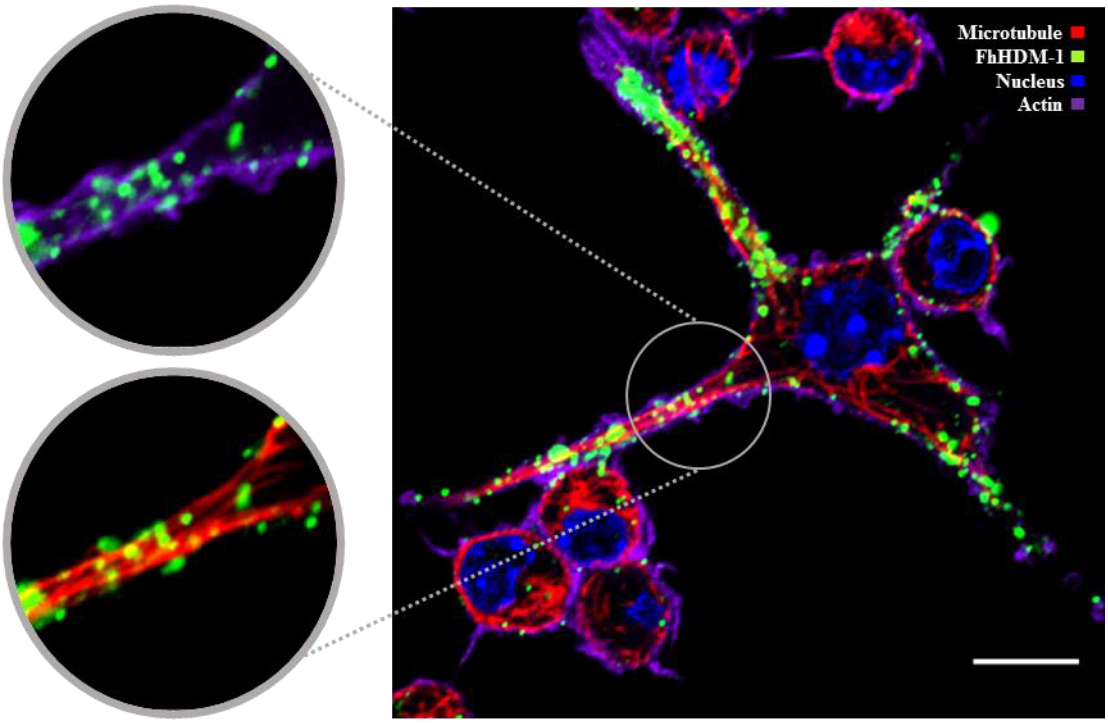

Figure 3.2 FhHDM-1 is internalised by macrophages and localises in close proximity to cytoskeletal networks. Representative immunofluorescence images obtained by confocal microscopy of murine RAW264.7 macrophages that were incubated with RecFhHDM-1 (for 45min at 37°C), which was identified using anti-RecFhHDM-1 and Alexa 488 primary and secondary antibodies, respectively (green fluorescence). Cells were stained with anti-tubilin and Alexa 568 antibodies (red fluorescence) for microtubule detection, and with phalloidin (violet) and DAPI (blue) for actin network and nuclear identification, respectively (100X objective; Scale bar: 5µm).

Given the relatively small molecular size of FhHDM-1 (~8 kDa)[115] and its cytoplasmic distribution observed in the current study, it was proposed that the uptake of FhHDM-1 likely occurred via clathrin-dependent endocytosis. This premise was corroborated by two observations: (i) the preferential binding of FhHDM-1 to cholesterol, which is essential for the formation of clathrin coated pits and all currently characterised endocytic pathways[162], and, (ii) the localisation of FhHDM-1 in close proximity of both actin (which enables the movement of cargo containing clathrin coated pits)[162] and microtubule networks (which allows the motility of the endocytotic vesicles, early endosomes, for their rapid maturation into late endosomes and lysosomes)[163].

Accordingly, the uptake and internalisation of RecFhHDM-1 was assessed in the absence of cholesterol. Cholesterol depletion was achieved by incubating macrophages with the glucose oligomer, methyl-β-cyclodextrin (MCD), which gently removes cholesterol by sequestering the lipid within its hydrophobic core, thereby increasing the solubility of the resultant cholesterol complexes[164]. This inhibitor was selected because alternative cholesterol depleting agents, such as nystatin, were found to be too potent, resulting in membrane damage and cell death. In contrast, the morphology of macrophages observed after MCD treatment indicated that negligible cell damage was induced. Incubation of macrophages with MCD, prior to incubation with RecFhHDM-1, did not prevent the localisation of FhHDM-1 within areas of the plasma membrane (Figure 3.3 D). However, this treatment did inhibit the internalisation of RecFhHDM-1 into cytoplasmic regions of macrophages.

The fungal toxin, cytochalasin D, inhibits actin polymerisation by binding to F-actin filaments, thereby halting their extension and/or shortening them, which prevents the cross-linking of individual filaments[165]. In the presence of cytochalasin D, an abnormal distribution of actin was observed within macrophages, in which actin co-localised with RecFhHDM-1 (Figure 3.3 E). A similar result was observed when microtubules were depolymerised by pre-incubating macrophages with nocodazole, which stimulated the contraction of microtubule networks, as observed by the use of an anti-tubulin antibody. This resulted in RecFhHDM-1 being trapped between the plasma membrane and the microtubule ring that was formed (Figure 3.3 F). Identical trends were observed when these experiments were performed using sFhHDM-1 conjugated to

Alexa 488. These data suggest that FhHDM-1 internalisation into the cytoplasmic region of macrophages occurs as a result of an active, cholesterol-, actin- and microtubule-dependent process. Furthermore, these data suggested that sFhHDM-1 and Rec-FhHDM-1 were analogous in function (just as they had been shown to be in structure) because the recombinant and synthetic versions of the peptide exhibited similar intracellular localisation patterns when incubated with macrophages.

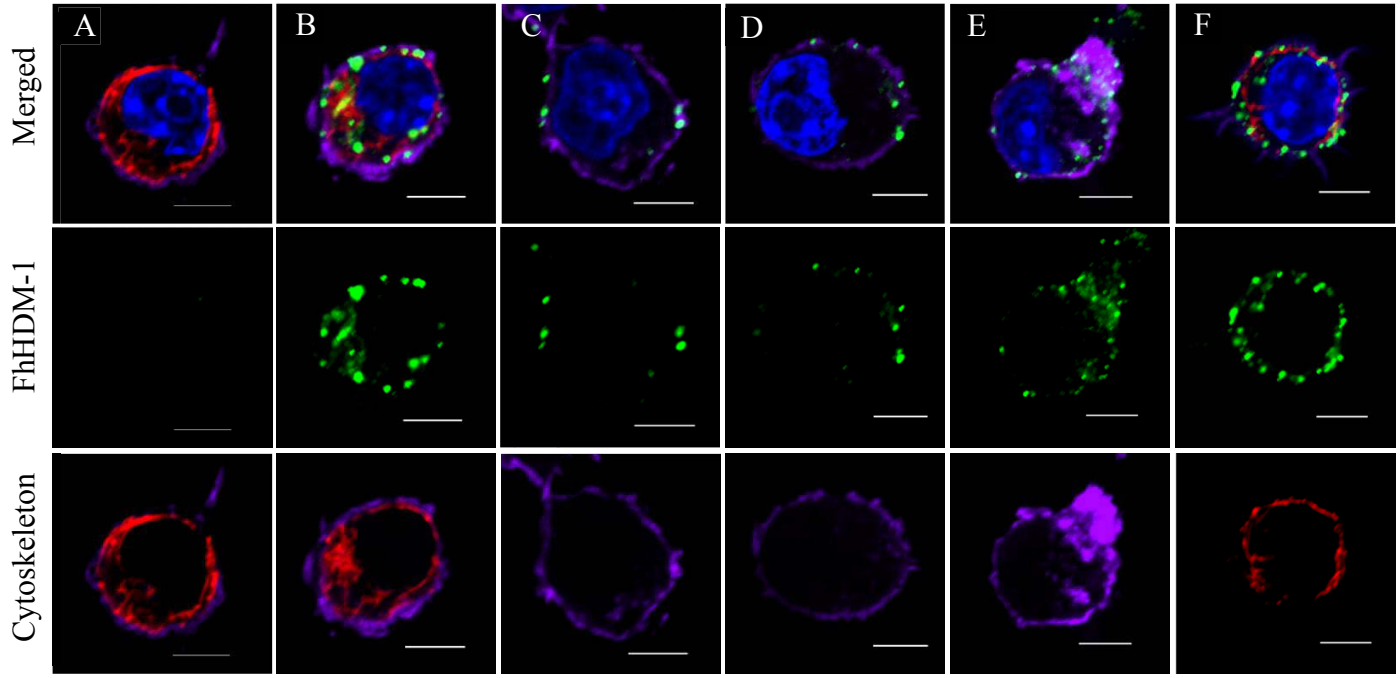

Figure 3.3 Internalisation of FhHDM-1 by macrophages is an active process dependent upon cholesterol, as well as actin and microtubule networks. Representative immunofluorescence images obtained by confocal microscopy of RAW264.7 macrophages that were untreated (A) or incubated with RecFhHDM-1 for 45min at 37°C (B, D-F) or 4°C (C). Additionally, samples were incubated with the cholesterol depleting agent, methyl-β-cyclodextrin (MCD) (D), or pre-incubated with the inhibitors cytochalasin D (E) or nocodazole (F), which block actin polymerisation and induce microtubule depolymerisation, respectively. Cells were stained with anti-RecFhHDM-1 (A; antibody specificity control & B-F) and anti-tubulin antibodies (A & F) that were detected with Alexa 488 (green) and 568 (red) conjugated antibodies, respectively. Actin networks and nuclei were identified using phalloidin (violet) and DAPI (blue) staining, correspondingly (100X objective; Scale bar: 5µm). Provided images represent cells in triplicate fields of view collected for each sample and the experiment was performed twice.

3.3.3. ENDOCYTOSIS OF FHHDM-1 INVOLVES EARLY ENDOSOMAL AND LYSOSOMAL CO-LOCALISATION

Multiple endocytic pathways, including caveolae-dependent and clathrin-mediated mechanisms, are dependent upon both cholesterol and actin networks[162, 164]. Therefore, the current study determined if lipid rafts mediated the endocytosis of FhHDM-1. This premise was supported by observations that RecFhHDM-1 co-localised with this membrane domain (Figure 3.1 B). Lipid rafts can exist as flat or invaginated regions on the plasma membrane. The latter are known as caveolae and the structural difference has been attributed to the presence of the cholesterol receptor, caveolin-1 (cav-1)[158]. Caveolae play roles in signal transduction as well as clathrin-independent endocytosis[157]. However, co-localisation of RecFhHDM-1 and caveolin-1 containing regions was not observed in macrophages that had internalised RecFhHDM-1 (Figure 3.4). This finding suggested that caveolae-dependent endocytosis was not the mechanism by which RecFhHDM-1 was internalised.

Therefore, the alternative possibility that FhHDM-1 was internalised via 'classical' (clathrin-dependent) endocytosis was next explored. In this pathway, molecules interact with the cell surface, where they associate with clathrin-coated pits. These pits pinch off sections of the plasma membrane, which become clathrin-coated vesicles that fuse with early endosomes[166]. Intracellular localisation of fluorescently labelled sFhHDM-1 was determined by staining macrophages with the early endosome marker, Rab5, which is a small GTPase that is an essential component of the clathrin-dependent endocytic pathway[160, 166-168]. Co-localisation of sFhHDM-1 and Rab5 appeared as yellow foci of fluorescence, which were observed at all time points examined (5-45min inclusively) (Figure 3.5). This data suggested that sFhHDM-1 was initially internalised into the macrophage cytoplasmic region via encapsulation within early endosomes. It was also noted that at the later time points, notably at 45min, a proportion of cytoplasmic sFhHDM-1 did not localise to areas identified as early endosomes. These observations suggested the possibility that sFhHDM-1 co-localised with other cytoplasmic vesicular regions during the later stages of endocytosis (Figure 3.5 F).

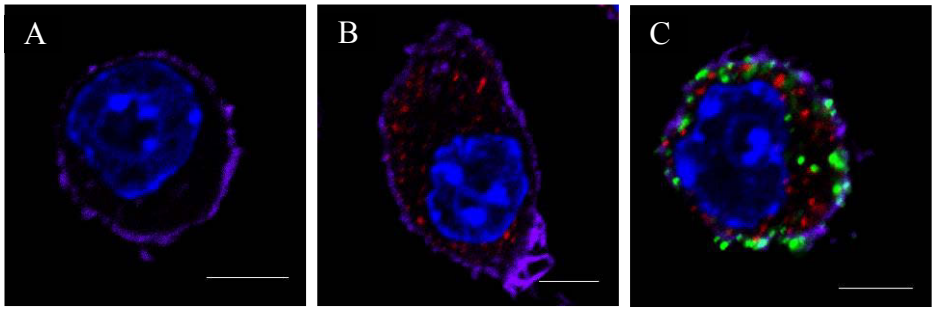

Figure 3.4 FhHDM-1 endocytosis was not mediated by caveolae. Representative immunofluorescence images obtained by confocal microscopy of RAW264.7 macrophages that were untreated (A & B), or incubated with RecFhHDM-1 for 45min at 37°C (C), which was identified with anti-RecFhHDM-1 and Alexa 488 antibodies (green). An untreated control (A) was also stained for RecFhHDM-1 detection to evaluate the specificity of the antibody. Caveolae were detected by incubating cells with anti-caveolin-1 and Alexa 568 conjugated antibodies (red). A sample stained for caveolin-1 identification only (B), in the absence of FhHDM-1, was also included. Nuclei and plasma membranes were identified by DAPI (blue) and phalloidin (violet) staining, respectively (100X objective; Scale bar: 5μm). Images represent cells from triplicate fields of view collected for each sample.

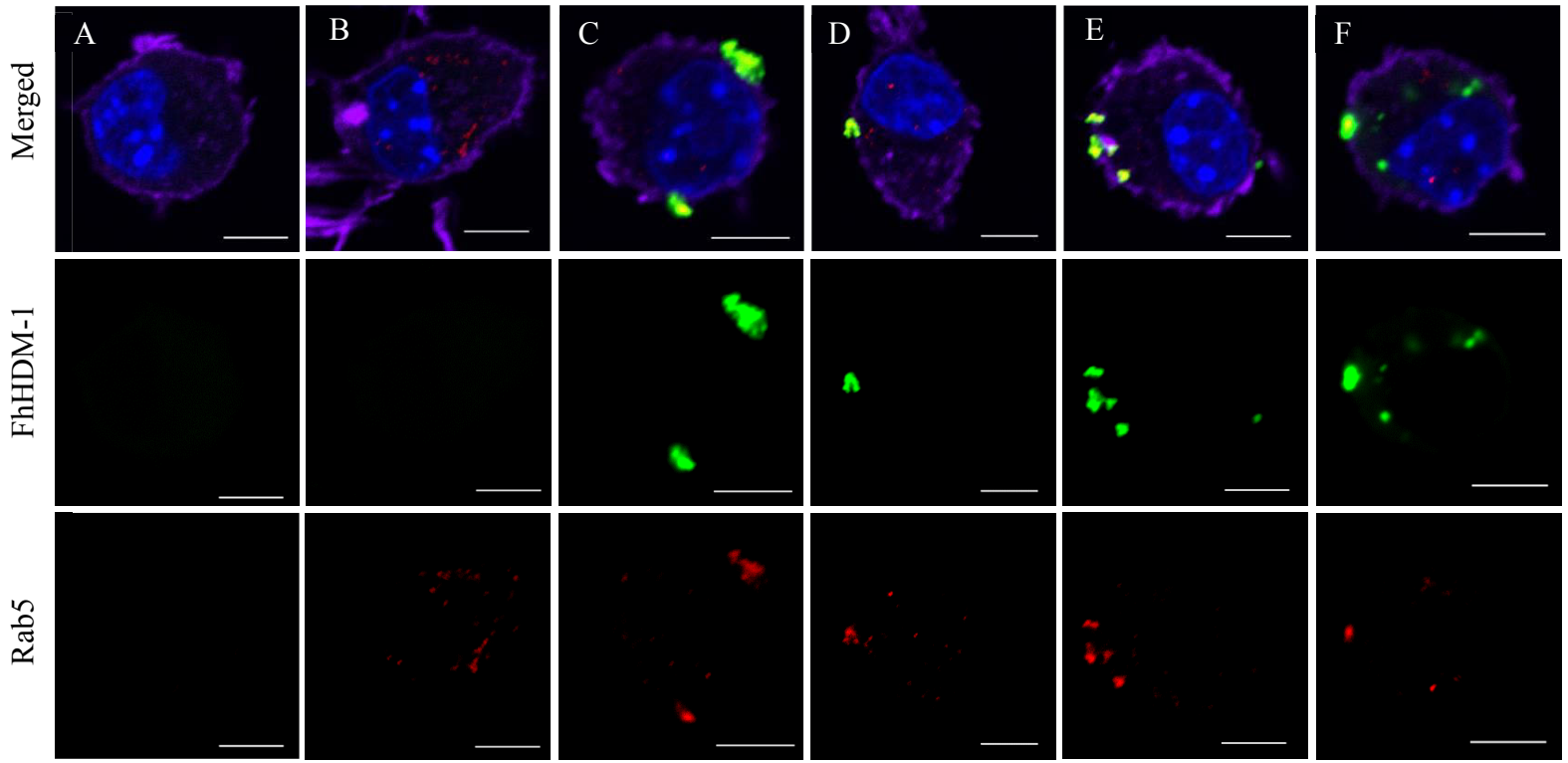

Figure 3.5 FhHDM-1 co-localised with early endosomes. Representative immunofluorescence images obtained by confocal microscopy of RAW264.7 macrophages that were untreated (A & B), or incubated with sFhHDM-1-Alexa 488 (green) for 5 (C), 15 (D), 30 (E) and 45 (F) min, and stained with anti-Rab5 (B-F) and Alexa 568 (A-F) antibodies to identify early endosomes (red) (B-F). Omission of primary antibody (A) and detection of resting early endosomes (B) controls were also included. Co-localisation was observed as yellow fluorescence (C-F). Nucleus and plasma membranes were identified by DAPI (blue) and phalloidin (violet) staining, respectively (100X objective; Scale bar: 5µm). Images represent cells from triplicate fields of view (collected per sample) and the experiment was performed twice.

Early endosomes sort endocytosed cargos to their final destination for functional purposes (such as nutrient delivery), recycling (of membrane lipids, for example), and degradation or processing[169, 170]. The latter two events involve the maturation of vesicles, a process in which early endosomes are transformed into late endosomes, and subsequently into lysosomes, by a series of fusion mechanisms[163, 171]. During this maturation process, the intravesicular pH decreases[166, 171], and the increasing acidity allows visualisation of mature vesicles using the acidotropic probe, LysoTracker, which is a recognised endolysosomal marker. Therefore, macrophages were incubated with sFhHDM-1, for varying periods of time, to determine if localisation of sFhHDM-1 occurred within late endosomes or lysosomes. Co-localisation of FhHDM-1 with LysoTracker was prominent at 15min (Figure 3.6 B) when the intensity of staining with LysoTracker was also optimal (i.e. of sufficient fluorescence intensity). At later time points a proportion of the sFhHDM-1 molecules were localised in the same regions as the marker (Figure 3.6 C & D), however due to the decreased intensity of the LysoTracker staining, areas of distinct co-localisation (observed as yellow fluorescence) decreased in both intensity and abundance.

In order to improve the ability to detect acidic vesicles using LysoTracker, and consequently establish the co-localisation of sFhHDM-1 and lysosomes, live cell imaging was performed on primary murine (BALB/c) BMDMs that had been incubated with sFhHDM-1 for 30 min. Cell viability was morphologically monitored using transmission detection (Figure 3.7 A) and internalization of *E.coli* BioParticles utilized as a positive control to confirm the ability of macrophages to endocytose extracellular material. Under these live conditions, the immunofluorescence signal from LysoTracker was significantly more intense (Figure 3.7 B), and this analysis confirmed that co-localisation with sFhHDM-1 had occurred, as observed by the presence of yellow/orange areas of fluorescence (Figure 3.7 A & C). Furthermore, quantitation analysis of the generated images suggested that approximately 93% of macrophages had internalised sFhHDM-1, and on average 88% had identifiable lysosomes. Additionally, in virtually all of these cells co-localisation of FhHDM-1 and LysoTracker was observed (Figure 3.7 E). These data suggested that FhHDM-1 indeed localised with lysosomal components after uptake by macrophages.

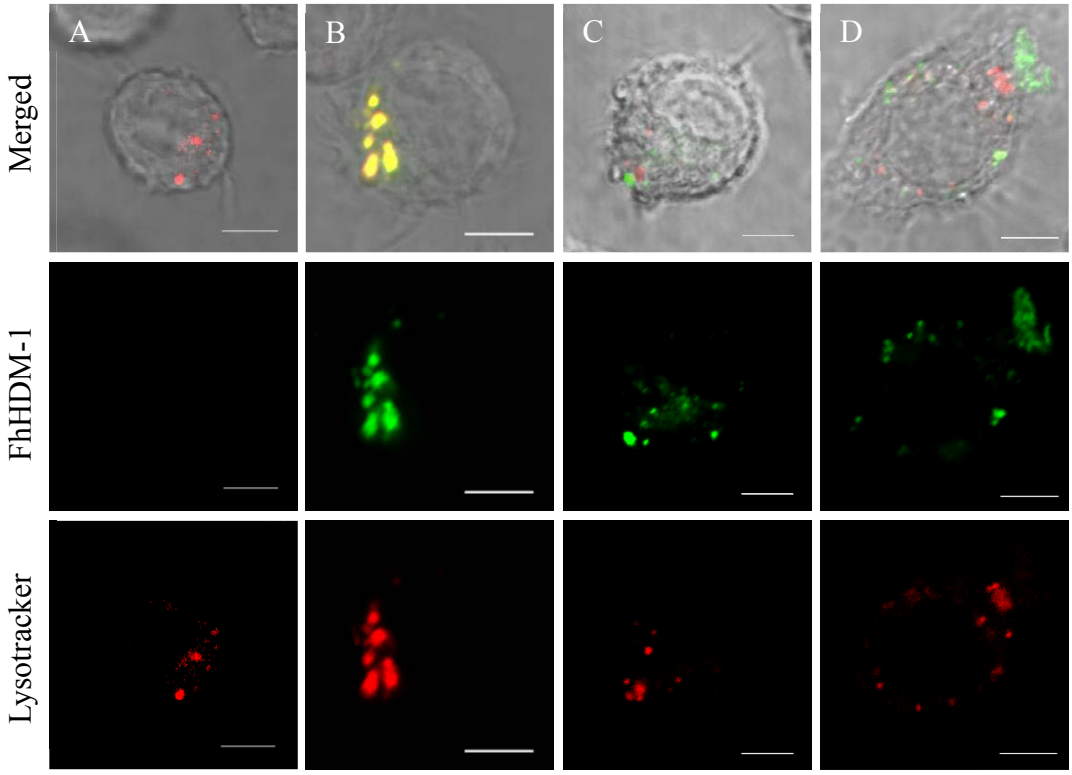

Figure 3.6 FhHDM-1 co-localised with endolysosomes of fixed RAW264.7 macrophages. Representative immunofluorescence images obtained by confocal microscopy of RAW264.7 macrophages that were untreated (A), or incubated with sFhHDM-1-Alexa 488 (green) for 15 (B), 30 (C) and 45min (D). Cells were also incubated with the endolysosomal dye, LysoTracker (red). Yellow/orange fluorescence corresponds to co-localisation of sFhHDM-1 and lysosomal components. Panel (A) represents LysoTracker only/resting endolysosomes control sample (100X objective; Scale bar: 5µm). Provided images represent cells from triplicate fields of view per time point. Results were confirmed by two subsequent experiments.

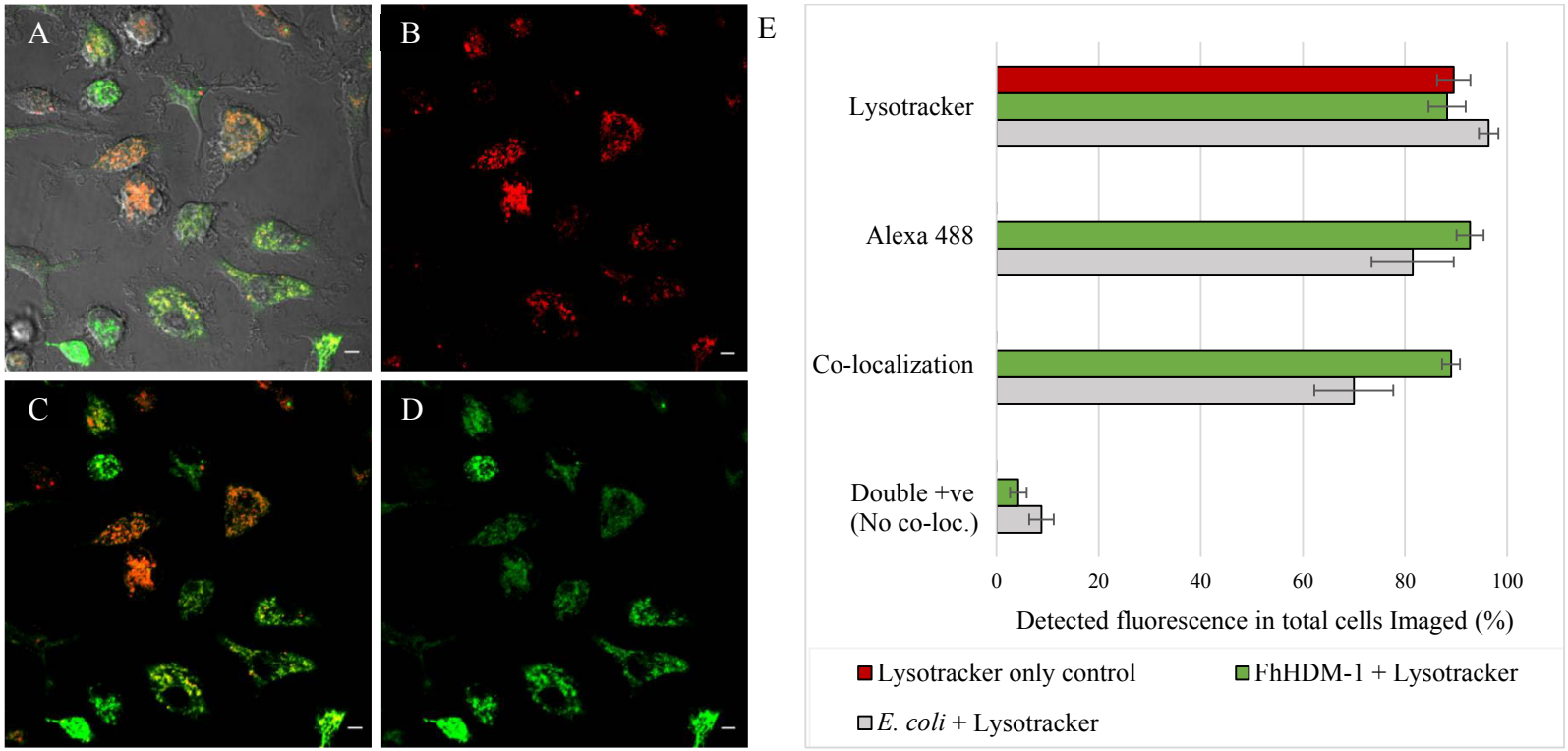

Figure 3.7 FhHDM-1 co-localised with endolysosomes of live BALBc BMDMs. Representative immunofluorescence images obtained by live cell confocal microscopy of BALBc BMDMs incubated with sFhHDM-1-Alexa 488 (D) for 30 min. Cells were also incubated with the endolysosomal dye, LysoTracker (red) (B). Co-localisation was observed as orange/yellow fluorescence (A & C) and cell morphology visualised by transmission detection (grey) (A) to monitor cell viability throughout the imaging process (100X objective; Scale bar: 5µm). An average of 150 cells per sample treatment were imaged for quantitative analysis (E) of LysoTracker detection and sFhHDM-1/*E. coli* uptake, as well as co-localisation or the detection of both signals within different regions of a given cell, which was denoted as not being co-localized (No co-loc).

To determine if sFhHDM-1 was trafficked to other organelles in the cytoplasmic region, additional confocal microscopy experiments were performed. Some endocytic routes directly deliver their cargo to the Golgi apparatus, as is the case for the internalisation of Cholera toxin subunit B (ChTx). This trafficking process is reportedly mediated by caveolae-dependent endocytosis[160, 172]. The lack of co-localisation of sFhHDM-1 with caveolin-1, observed previously, did not necessarily eliminate the possibility that FhHDM-1 may be delivered to the Golgi apparatus, since caveolae depleted cells are capable of alternatively transporting ChTx in clathrin coated pits[172]. Furthermore, on occasions clathrin-mediated endocytosis can result in early endosomal structures trafficking their cargo directly to the Golgi network, as occurs during the internalisation of Shiga toxin[160, 173]. However, despite the observation that FhHDM-1 co-localised with ChTx at the plasma membrane, internalisation of sFhHDM-1 by macrophages did not result in its co-localisation with the Golgi apparatus, as determined by staining using an anti-giantin antibody as a marker for Golgi (Figure 3.8 A-C). Therefore, these data demonstrate that FhHDM-1 does not share the same route of uptake as ChTx.

The presence of α-helices in certain protein and peptide segments can serve to target molecules to receptors located in the mitochondrial outer membrane. This has been reported for mitochondrial pre-sequences as well as for certain basic antimicrobial peptide precursors, such the salivary human host defence peptide, histatin-5[174, 175]. However, despite its α-helical structure, internalised sFhHDM-1 did not co-localise with the mitochondrial marker, MitoTracker (Figure 3.8 E). Collectively, these results suggested that after internalisation by macrophages, sFhHDM-1 localised to early endosomes and lysosomes, but not to the Golgi apparatus or mitochondria.

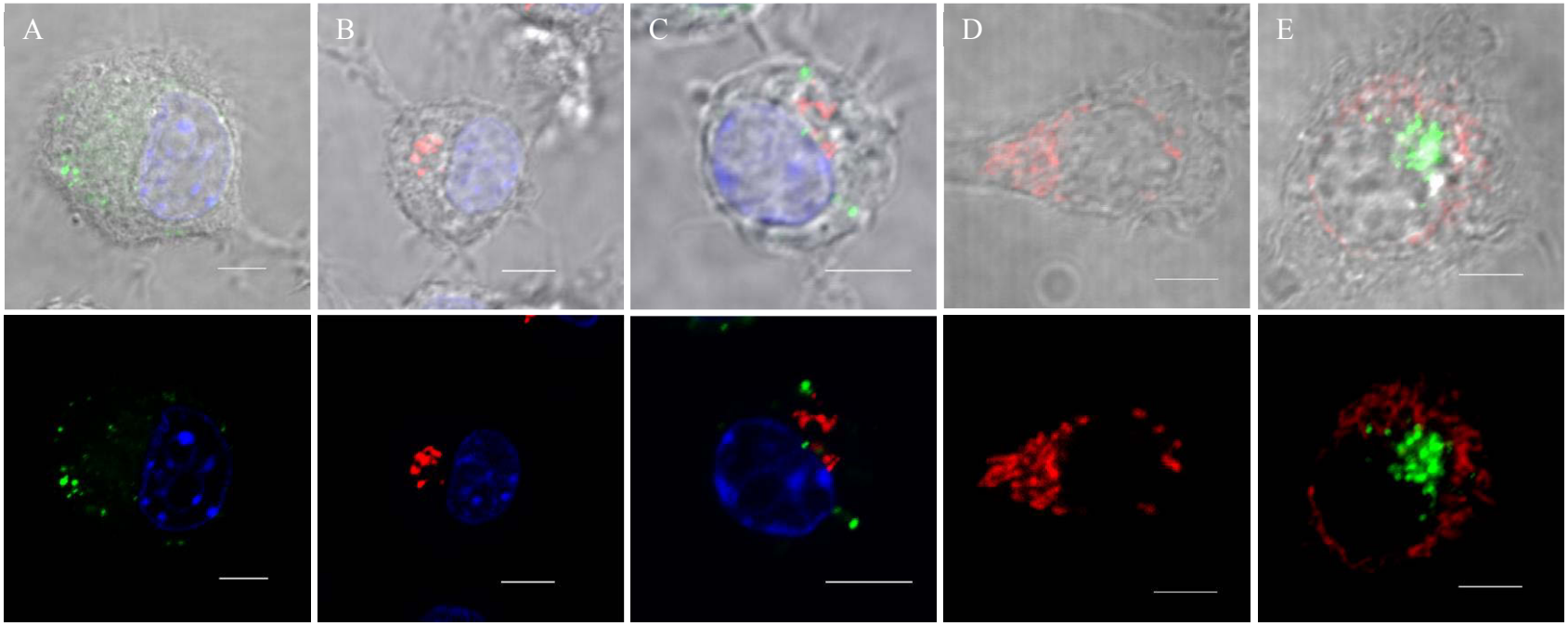

Figure 3.8 FhHDM-1 did not co-localise with the Golgi apparatus or mitochondria in RAW264.7 macrophages. Representative immunofluorescent images obtained by confocal microscopy of RAW264.7 macrophages that were untreated (B & D), or incubated with sFhHDM-1-Alexa 488 (A, C & E) (green) for 45min at 37°C. Golgi networks (red) were identified with anti-giantin (B & C) and Alexa 568 conjugated antibodies (A-C), and mitochondria (also red) by MitoTracker staining (D & E). Sample (A) corresponds to the omission of primary antibody (anti-giantin) control and (B & D) to untreated samples stained for Golgi and mitochondria detection only (100X objective; Scale bar: 5µm). Images represent cells from triplicate fields of view collected for each sample treatment.

3.4. Discussion

Confocal microscopy enabled the identification of an initial interaction between FhHDM-1 and lipid rafts within the plasma membrane of macrophages, which was followed by the active internalisation of FhHDM-1. To date, multiple endocytic mechanisms have been described and several of these share characteristics, such as cholesterol and actin dependence, and the vesicular entrapment of cargo within early endosomes and endolysosomes[160]. In the current study, all of these common features were found to play roles in the trafficking of FhHDM-1 within the cytoplasmic regions of macrophages. Collectively, this data suggests that the mechanism by which FhHDM-1 is internalised is likely mediated by classical (clathrin-mediated) endocytosis.

Endocytosis of LL-37-coated DNA plasmids is both time and temperature dependent, and occurs by a cholesterol-sensitive, caveolae-independent mechanism with co-localisation to lipid rafts and early endosomal compartments[150, 176]. Furthermore, Lau *et al.* revealed that the internalisation of the cathelicidin, LL-37, is microtubule-dependent, but actin-independent[148]. The resemblance between the endocytic mechanisms responsible for the internalisation of both LL-37 and FhHDM-1 are likely attributable to their structural similarities.

Amphipathic helices possess structural characteristics that make them suitable candidates for interaction with plasma membranes. The unfolded peptides containing the helices preferentially accumulate near negatively charged membrane regions, through electrostatic interactions. Then, via a hydrophobic effect, their hydrophobic residues become inserted between lipid acyl-chains, and the hydrophilic residues of the helix orient themselves towards the lipid polar heads[177]. Occasionally, the interaction of amphipathic helices with membranes induces membrane curvature, which is necessary for vesicle formation, and the initiation of membrane trafficking events. For example, the hydrophobic regions of the protein epsin, become inserted between lipids, thereby separating them to induce membrane curvature towards the cytoplasmic region, and subsequent formation of clathrin coated vesicles [177, 178].

Several molecules that interact with lipid rafts become anchored/absorbed to plasma membranes, via targeting of their transmembrane domains or membrane proximal determinants. Such is the case for the membrane proximal amphipathic helix

of the tyrosine kinase interacting protein (Tip) of *Herpesvirus saimir* (HVS), and the lipid raft residing protein, α synuclein[179, 180]. In case of Tip, it has been suggested that the principal mechanism by which this binding occurs is via the hydrophobic residues (especially isoleucine and leucine) on its membrane proximal helical motif, which facilitate the targeting of this protein directly to lipid rafts[179]. Furthermore, when Tip binds to lipid rafts in T cells, it stimulates the translocation of the endolysosomal protein, p80, and the aggregation of TcR/CD3 complexes into this membrane region. It has also been proposed that Tip induces membrane budding and its interaction with p80 induces internalisation of the lipid raft associated components, as well as the formation and enlargement of lysosomes. The endocytosed contents are destined for degradation within lysosomes, and the specific targeting to this organelle is dependent upon the integrity of the amphipathic helical motif of Tip[179, 181, 182].

Bearing this in mind, the amphipathic helix of FhHDM-1 may also be involved in the targeting of this peptide to lysosomes, which may represent its final destination. Interestingly, like Tip, the amphipathic helix of FhHDM-1 is also rich in both isoleucine and leucine hydrophobic residues[115]. Therefore, the interaction of FhHDM-1 with lipid rafts may also be facilitated by its C-terminal amphipathic helix, which could target FhHDM-1 to these plasma membrane domains. Although FhHDM-1 was not recovered along with integral membrane proteins after cellular fractionation[115] (Section 1.5.1), an association with lipid rafts remains feasible, since it has been demonstrated that only proteins that are strongly associated with lipid rafts remain in the insoluble fractions, whereas weakly associated proteins are extracted when this type of technique is employed[182].

The positively charged residues within Tip also facilitate its interaction with lipid rafts, as they bind to negatively charged lipids[179]. Although the amphipathic helix containing peptide of FhHDM-1 is capable of binding to multiple phospholipid species (independent of their charge or saturation, but dependent upon the differential spacing of their head groups in the phospholipid bilayer[115]), it is still possible that the affinity of FhHDM-1 for cholesterol aids its interaction in an analogous manner, especially given the high abundance of this lipid within lipid rafts[158]. Therefore, it is hypothesised that an interaction, possibly mediated via the amphipathic helix, could induce membrane curvature[183], resulting in vesicular formation (as is induced by epsin[178]) and FhHDM-1

internalisation, with potential targeting to lysosomes. This premise is corroborated by the findings of the current study.

Cholesterol depletion using MCD, reduced, but did not abolish, the interaction between FhHDM-1 and the plasma membrane of macrophages (Figure 3.3 D). Therefore, it is possible that the amphipathic helix may enable the interaction of FhHDM-1 with the plasma membrane, via a mechanism that is independent of cholesterol binding. However, it has to be taken into account that in the current study the depletion of cholesterol may not have been absolute and a proportion of residual cholesterol may have remained within the lipid rafts. Furthermore, truncation of the cholesterol binding motif in FhHDM-1 reduced, but did not abolish, binding to this lipid, which indicates that while the motif may enhance binding specificity, this structure may not be essential for the interaction to occur[114].

While the localisation pattern of fluorescently tagged RecFhHDM-1 and sFhHDM-1 was identical, significant differences were found when RecFhHDM-1 was visualised intracellularly, using anti-RecFhHDM-1 antibody, as opposed to an antibody specific for the C-terminal His-tag attached to the recombinant peptide (Figures 3.1 B & 3.2). It has been reported that RecFhHDM-1 is susceptible to cleavage by cysteine proteases, an event which results in the release of smaller peptide fragments, which are undetectable using anti-His antibodies, but are recognised by the anti-RecFhHDM-1 antibody[115]. Therefore, it is possible that after the initial interaction of RecFhHDM-1 with the macrophage surface, the C-terminal His-tag was cleaved, and remained attached to the cell surface whilst the released peptide fragment (identifiable by anti-RecFhHDM-1 antibody) was internalized by macrophages.

This type of cleavage event is reportedly essential for the activation of homologous HDPs[147]. For example, within immature neutrophils, the human cathelicidin precursor, hCAP-18, is stored within cytoplasmic specific granules that do not possess catalytic activity[184, 185]. When the cells become fully matured, hCAP-18 is exocytosed and extracellular exposure to proteases cleaves the cathelin-like pro-segment of the precursor, releasing the active LL-37[145, 186]. However, when the storage of hCAP-18 is mistargeted to azurophil (lysosome-like) granules, premature cleavage occurs, which induces the early activation of this cathelicidin[185].

Endocytosed LL-37 (as well as LL-37-coated DNA plasmids) has been reported to accumulate at perinuclear locations[148, 150]. However, the final destination of specific molecules coated with this peptide (to aid their uptake) seems to be dependent upon the nature of its cargo, as occurs after endocytosis of LL-37-coated LPS complexes that are delivered to lysosomes in DCs[187]. The ability of FhHDM-1 to associate with plasma membranes, its endocytosis, and localisation to lysosomes may render it a potential carrier protein, since cargo molecules could be entrapped through rearrangements of the amphipathic helical region, which would allow the formation of a hydrophilic pore (as has been reported for carrier peptides)[153]. This ability could potentially be exploited for FhHDM-1 mediated drug delivery to lysosomes. Furthermore, targeting of FhHDM-1 towards lysosomes, and the subsequent release of its peptide by protease cleavage may have a biological impact on macrophages, especially given the crucial role that lysosomes play in their function.

CHAPTER 4 FHHDM-1 MODULATES THE PROCESSING OF ANTIGENS BY MACROPHAGES

4.1. Introduction

Historically, macrophages have been considered professional phagocytes, due to the efficiency with which they eliminate pathogens and clear cellular debris (resulting from apoptotic and necrotic processes). However, it is also now widely recognised that macrophages play crucial roles in immunity, which determine, in a large part, the nature of the adaptive immune responses generated[17, 140]. Macrophages not only have the capability of recognising, internalising and degrading pathogens and dying cells, but also produce a wide array of cytokines, and other immune regulatory molecules, that promote either pro- or anti-inflammatory adaptive immune responses. Furthermore, macrophages play a major role in the activation of T cells, due to their ability to process phagocytosed material and present the resultant antigenic peptides to T cells[17, 140, 188, 189]. A process that is possible due to the expression of major histocompatibility complexes (MHCI and II) and activation markers (CD80 and CD86) by macrophages[17, 140, 188]. Altogether, these functional roles form an integral link between innate and adaptive immune responses[17, 140, 141].

Fundamental to these biological activities of macrophages are the intracellular lysosomes. The process of endocytosis involves a series of vesicular maturation stages that culminate in the delivery of extracellular material to lysosomes (Section 3.3). These organelles, comprise the site for processing and degradation of internalised antigens, are involved in secretory pathways (lysosomal exocytosis), and contribute to the general maintenance of cellular homeostasis (including plasma membrane repair and recycling of intracellular contents)[190-194].

Lysosomes are delimited by a single phospholipid bilayer membrane that is rich in highly glycosylated integral proteins (predominantly LAMP1, LAMP2 and CD63). These proteins form a glycocalyx that lines the luminal face of the membrane[195, 196]. The lysosomal lumen houses a group of catalytic enzymes that are collectively known as hydrolases. Acid hydrolases, trafficked from the endoplasmic reticulum, are tagged with mannose-6- phosphate residues (in the Golgi cisternae), which then bind to mannose

phosphate receptors (MPR), located in the trans-Golgi network (TGN)[193, 197]. These complexes are then transported within clathrin-coated intermediate vesicles, which ultimately fuse with endosomes, where the acidic pH dissociates the ligand/receptor complexes[193, 197]. Clathrin plays an important role in returning the MPRs to the TGN for recycling, by forming coated vesicles and pits that facilitate their transportation. The endosomes containing hydrolases then fuse with lysosomes where they can most optimally perform their enzymatic roles[193].

The catalytic activity of lysosomal hydrolases is dependent upon the acidity of the luminal region where they reside[193, 198, 199]. Central to the maintenance of the low pH environment is the activity of the membrane vacuolar ATPases (vATPases). This multi-subunit enzyme complex consists of a soluble V_1 sub complex, which catalyses ATP hydrolysis, and a membrane-embedded V_0 sub complex that is responsible for proton translocation. Jointly, these subunits form the functional vATPase, which utilises ATP hydrolysis as source of energy to pump protons, against an electrochemical gradient, into the luminal region, thus establishing and maintaining pH levels between 4.6 and 5[193, 198, 200, 201].

During endocytosis, membrane receptors, which have bound to extracellular material, are internalised and delivered to early endosomes. The weakly acidic environment in these organelles induces dissociation between the internalised cargo and receptors, the latter being recycled to the membrane, whilst the former remain within the endosomes[193, 194, 202]. Endosome maturation is characterised by the conversion of Rab proteins, whereby Rab5 localisation to the early endosomes is lost and Rab7 localisation is acquired[193, 202-204]. However, the engulfed material has to be ultimately delivered to lysosomes, where it is fully processed. Several, often conflicting, hypotheses to describe the mechanism of this process have been proposed. However, it has been recently concluded that a combination of transient contacts (a process referred to as 'kissing') and fusion events, occurring between lysosomes and late endosomes (or lysosomes and autophagosomes in case of intracellular constituents) result in the formation of hybrid organelles that allow material transfer and mixing[193, 194, 202, 203, 205]. This process culminates in lysosome reformation where degradation/processing can occur[202, 203].

Degradation of endocytosed antigens by lysosomal hydrolases yields antigenic peptides, generally between 12-19 residues in length (however longer peptides can result)[193, 206, 207]. These peptides can then be loaded onto MHCII molecules, within the lysosomal compartment, and the complexes formed are then delivered to the plasma membrane for presentation to $CD4^+$ T cells. This presentation process, in combination with co-stimulation, induced by activation markers interacting with their cognate partners on the T cell, induce T cell activation and proliferation[189, 206-208].

Due to the dependence of hydrolase activity upon acidification of the lysosomal lumen[199], if the low pH environment is compromised, antigen processing is prevented, and, accordingly, cells are incapable of presenting processed antigens to T cells. However, if the native antigen is artificially processed, by chemical or enzymatic means, prior to co-incubation with APCs, such as macrophages, then enzymatic processing in the acidic environment of the lysosome is no longer required and antigen presentation can occur[207, 209]. These observations highlight the essential requirement for lysosomal acidification, and hence vATPase activity, for antigen processing. The localisation of FhHDM-1 to macrophage lysosomes (Chapter 3), and the previously mentioned proteomics analysis[142], suggest that FhHDM-1 can potentially exert a functional impact on this organelle. Therefore, the ability of this peptide to influence not only lysosomal conditions but also the ability of macrophages to process and present antigen to T cells was assessed.

4.2. Specific methods

4.2.1. ENDOCYTOSIS AND VESICULAR ACIDIFICATION STUDIES

4.2.1.1. DEXTRAN ENDOCYTOSIS STUDIES

4.2.1.1.1. Flow Cytometry

Triplicate samples of RAW264.7 murine macrophages were seeded into 24-well plates ($5x10^5$ cells per well) and incubated O/N to allow adherence. Two sets (of triplicate samples each) were either untreated or pre-incubated with sFhHDM-1 at concentrations of 10, 20, 50 or 100µg/mL for 1h or 20h. As comparative inhibitory controls, some samples were incubated with the vATPase inhibitors, concanamycin A (Sigma), at a concentration of 0.866µg/mL (equivalent to 1µM) for 1h, or cytochalasin D (2µg/mL) (Sigma) for 30min. Supernatants were removed and one set as well as the concanamycin A-treated samples, were then incubated with 10µg/mL pHrodo™ green dextran (Life Technologies) for 1h. The second set of samples, in addition to the cytochalasin-treated samples, were incubated with Alexa 647-conjugated dextran (dextran-647; Molecular Probes) at 10µg/mL for 1h. All incubations were performed at 37°C/5% CO_2. For the cytochalasin D-treated samples, the inhibitor remained in culture during the entire dextran-647 incubation period. Cells were prepared for flow cytometry by washing them twice in 500µL FACS buffer (PBS, 1%w/v BSA, 2%v/v FBS and 0.05% Az). Then cells were scraped off the plate using the end of a pipette tip and transferred to FACS tubes for analysis using a BD LSR II Flow Cytometer System (BD Biosciences). Immediately prior to analysis, 1µM SYTOX blue dead cell stain (Molecular Probes) was added to each sample. The collected data was further analysed using the FCS express version 4 software and gating was applied on single live cells. ANOVA followed by Dunnett's statistical tests, using Graph Pad Prism version 6 software, were performed to determine significant differences between geometric mean values of sample treatments and the positive controls. An equivalent experiment was also performed in which samples were simultaneously incubated with sFhHDM-1 (at 10, 50 or 100µg/mL) and labelled-dextrans for a period of 1h.

4.2.1.1.2. Confocal microscopy

BALB/c BMDMs were seeded into 35mm microscopy dishes ($1x10^6$ cells per dish). One sample was pre-incubated with Alexa 488-conjugated sFhHDM-1 (50µg/mL for 2h, 37°C/5% CO_2) prior to washing twice with sterile PBS (RT), and then incubated with Alexa 647-conjugated dextran at a concentration of 10µg/mL in media (1h, 37°C/5% CO_2), or simultaneously incubated with both molecules (1h, 37°C/5% CO_2). In addition, samples of cells treated with vehicle only or dextran-647 only acted as controls. Cells were then prepared for microscopy, as outlined in Section 2.3. Once images were obtained, quantitative analysis was performed by identification of the uptake of sFhHDM-1 and/or dextran-647 as well as co-localisation in 100 cells per sample, by visual analysis using the NIS software. This experiment was repeated using primary human macrophages following the same procedure, with the exception that cells were incubated with 20µg/mL sFhHDM-1 for 1h. Furthermore, for the murine samples, t-tests, using Graph Pad Prism version 6 software, were performed to determine significant differences in the percentage of detected fluorescently positive cells per field of view, between the pre- and simultaneously FhHDM-1 treated samples.

4.2.2. EFFECTS OF FHHDM-1 ON ANTIGEN PROCESSING AND PRESENTATION

4.2.2.1. EFFECTS OF SFHHDM-1 ON DQ OVALBUMIN PROCESSING

Triplicate samples of RAW264.7 macrophages were seeded into 24 well plates ($7x10^5$ cells per well), incubated O/N at 37°C/5% CO_2 to allow adherence, and media was removed prior to sample treatment. One set of cells was pre-incubated with sFhHDM-1 for 1h (37°C/5% CO_2) at concentrations of 10, 50 or 100µg/mL, and then washed three times with sterile PBS (RT). Then this sample set was incubated with 10µg/mL DQ ovalbumin (Molecular Probes) for 1h, 37°C/5% CO_2. During this latter incubation another set of samples was simultaneously incubated with 10µg/ml DQ ovalbumin and sFhHDM-1, at concentrations of 10, 50 or 100µg/mL. Unstained and DQ ovalbumin only samples were also included as controls. All wells were washed, cells were removed by scraping (using the end of a pipette tip), resuspended in FACS buffer, and transferred to FACS tubes. Prior to analysis, 0.1mM of the nuclear stain, DAPI, was added to each sample to distinguish dead cells. Flow cytometric data was collected by Dr Suat Dervish (Centenary Institute, Sydney) using the BD Fortessa Flow Cytometer System (BD Biosciences). Further analysis using the FCS express version 4

software was performed with gating on single live cells. ANOVA followed by Dunnett's statistical tests, using Graph Pad Prism version 6 software, were performed to determine significant differences between geometric mean values for the sample treatments and the positive control.

4.2.2.2. EFFECTS OF FHHDM-1 ON ANTIGEN PRESENTATION TO TRANSGENIC MURINE CELLS

4.2.2.2.1. Antigen processing studies

Triplicate samples of C57BL6 BMDMs (Section 2.2.3.1) were seeded into a 96 well flat tissue culture grade plate ($2x10^5$ cells per well) containing 10ng/mL of mouse recombinant IFNγ (BD Biosciences), and incubated for 24h at 37°C/5% CO_2 to up regulate MHCII expression. Cells were then washed twice with sterile PBS (RT) and incubated with the inhibitor concanamycin A (0.866µg/mL) or FhHDM-1 (100µg/mL) for 1h at 37°C/5% CO_2. Media was removed and samples were incubated with either full-length ovalbumin (EndoFit Ovalbumin; Invivogen, San Diego, USA) at a concentration of 2mg/mL, or ovalbumin peptide (323-339) at 10µg/mL (AnaSpec Inc., Seraing, Belgium) for 6h at 37°C/5% CO_2. For simultaneous incubation experiments, cells were incubated with FhHDM-1 in combination with ovalbumin (full length or peptide) at the same concentrations and under the same conditions as described above.

4.2.2.2.2. T cell isolation

Spleens were isolated from OT-II mice (C57BL6 background) obtained from the Walter and Eliza Hall Institute (WEHI) (Victoria, Australia). These homozygous transgenic mice express the α-chain and β-chain TcR that pairs with the CD4 co-receptor and is specific for chicken ovalbumin 323-339 in the context of I-Ab. Procedures were performed under ethics approval number 2013-075 (UTS). Single cell suspensions of splenocytes were obtained by passing tissue through nylon cell strainers (70µm cut off) using the rubber ends of plungers from 1mL syringes. The resulting splenocytes were pelleted by centrifugation (15min at 300*g*). Red blood cells were lysed by resuspending cells in 2mL Hybri-Max lysis buffer (Sigma) followed by a 5min incubation period at RT. Cells were washed with RPMI 1640 media and pelleted (15min at 300*g*). T cells were purified by negative selection using a CD4 T cell isolation kit, according to the manufacturer's recommendations (Miltenyi Biotec). The resultant cell population was 90% $CD4^+$, as assessed by flow cytometry using PE-anti-

mouse CD3 molecule complex clone 17A2 and Pacific Blue-anti-mouse CD4 clone RM-4-5 antibodies (BD Pharmingen; Section 2.4). Cells were resuspended at a density of $5x10^5$ cells per mL in RPMI 1640 media, supplemented with L-glutamine, 10% HI FBS, 1% penicillin/streptomycin, and 0.004% 2-mercaptoethanol.

4.2.2.2.3. Antigen presentation studies

Media was removed from wells containing ovalbumin treated C57BL6 BMDM samples (Section 4.2.2.2.1) and $CD4^+$ T cells ($1x10^5$) were added for co-incubation over 24h to allow antigen presentation to occur. After this, cells were pelleted (5min at 300*g*) and supernatants were collected, diluted 1/10, and assayed for IL-2 by ELISA (BD Biosciences; Section 2.5). ANOVA followed by Dunnett's statistical tests, using Graph Pad Prism version 6 software, were performed to determine significant differences in IL-2 secretion between sample treatments and the positive control.

4.2.3. EFFECTS OF FHHDM-1 ON MHCII SURFACE EXPRESSION BY BMDMS

BALB/c BMDMs were seeded into 6 well plates ($2x10^6$ cells per well) and incubated O/N to allow adherence. One set of duplicate samples was pre-incubated for 2h with sFhHDM-1 (50µg/mL), washed three times, and incubated with IFNγ (10ng/mL) for 2h. Remaining samples (in duplicate) were incubated with either sFhHDM-1 (50µg/mL) or IFNγ (10ng/mL) for 2h, or left untreated. Then cells were washed twice with FACS buffer, removed by scrapping, and 1mL FACS buffer was added prior to cells being transferred into individual eppendorf tubes. Each sample was split into two aliquots and stained using rat anti-mouse MHCII-Alexa 488 antibody (BD Pharmingen) or anti-rat-Alexa 488 (BD Pharmingen) (isotype control), following the protocol described in Section 2.4. Then, cells were transferred to FACS tubes for analysis by flow cytometry. Immediately prior to analysis, using the BD LSR II flow Cytometer System (BD Biosciences), 2µg/mL propidium iodine (Life Technologies) was added to each sample to identify dead cells. Collected data was further analysed using the FCS express version 4 software and gating applied on single live cells. ANOVA followed by Dunnett's statistical tests, using Graph Pad Prism version 6 software, were performed to determine significant differences between geometric mean values of the sample treatments and the untreated control.

4.3. Results

4.3.1. FhHDM-1 REDUCES VESICULAR ACIDIFICATION AND ENHANCES ENDOCYTOSIS BY MACROPHAGES

Collectively, the microscopic studies presented in Section 3.3 suggested that, following endocytosis by macrophages, lysosomes were the final intracellular destination of FhHDM-1. Accordingly, it was hypothesised that FhHDM-1 exerted its biological activity within this organelle. During endocytosis the vesicles that transport extracellular cargo become progressively acidified, from a luminal pH of 6 in early endosomes to an acidic environment of pH 4.5 within lysosomes[198]. Considering the importance of luminal pH in the control of lysosomal functions, notably antigen processing, it was initially determined if FhHDM-1 influenced the maintenance of lysosomal pH within macrophages.

Conjugated dextran molecules were used for the purposes of these studies as they are known to be internalised via endocytosis; the molecule being first encapsulated in early endosomes, which then mature into late endosomes and finally into lysosomes[210-212]. Two conjugated versions of dextran were selected to assess the impact of FhHDM-1 on lysosomal activity. The uptake and internalisation of dextran was assessed by incubating cells with Alexa647-conjugated dextran, which fluoresces intracellularly in a pH-independent manner. In contrast, pHrodo dextran is pH sensitive and, upon internalisation, its conjugated fluorophore emits a signal that increases in intensity proportionately to the degree of acidification of the environment in which the molecule is contained. Additionally, pHrodo dextran is non-fluorescent within extracellular spaces or at neutral pH environments, thereby preventing its detection when it is non-specifically bound or when it is not endocytosed[212].

Thus, to investigate the effect of FhHDM-1 on lysosomal acidification, RAW264.7 macrophages were pre-incubated (for periods of 1 or 20h), or simultaneously treated with increasing concentrations of FhHDM-1, and subsequently incubated with the dextran-conjugates (for a period of 1h to allow sufficient time for maturation of early endosomes to lysosomes; a process that takes approximately 40 min[194]). In addition, some samples were pre-incubated with cytochalasin D, which inhibits actin polymerisation (to prevent vesicular transportation and thus endocytosis[61,

[165]) or with the known specific vATPase inhibitor, concanamycin[213] (to assess the effects on acidification), instead of FhHDM-1 treatment, prior to incubations with dextran conjugates to act as inhibitory controls for comparative purposes.

As expected, the incubation of macrophages with cytochalasin D significantly reduced the uptake of dextran-647 ($p \leq 0.001$). In contrast, cells pre-treated for 1h with the highest concentration of FhHDM-1 used (50µg/mL) showed a significant increase in the amount of fluorescence attributable to dextran-647 uptake ($p \leq 0.001$) (Figure 4.1 A & B: right panels). Similar to the 1h FhHDM-1 pre-treatment period, the extended treatment protocol of 20h, also significantly ($p \leq 0.0001$) enhanced the endocytosis of dextran (Figure 4.1 C: right histograms) by macrophages.

The intensity of fluorescence emitted by pHrodo dextran (Figure 4.1 A & B left panels) was significantly reduced after a 1h pre-incubation of macrophages with concanamycin A ($p \leq 0.0001$). A slight increase in lysosomal acidification levels (pHrodo dextran detection) was observed in samples where macrophages had been pre-incubated for 1h with 20µg/mL FhHDM-1 ($p \leq 0.05$), which was consistent with an increase in dextran uptake. These observations are likely attributable to an accumulation of undigested endocytosed material, which normally induces an increase in lysosome numbers and therefore expands the overall availability of acidified vesicles[194]. However, a significant decrease ($p \leq 0.0001$) in the detected fluorescent signal was evident when macrophages were pre-treated with 50µg/mL FhHDM-1 for 1h, prior to the addition of pHrodo dextran (Figure 4.1 A & B: left panels). Analyses of fluorescence emission by pHrodo dextran in macrophage samples pre-treated with FhHDM-1 for 20h was not possible, as a resultant increase in auto fluorescence in the pHrodo dextran detection channel made the interpretation of results unreliable (Figure 4.1 C: left panels). Collectively, these data indicate that, the highest concentration FhHDM-1 tested at 1h pre-incubation, was capable of compensating for the increase in dextran uptake/lysosomal number in macrophages, and resulted in an overall decrease in lysosomal acidification.

Simultaneous incubation with 50 and 100µg/mL FhHDM-1 and dextran-647 for 1h revealed a significant increase in dextran endocytosis (Figure 4.2 A: right panels) ($p \leq 0.0001$) which, as can be seen in both the histogram and graphic representations (Figure 4.2 A & B), was even more profound than the increase in uptake induced by 1h

pre-treatment of macrophages with FhHDM-1 prior to dextran-647 incubation (Figure 4.1). However, simultaneous incubation of macrophages with FhHDM-1 and pHrodo dextran revealed that vesicular acidification was maintained at the levels observed when only pHrodo dextran was incubated with the cells, that is, FhHDM-1 did not induce any changes to lysosomal pH, at least at the concentrations tested. Even increasing the FhHDM-1 concentration up to 100μg/mL exerted no effect under these conditions (Figure 4.2 A: left panels).

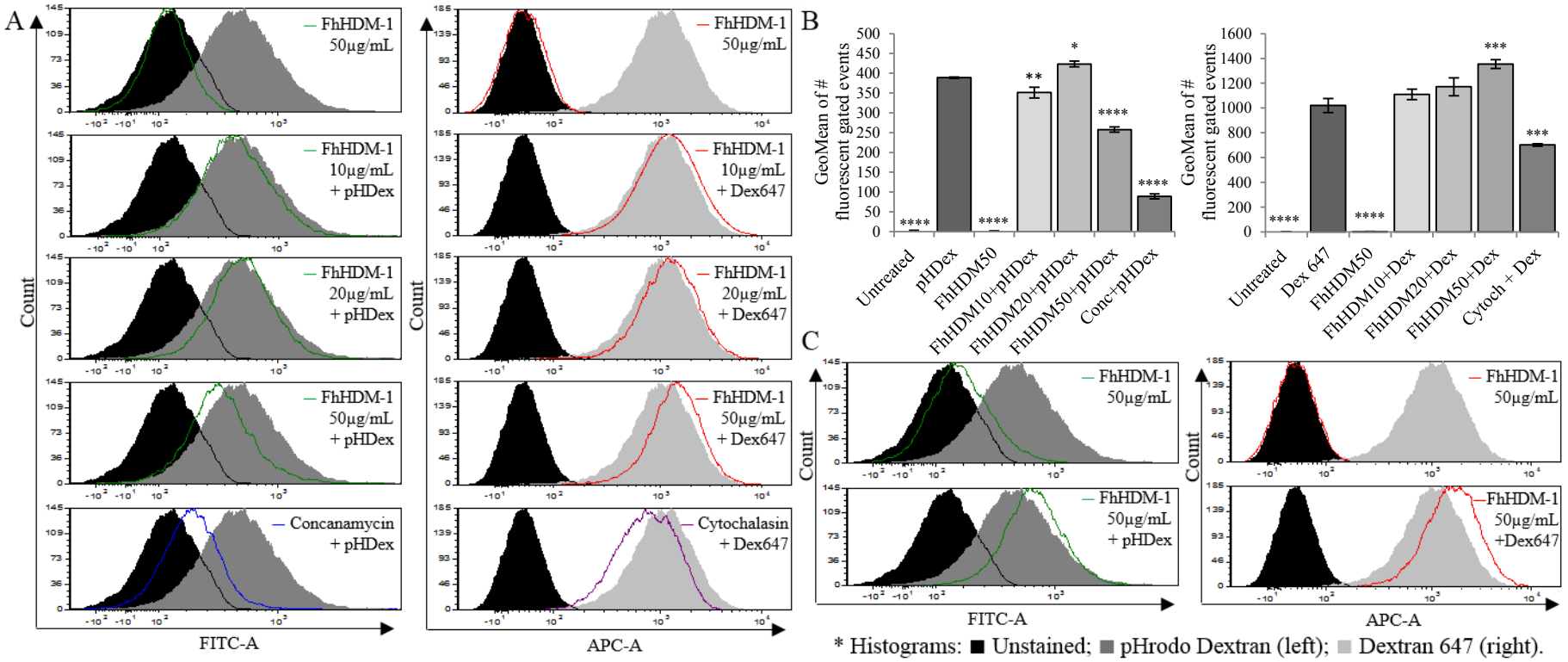

Figure 4.1 Macrophage pre-treatment with FhHDM-1 decreased dextran detection in acidified vesicles but not its endocytosis. Histograms (A) and geometric mean analyses (B) of fluorescence intensity measured in RAW264.7 murine macrophages pre-incubated with FhHDM-1 or concanamycin (0.866µg/mL) for 1h, or co-incubated with cytochalasin D (2µg/mL), followed by incubation with 10µg/mL pHrodo dextran (left panels) or with dextran-647 (right panels). Data representative of two individual experiments performed in triplicate. Statistically significant differences were determined by ANOVA followed by Dunnett's test, using pHDex or Dex647 as controls (*, $p \leq 0.05$; **, $p \leq 0.01$; ***, $p \leq 0.001$; ****, $p \leq 0.0001$). Histograms in (C) correspond to results using an FhHDM-1 pre-incubation period of 20h, as opposed to 1h.

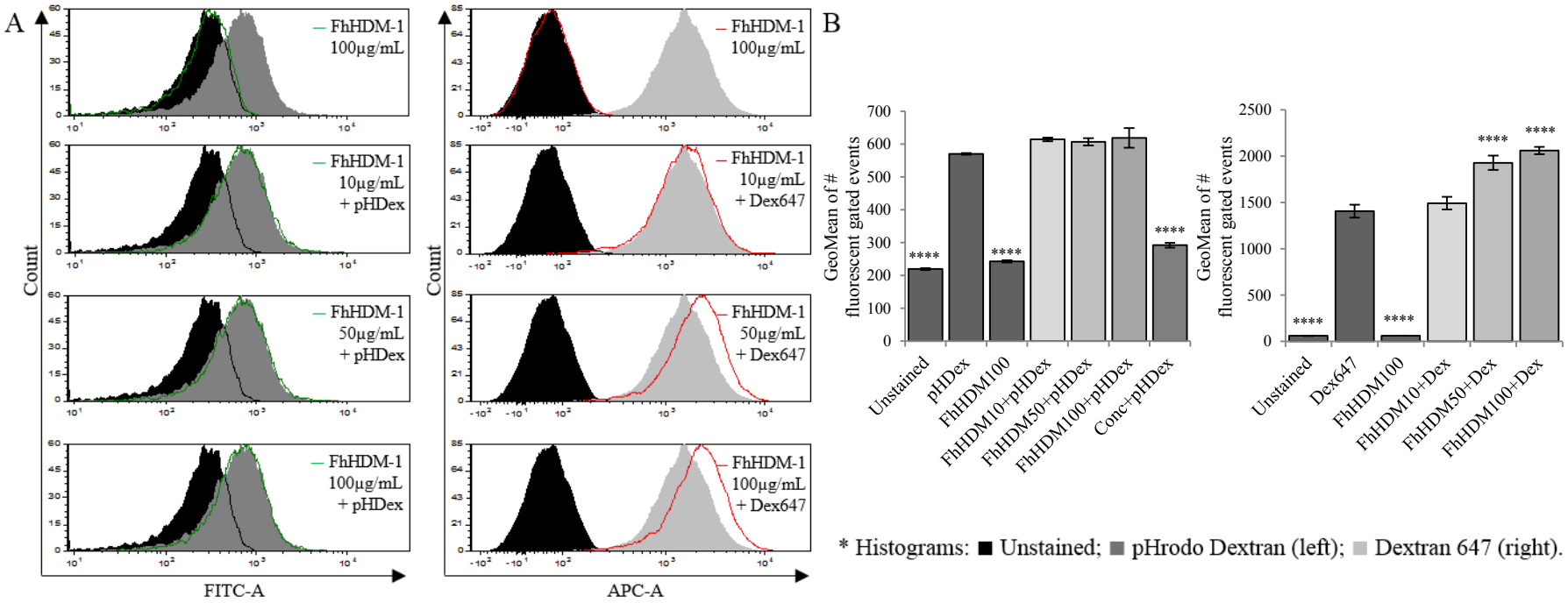

Figure 4.2 Simultaneous incubation of macrophages with FhHDM-1 did not affect the detection of dextran in acidified vesicles, but it did increase the uptake of dextran. Histograms (A) and geometric mean analysis (B) of RAW264.7 murine macrophages simultaneously incubated with FhHDM-1 (at increasing concentrations) and pHrodo Dextran (A & B left panels) or Dextran 647 (A & B right panels). The provided data is representative of two individual experiments performed in triplicate for each sample treatment. Statistically significant differences were determined by ANOVA followed by Dunnett's test, using pHDex or Dex647 as controls (****, $p \leq 0.0001$).

Although flow cytometry is a useful quantitative technique, it cannot establish the intracellular location of a fluorescent signal. Considering that pHrodo Dextran does not emit a fluorescent signal unless it is exposed to an acidic pH[212], it was important to determine whether the decrease in emissions of fluorescence by this molecule, in the presence of FhHDM-1, was attributable to a reduction in lysosomal acidification or to impaired endocytosis of dextran. The obtained data after incubation of macrophages with FhHDM-1 and dextran-647 suggested that an increase in lysosomal pH was most likely occurring. However, as an additional method of assessment, confocal microscopy was employed. For these experiments, BALB/c BMDMs were incubated with a combination of dextran-647 and Alexa 488-conjugated FhHDM-1 (Figure 4.3). Corroborating the flow cytometry data, neither pre-treatment nor simultaneous incubation of macrophages with FhHDM-1 impaired the endocytosis of dextran. In fact, in comparison to cells treated with dextran only, macrophage populations additionally treated with FhHDM-1 had larger numbers of dextran-containing cells with brighter foci of fluorescence emitted by dextran, suggesting that endocytosis was increased in the presence of FhHDM-1. Furthermore, comparison of pre-incubated versus simultaneously incubated samples indicated that the latter conditions induced a significantly higher rate of dextran endocytosis (Figure 4.3 G $p= 0.0044$), which is in agreement with the flow cytometry analyses. Additionally, a degree of co-localisation (observed as yellow fluorescent foci) of FhHDM-1 and dextran was observed, which suggested that both molecules were simultaneously contained within the same endocytic compartments, when macrophages were both pre-treated and simultaneously treated with FhHDM-1 and dextran (Figure 4.3 C, D & G). However, the latter experimental conditions seemed to facilitate a greater degree of co-localisation (Figure 4.3 G $p= 0.0038$). Additionally, simultaneous incubation of FhHDM-1 and dextran with primary human macrophages yielded similar results, indicating that this effect was not species specific (Figure 4.3 E & F).

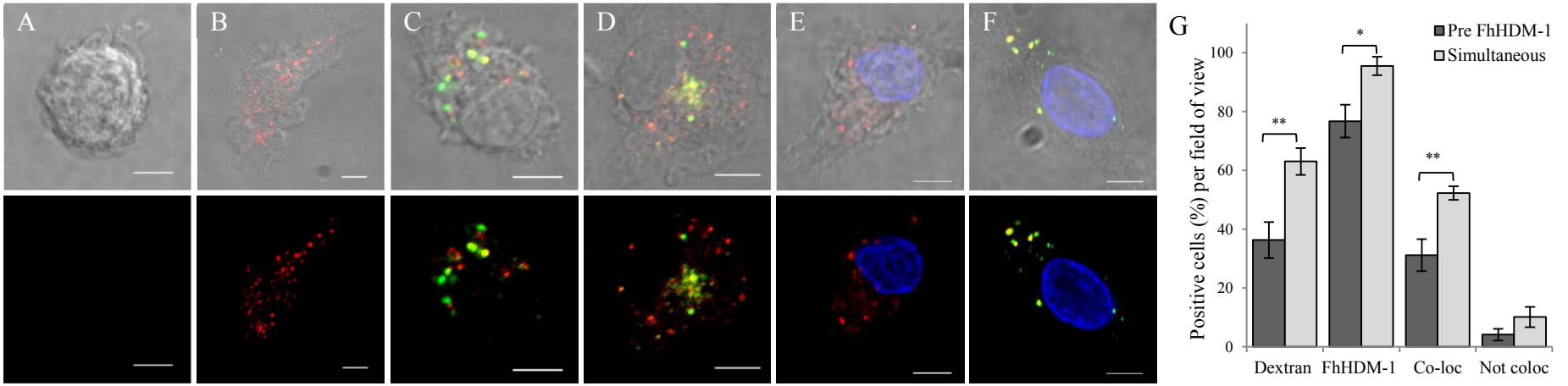

Figure 4.3 Macrophages treated with FhHDM-1 can endocytose dextran and simultaneous incubation with both molecules enhanced the co-localisation of FhHDM-1 and dextran. Representative immunofluorescence images obtained by confocal microscopy of BALB/c BMDMs (A-D) or primary human macrophages (E & F) that were either untreated (A), incubated with dextran-647 (red fluorescence) only (B & E), pre-treated with Alexa 488-conjugated sFhHDM-1 (green fluorescence) prior to incubation with dextran-647 (C), or simultaneously incubated with both molecules (D & F). Co-localisation (C, D & F) can be observed as yellow fluorescence and DAPI (E & F; blue fluorescence) was used for nuclear identification (100x objective; scale bar: 5µm). Provided images are representative of five fields of view per sample treatment and the experiment was performed twice. Graphical representation (G) after quantitation of numbers of cells imaged per field of view of samples (C- pre-treatment) and (D- simultaneous) where Dextran 647 and sFhHDM-1 uptake were detected (Co-loc denotes the presence of co-localisation and Not-coloc refers to cells where both molecules were identified but did not co-localise to the same vesicular region). Statistically significant differences between sample treatments were determined by t-tests (*, $p \leq 0.05$; **, $p \leq 0.01$).

4.3.2. FhHDM-1 REDUCES ANTIGEN PROCESSING BY MACROPHAGES

Given the ability of FhHDM-1 to reduce lysosomal acidification within macrophages, it was of interest to determine the impact that this phenomenon would have on the biological activity of these cells. The best characterised function of the acidified lysosome is the enzymatic degradation of proteins into smaller peptides, for presentation by MHCII molecules to $CD4^+$ T cells. To assess this, DQ ovalbumin (DQ Ova), a full-length ovalbumin protein heavily labelled with the fluorescent pH independent dye, BODIPY[214, 215], was used. This dye is present in such an abundance that its molecules interact, such that the complex becomes spontaneously quenched within the folded ovalbumin protein, thereby rendering the unprocessed DQ Ova non-fluorescent. However, upon protease digestion of the ovalbumin protein, this quenching effect is lost, and the resulting DQ Ova peptides become highly fluorescent[214, 215]. Furthermore, the accumulation of the digested peptides within lysosomes, results in high concentrations of the fluorescent dye in a confined space, leading to the formation of excited dimers (excimers). The presence of these excimers causes a gradual shift in fluorescence emission from green (516nm) to red (540-600nm). Therefore, the intensity of red fluorescence is indirectly proportional to the enzymatic activity of lysosomal hydrolases, and reflects the efficiency of antigen processing[214-216].

RAW264.7 murine macrophages were either pre-treated or simultaneously treated with FhHDM-1 (10, 50 or 100μg/mL) and with DQ Ova (Figure 4.4 B-D). Only the simultaneous incubation of FhHDM-1 (at 50 or 100μg/mL) and DQ Ova resulted in a significant reduction in fluorescence emitted by processed DQ Ova aggregates, as detected by flow cytometry, in a concentration-dependent manner (Figure 4.4 C&D $p \leq 0.0001$). Analysis of cells treated with FhHDM-1 only further indicated that FhHDM-1 was not contributing to the detection of red fluorescence, and, accordingly, this observation was attributable to fluorescence emitted by DQ Ova only (Figure 4.4 A).

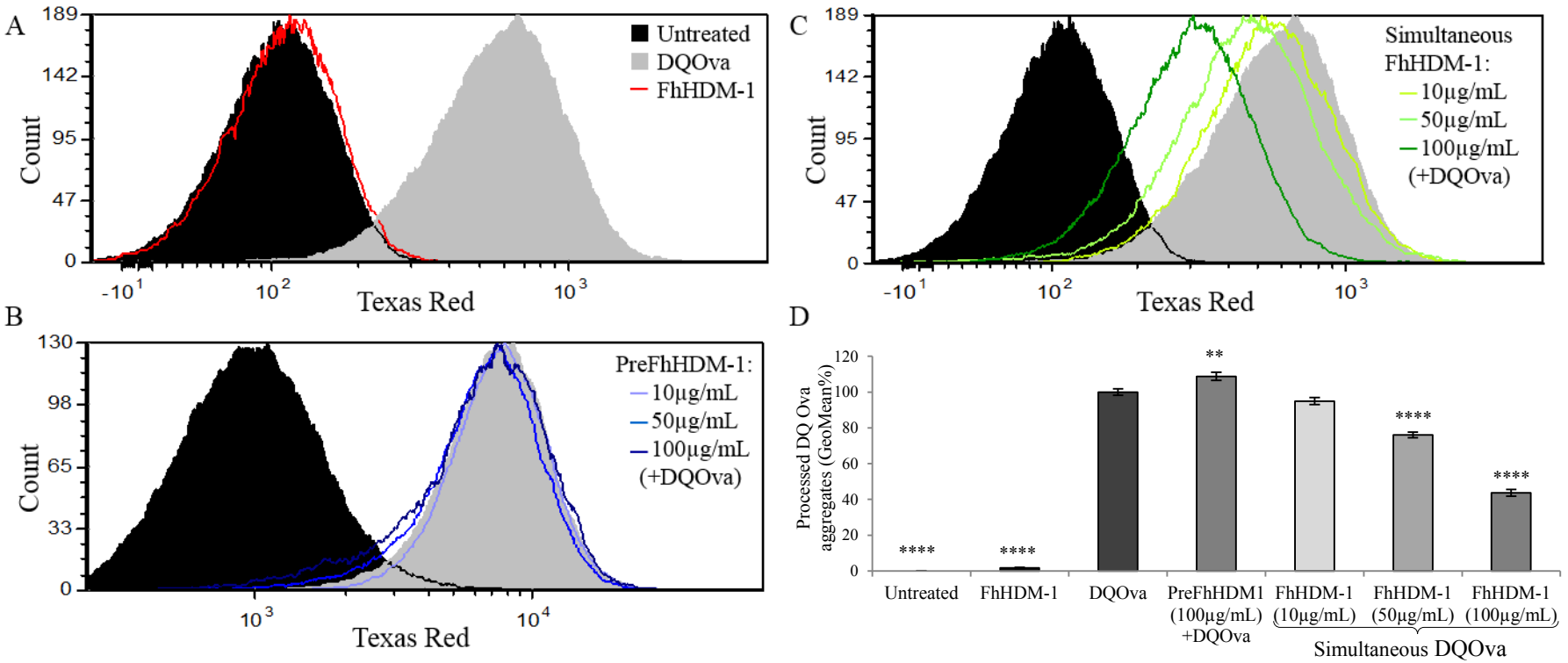

Figure 4.4 Simultaneous incubation with FhHDM-1 and ovalbumin reduces the ability of macrophages to process antigen. RAW264.7 murine macrophages were untreated, incubated with DQ Ova only, or sFhHDM-1 only as controls. Also cells were either pre-incubated with sFhHDM-1 prior to incubation with DQ Ova, or simultaneously treated with both sFhHDM-1 and DQ Ova, with increasing concentrations of sFhHDM-1. Fluorescence emitted by the degraded aggregates of processed DQ Ova was detected by flow cytometry. Histograms (A-C) and graphed geometric means (D) with their respective statistical analysis (ANOVA followed by Dunnett's test using the DQ Ova sample as control) are provided (**, $p \leq 0.01$; ****, $p \leq 0.0001$). Data is representative of two individual experiments performed in triplicate.

4.3.3. EFFECTS OF FHHDM-1 ON ANTIGEN PRESENTATION BY MACROPHAGES

The significant reduction in ovalbumin processing by macrophages, induced by FhHDM-1, suggested that the ability of these cells to present antigenic peptides to $CD4^+$ T cells was likely to be impaired. To assess this, C57BL6 BMDMs were primed with IFNγ for 24h (to make the cells conducive to antigen presentation via inducing up regulation of MHCII expression levels[141]), followed by 1h incubation with the vATPase inhibitor, concanamycin A[213], or FhHDM-1. After this, macrophages were incubated with full-length ovalbumin (Ova) for 6h, which is sufficient time to allow uptake and initiation of antigen processing. A second set of samples was simultaneously incubated with FhHDM-1 and Ova. To confirm that any effects on T cell proliferation observed were attributable to impaired processing, as opposed to an effect on the presentation of peptides, cells were also incubated with pre-processed ovalbumin antigenic peptide (323-339). In this latter case, the presentation of peptide would occur independently of processing mechanisms[141].

Subsequent to their incubation with Ova or Ova peptide, macrophages were co-incubated with splenic $CD4^+$ T cells, isolated from transgenic mice (OTII mice) whose T cells express a TcR that specifically recognises ovalbumin peptides[217]. After 24h, culture supernatants were collected, and the secretion of IL-2 by T cells was measured as an indication of their activation and expansion due to presentation of cognate antigen, Ova[141]. As expected, IL-2 was secreted by T cells that were co-incubated with macrophages treated with Ova and Ova peptide (Figure 4.5). In agreement with the DQ Ova data, pre-incubation of macrophages with FhHDM-1 had no significant impact on T cell proliferation. In contrast, the simultaneous incubation of macrophages with FhHDM-1 and Ova resulted in a significant reduction ($p \leq 0.001$) in the secretion of IL-2 by T cells, indicating a reduction in T cell proliferation. A significant reduction ($p \leq 0.0001$) in IL-2 secretion was also observed when T cells were co-incubated with macrophages pre-treated with concanamycin A. Incubation of macrophages with FhHDM-1 had no impact on their ability to present Ova peptide to T cells, as the levels of IL-2 secreted were the same as those observed for the positive control samples. These data thus confirmed that FhHDM-1 was specifically inhibiting the processing of proteins into peptides for presentation by MHCII molecules.

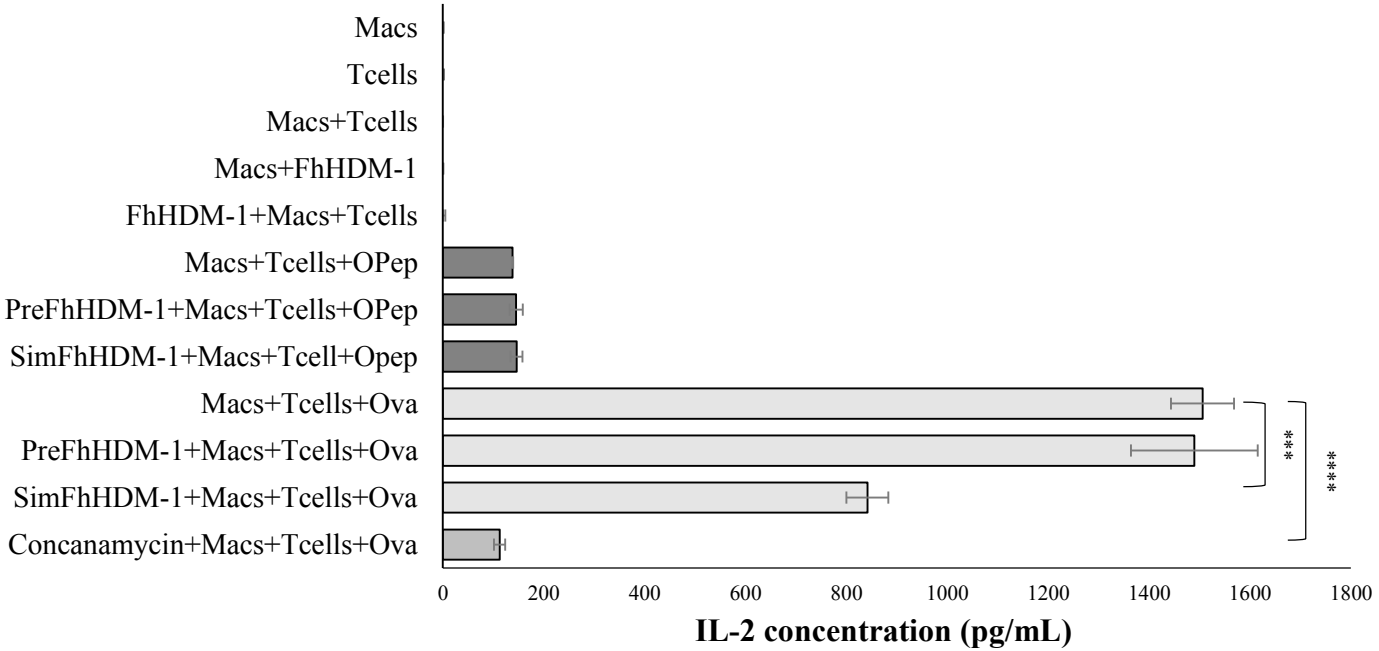

Figure 4.5 FhHDM-1 reduces the ability of macrophages to process antigenic peptides for their presentation to T cells. C57BL6 BMDMs were primed with IFNγ (to up regulate MHCII expression) prior to either pre-treatment or simultaneous incubation with FhHDM-1 and full-length ovalbumin (Ova) or ovalbumin peptide (OPep); to independently assess the effects of FhHDM-1 on antigen processing or presentation by macrophages, respectively. As a readout for antigen presentation, macrophages were then co-cultured with T cells isolated from OTII mice, which specifically proliferate in response to presentation of ovalbumin derived antigenic peptide. An ELISA was used to measure IL-2 secretion by T cells, which is indicative of T cell activation and subsequent proliferation. Triplicate optical density readings detected at 450nm (with a 570nm correction), were converted to IL-2 concentrations for graphical representation. Statistically significant differences in samples treated with Ova were determined by ANOVA followed by Dunnett's test, using the Macs+Tcells+Ova sample as control (***, $p \leq 0.001$; ****, $p \leq 0.0001$).

These findings support the hypothesis that the lysosomal localisation of FhHDM-1 allows this peptide to exert its biological impact on the organelle, that is, by inhibiting the ability of macrophages to process, and subsequently present antigens. However, to further confirm the specific nature of this inhibition, the influence of FhHDM-1 on the expression of MHCII was assessed. Expression levels of MHCII molecules are increased after exposure to IFNγ, via mechanisms which are lysosomal-independent[218]. Thus, BALB/c BMDMs were incubated with FhHDM-1 (50μg/mL), IFNγ (10ng/mL), or the combination of FhHDM-1 and IFNγ for periods of 2h (untreated cells served as a negative control). Macrophages were stained with antibody against MHCII molecules and analysed by flow cytometry. Importantly, the expression of surface MHCII was above the fluorescence detected for isotype only treated samples, thereby indicating antibody specificity (Figure 4.6 Histogram).

Incubation of macrophages with FhHDM-1 alone did not significantly increase expression levels of MHCII molecules above the levels observed for untreated macrophages (Figure 4.6). This data suggested that FhHDM-1 did not activate macrophages. In contrast, and as expected, incubation of macrophages with IFNγ significantly enhanced MHCII expression levels ($p \leq 0.0001$), which were not influenced by the presence of FhHDM-1, even with incubation periods of up to 2h in duration, which were longer than those used for the antigen presentation experiments.

Overall, these results suggest that the observed decreases in antigen processing and subsequent presentation by macrophages, induced by exposure to FhHDM-1, occurred as a result of reduced endolysosome acidification, and were not attributable to an effect on the surface expression levels of MHCII molecules.

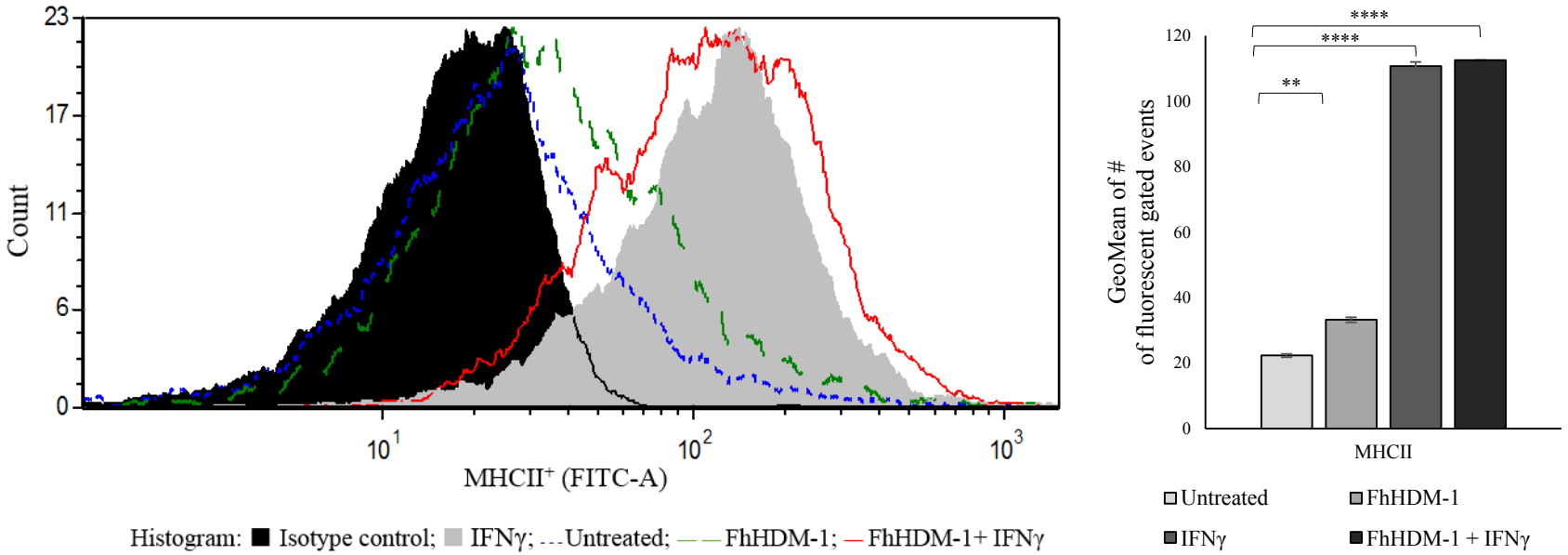

Figure 4.6 FhHDM-1 did not alter MHCII expression levels by macrophages. BALB/c BMDMs were either untreated or incubated with FhHDM-1 (50µg/mL), IFNγ (10ng/mL), or with both FhHDM-1 and IFNγ, for periods of 2h, and then stained with anti-MHCII or isotype control antibodies. Histogram and graphical representation (geometric means) of MHCII expression levels, as determined by flow cytometry analyses, are provided and are representative of two individual experiments performed in duplicate for each sample treatment. Statistically significant differences between sample treatments were determined by ANOVA followed by Dunnett's test, using the untreated sample as control (**, $p \leq 0.01$; ****, $p \leq 0.0001$).

4.4. Discussion

The capacity of macrophages to endocytose extracellular material was not prevented by their incubation with FhHDM-1. However, treatment of macrophages with this peptide did interfere with the generation and/or maintenance of optimally acidified environments within the lysosomal luminal regions. As a consequence, FhHDM-1 prevented the efficient processing of proteins into peptides by hydrolases. This phenomenon exerted a direct negative impact upon the ability of macrophages to subsequently present antigenic peptides (in the context of MHCII) to $CD4^+$ T cells, thus preventing T cell activation and proliferation. Collectively, this data provides evidence for a mechanism by which FhHDM-1 may regulate the mammalian immune system; namely by modifying the lysosomal-related functions of macrophages.

The data obtained from the dextran endocytosis experiments, suggested that FhHDM-1 did not impair the efficiency with which macrophages internalised dextran (Figures 4.1-4.3). In fact, simultaneous incubation of macrophages with both FhHDM-1 and dextran, actually induced increased endocytosis of the latter. This could simply be a result of macrophages being activated, and thus more prone to phagocytosis, as a consequence of their interaction with extracellular peptides. To establish if this is the case, or if by the contrary, is an effect specifically induced by FhHDM-1, similar experiments using alternative peptides or proteins, in parallel to FhHDM-1, in dextran internalization studies would be required.

The fluorescence emitted by endocytosed pHrodo dextran, in macrophages pre-incubated with FhHDM-1, was reduced, suggesting an impairment in endolysosomal acidification within these cells. However, such reduction did not occur with simultaneous incubation of macrophages with FhHDM-1 and dextran, as in this scenario basal acidification levels within lysosomes were maintained (Figures 4.1-4.2). Taken together, the suggested maintenance of consistent vesicular acidification with increasing rates of endocytosis (detected in the simultaneously treated samples), essentially imply that FhHDM-1 could be preventing the overall rise in vesicular acidification, that would otherwise occur as a result of undigested endocytosed material stimulating an increase in number of available acidified endolysosomes within the cells[194]. This likely signifies that the resulting endolysosomes are not optimally acidic, thereby justifying the observed reduction in processing of DQ Ova (Figure 4.4). Pre-

incubation with the highest concentrations of FhHDM-1 tested appeared to overcompensate for the increased rate of internalisation, causing a more profound reduction in the detection of pHrodo dextran fluorescence (suggesting a decrease in acidification levels). However, if these effects on vesicular acidification were only transient, it is possible that macrophages were capable of recovering their processing abilities upon removal of FhHDM-1 (Figure 4.4). This premise would explain why no significant changes in antigen processing or presentation were detected when macrophages were pre-incubated (as opposed to co-incubated) with FhHDM-1 (Figure 4.5).

Based on the data presented here, there are two potential mechanisms by which FhHDM-1 may be modulating macrophage function. Firstly, the internalised cargo (dextran or ovalbumin) could have been successfully transported to reach its final lysosomal destination. However, due to a more alkaline lysosomal lumen (as indicated by decreased pHrodo dextran fluorescence), induced by the direct effects of FhHDM-1 on lysosomal vATPase function, the internalised cargo could not be efficiently processed. An alternative mechanism supported by the data is that, FhHDM-1 may be interfering with the process of endocytosis-associated vesicular maturation, thereby preventing the reformation of fully acidified (cargo containing) lysosomes.

The possibility that FhHDM-1 was directly inhibiting vATPase activity corroborates previous *in vitro* studies, which demonstrated that FhHDM-1 inhibited ATPase activity in endolysosome enriched membrane preparations, which contain vATPases[114]. Evidence demonstrating that several cationic peptides, which also display characteristic α-helical amphipathic structures, act as potent ATPase inhibitors, supports such an inhibitory role for FhHDM-1[219-221]. This biochemical data, in combination with the cellular localisation of FhHDM-1, support the premise that FhHDM-1 directly inhibits the acidification of lysosomal vesicles, via inhibition of vATPase activity (Figures 4.1, 4.2, 4.4 & 4.5). However, definitive experiments where a direct interaction between FhHDM-1 and vATPases is demonstrated to exist, are yet to be completed.

While confocal microscopy analyses clearly demonstrated the internalisation and localisation of dextran to the cytoplasmic regions of macrophages (Figure 4.3), it did not specifically reveal the identity of the endocytic vesicles that contained the cargo. On that account, FhHDM-1 may be alternatively functioning to prevent the full maturation

of intracellular endolysosomal structures into acidified vesicles. Aside from its role in maintaining optimal luminal pH, vATPase subunits are also involved in the process of endocytic vesicle maturation, transportation, interaction, and fusion with lysosomes, although the specific mechanisms are yet to be fully elucidated[194, 222-224]. Preliminary proteomic analyses of macrophages incubated in the presence of FhHDM-1, revealed a significant reduction in expression levels of the vATPase subunit, V_0-isoform a3, which is specific to vATPases located within lysosomal membranes[142, 222, 225, 226]. In the absence of this subunit, vATPases may not assemble correctly, thereby rendering them unable to perform their functions as proton pumps or to exert effects required at earlier points in the process of endolysosomal maturation. Further evidence that acidic vesicles may not be formed correctly after treatment with FhHDM-1, comes from the demonstration that the expression levels of lysosomal membrane proteins, such as CD63 and LAMP1, were also significantly down-regulated in FhHDM-1 treated macrophages, as compared to control cells[142]. It has been suggested that, via inducing a sequence of functional associations between ATPase subunits and clathrin adaptor complexes, CD63 assists in the extended transportation of associated proteins from the cell surface to late endosomes and lysosomes[227]. Additionally, it has been demonstrated that LAMP1 performs roles in endosomal motility within microtubules, vesicular interactions, and recruitment of Rab7, thereby regulating endocytic vesicular maturation events. Furthermore, LAMP1 depletion, along with that of LAMP2, has been shown to result in an arrest of endocytosis[228].

Fully elucidating the impact of FhHDM-1 upon the maturation process of endocytic vesicles, and, therefore, the complete transportation pathway from uptake to delivery to lysosomes, is a challenging objective. Endocytosis is a continuous and asynchronous process, and, therefore, particles at different stages of the internalisation process can be detected at any one point in time. Additionally, due to the transient association of molecular markers with the different stages of the maturing organelles, even pulse chase approaches are unable to completely elucidate the endosome maturation process[204]. One approach to achieve this aim would be to perform quantitative confocal microscopy studies, in which macrophages are simultaneously labelled with early and late endosomal, as well as lysosomal markers, in the presence of dextran or ovalbumin, fluorescently labelled with a pH-independent fluorophore. Alternatively, electron microscopic studies, after the labelling of organelles with

colloidal gold conjugated antibodies, could be employed to track the internalisation of molecules and particles and to identify endolysosomal fusion events in FhHDM-1-treated macrophages[204, 229]. Additionally, a detailed profile of the maturation process could be achieved by subcellular fractionation of macrophages. By separating the specific cellular fractions using sucrose gradients, analysis of individual organelles could then be performed by SDS-PAGE and western blotting (using organelle specific markers, such as Rab5 for early endosomes, Rab7 or mannose 6 phosphate receptors for late endosomes, and LAMP1 or LAMP2 for lysosomes)[204, 230]. This approach may aid in identifying the relative abundance of each vesicular maturation stage occurring after dextran internalisation by FhHDM-1 treated macrophages, thereby enabling indirect tracking of the degree of endocytic vesicle maturation. Furthermore, proteomic analysis of isolated lysosomes would provide reliable data to determine the specific lysosomal proteins (including vATPase subunits) that are modulated by FhHDM-1.

Both scenarios proposed to explain the mechanism by which FhHDM-1 may be modulating macrophage activity (namely; that FhHDM-1 may be inhibiting the ability of vATPases to maintain fully acidified lysosomal lumens or alternatively that FhHDM-1 could be preventing vesicular maturation during endocytosis), support the ultimate reduction in antigen presentation by macrophages observed after treatment with FhHDM-1. In fact, the scenarios proposed may not be mutually exclusive and may operate synergistically to modulate the ability of FhHDM-1 treated macrophages to process antigen. Additionally, the current study showed that FhHDM-1 exerted no direct effect on the ability of macrophages to present pre-processed ova peptide, and subsequently activate T cells. The observation that FhHDM-1 did not modulate surface expression levels of MHCII further corroborates the premise that antigen presentation events were not being directly influenced. Antigen presentation not only relies on the availability of sufficient numbers of MHCII molecules to present antigen on the cell surface, but also on the actions of lysosomal hydrolases. Cathepsin S is responsible for cleaving the invariant chain that occupies the antigenic peptide binding groove of MHCII molecules prior to peptide loading. Contrary to other lysosomal cysteine proteases, cathepsin S is stable at neutral and slightly alkaline pH environments[199], which would indicate that changes in lysosomal pH, as are induced by FhHDM-1, would not interfere with this process, as was observed in the current study.

In addition to a reduction in lysosomal processing of internalised antigen, the modulation in lysosomal acidification induced by FhHDM-1, is likely to impact upon additional pathways that rely on the establishment of a low pH environment. For example, the activation of many endosomal/lysosomal TLR receptors is dependent upon vesicular maturation and the acidic environment of the macrophage lysosome[231-233]. Furthermore, a number of lysosomal cysteine proteases, which require luminal acidification to become activated, translocate to the cytoplasm, where they initiate signalling cascades, which lead to inflammasome activation[210, 234, 235], as well as modulating the processes that regulate apoptosis[236-238]. Therefore, by targeting lysosomal function, FhHDM-1 may exert downstream effects on multiple intracellular pathways, which collectively may cause immune modulation. Accordingly, FhHDM-1 may offer novel therapeutic strategies for the prevention and treatment of pathologies arising as a consequence of defective or excessive lysosomal activity.

CHAPTER 5 FHHDM-1 REDUCES NLRP3 INFLAMMASOME ACTIVATION IN MACROPHAGES

5.1. Introduction

The ability of FhHDM-1 to reduce lysosomal acidification suggested that this peptide likely affects a number of biological functions that are mediated by macrophages, aside from disrupting the processing (and so, by default, presentation) of antigens. In general, lysosomal proteases display optimal enzymatic activity in acidic pH environments. However, cathepsin B activation is particularly dependent upon such conditions, as it undergoes structural relaxation at low pH, which optimises its conformation for interaction with substrates[199, 208]. Beyond its role within the lysosome, the release of cathepsin B into the cytosol has been linked to the activation of the NLRP3 inflammasome[210, 239, 240]. Therefore, by inhibiting the acidification of lysosomes, and thus the activation of lysosomal proteases, FhHDM-1 may prevent NLRP3 activation.

Inflammasome protein complexes are formed in response to cellular danger or stress signals, and their assembly relies upon the activity of the cytosolic sensors, nucleotide-binding oligomerisation domain protein (NOD)-like receptors or NACHT-leucine-rich repeat receptors (NLRs)[241-243]. These receptors trigger a cascade of events that culminate in the production of the cytokines IL-1β and IL-18[241, 244, 245]. Through interaction with their specific receptors, these cytokines drive various downstream effects, such as the activation of innate immune cells (monocytes, macrophages and neutrophils), stimulation of cytokine secretion (including IL-6, IFNγ and IL-4), induction of leukocyte migration, as well as the activation and differentiation of T cells towards Th17 or Th1 (via the actions of IL-1β or IL-18, respectively)[241, 244, 245]. In addition, excessive inflammasome activation can also drive cells towards pyroptosis, which is a caspase-1-mediated programmed cell death process[245-247].

Although a number of subfamilies of NLRs exist, only NLRP1, NLRP3, NLRC4 (IPAF), and absent in melanoma 2 (AIM2) are known to be involved in the formation of inflammasomes[241, 243, 245, 248]. Of these, the NLRP3 inflammasome, which is primarily expressed in cells that perform immune-related functions, including macrophages,

epithelial cells, and osteoblasts[243], is arguably the best characterised inflammasome to date[245]. For the NLRP3 inflammasome to become activated, two major events must occur. Firstly, cells need to be primed (Signal I). Typically, this occurs through the activation of TLR4[246], which leads to the activation of NF-κB, and the subsequent transcription of the inactive precursors of the inflammatory cytokines, IL-1β and IL-18 (proIL-1β and proIL-18, respectively)[245, 246, 248, 249] (Figure 5.1 A). This priming event also increases the rate of transcription and translation of NLRP3[245, 246, 249].

In its resting state, NLRP3 exists in a monomeric form (Figure 5.1 B), which renders it inactive. A second trigger (Signal II), typically associated with cellular damage or stress (Figure 5.1 C), induces the oligomerisation of NLRP3 in the NACHT domain, yielding a multi-protein, high molecular weight complex that comprises the functional inflammasome (Figure 5.1 D)[241, 243, 245]. The assembly of the NLPR3 inflammasome complex brings pro-caspase-1 molecules into close proximity, allowing auto-catalysis to occur, which releases the activated form of caspase-1 (Figure 5.1 E). Caspase-1 then cleaves proIL-1β and proIL-18 (Figure 5.1 F), which is required for the activation and extracellular release of these cytokines. The secretion of active IL-1β by cells, is widely accepted to represent the end point of the process of NLRP3 inflammasome activation[241, 248, 250].

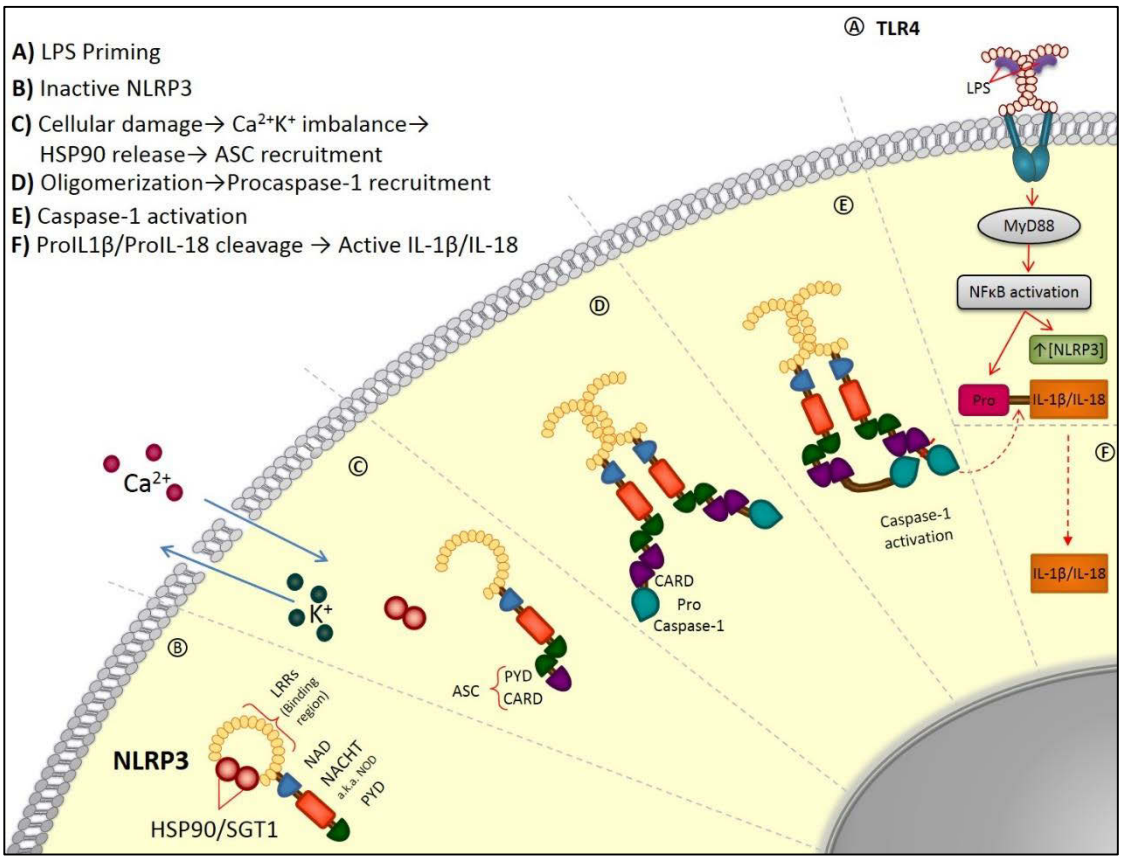

Figure 5.1 NLRP3 activation pathway. The first trigger (Signal I) required for NLRP3 activation is a priming event (A) that consists of LPS-induced activation of TLR4, which stimulates the production of proIL-1β, proIL-18, and enhances NLRP3 expression levels, via a MyD88/NF-κB dependent pathway[245, 246, 248, 249]. Inactive monomeric NLRP3 (B) contains a HSP90/SGT1 motif that acts as a chaperone molecule (which stabilises NLRs allowing their accumulation whilst simultaneously preventing aggregation). HSP90/SGT1 dissociates (C) upon the presence of cellular damage/stress signals (Signal II)[241, 243, 251, 252]. This causes apoptosis associated speck like protein (ASC)[243] recruitment and enables the oligomerisation of available NLRP3 monomers into a complex that comprises the functional NLRP3 inflammasome (D). The presence of ASC adaptor proteins in this complex mediates pro-caspase-1 recruitment (D). Subsequent autocatalysis of the associated pro-caspases-1 leads to caspase-1 activation (E), consequent proIL-1β and proIL-18 cleavage, and release of the biologically active forms of IL-1β and IL-18 (F)[241, 248].

An increasing number of diverse signals have been identified as activating factors for the NLRP3 inflammasome. Initially, it was suggested that the sole trigger was the efflux of potassium ions and influx of calcium ions, due to a compromised cellular membrane (Figure 5.1 C)[253]. However, further research has identified multiple alternative events that can also deliver this second signal[245], these include the release of mitochondrial reactive oxygen species (ROS)[239] and lysosomal dysfunction[210].

The uptake of large, endogenous, host-derived, damage-associated molecules and environmental irritant aggregates, such as crystals (including mono sodium urate [MSU], silicon dioxide nanoparticles [Nano-SiO_2] and aluminium salts [ALUM]), has been directly associated with lysosomal swelling. This process eventually leads to destabilisation of the lysosome, and subsequent release of active cathepsin B into the cytoplasmic region, which induces the activation of the NLRP3 inflammasome[210, 234, 235, 245, 248]. It is widely accepted that the release of hydrolases into the cytosol, as opposed to the actual rupture of lysosomes, directly activates the inflammasome[210, 239, 240]. Indeed, inhibition of either cathepsin B activity or lysosomal acidification prevents the activation of NLRP3, even if lysosomal rupture does occur, suggesting that the released cathepsin B must be enzymatically active to perform its role in activating the inflammasome.

The lysosomal-associated pathway of NLRP3 activation described above contributes towards the development of several disease pathologies, including atherosclerosis (characterised by the aggregation of cholesterol crystals[254]), Alzheimer's disease (via amyloid beta accumulation in microglia lysosomes[234]), gout and pseudogout (via aggregation of monosodium urate [MSU] crystals[210, 240, 255]), and silicosis (with accumulation of silicon dioxide crystals[210]). Therefore, exploring the possibility that FhHDM-1 may interfere with lysosomal-associated NLRP3 activation may represent a putative therapeutic application for inflammatory diseases that involve NLRP3 inflammasome action.

5.2. Specific methods

5.2.1. FhHDM-1 effects on NLRP3 Inflammasome Activation

5.2.1.1. NLRP3 activation

BMDMs from BALB/c mice (Section 2.2.3.1.) were plated in 6 well plates ($2.5x10^6$ cells per well). Duplicate wells (i.e. $5x10^6$ cells in total) were used per sample treatment. Cells were primed by incubation with LPS (500ng/mL) in media (with equivalent volumes of PBS in media for vehicle control samples) for 3h at 37°C/5% CO_2[210]. Cells were then washed twice with PBS (RT) and incubated with FhHDM-1 at concentrations of 2.5, 5, 10, and 25μM (corresponding to 20, 40, 80, and 200μg/mL, respectively) in media, for 1h at 37°C/5% CO_2. After this time, cells were washed twice with PBS (RT) and incubated with the NLRP3 inflammasome activators: silicon dioxide nanoparticles (Nano-SiO_2) (Invivogen) for 6h, or aluminium crystals (ALUM) (Invivogen) O/N at a concentration of 500μg/mL in Opti-MEM reduced serum medium (Life Technologies).

Primary human macrophages (Section 2.2.3.2.), were plated into 96 well plates ($2x10^5$ cells per well in triplicate) and treated as described above for LPS primed, ALUM mediated NLRP3 activation, using FhHDM-1 at a concentration of 15μM (equivalent to 120μg/mL).

5.2.1.2. Cytokine detection by ELISA

Supernatants of NLRP3 activated cells (300μL/sample) were collected and stored at -20°C. Mouse and human IL-1β (BD OptEIA, California, USA) and mouse TNF (BD OptEIA) were assayed by ELISA, and protocols were performed according to manufacturer's recommendations (Section 2.5).

5.2.1.3. Detection of activated IL-1b and Caspase-1 by Western Blot

After the completion of ELISAs, the remaining supernatants (~4.5mL) were collected and stored at -20°C for protein precipitation. Adherent cells for each sample treatment were washed twice with PBS (RT), removed by scraping, and pelleted into single eppendorf tubes. Cell lysates were prepared by resuspending pellets in lysis buffer solution (10μL of radioimmunoprecipitation assay [RIPA] buffer [Sigma] per $1x10^6$ cells plus Halt protease inhibitor cocktail [Thermo Scientific, Massachusetts, USA] diluted 1/100 in RIPA buffer), and then incubating cells at 4°C for 30 min. This

was followed by centrifugation (16100*g*, 4°C for 15min). Supernatants were transferred to new eppendorf tubes, and, if not immediately used, stored at -20°C. Samples were prepared for western blotting by dilution in 4x loading dye (Life Technologies) to achieve a 1x solution containing a 1/25 dilution of 1M DTT (Life Technologies), followed by boiling at 95°C for 5min.

5.2.1.3.1. TCA supernatant protein precipitation

A 100% (w/v) working solution of trichloroacetic acid (TCA) (Sigma) was freshly prepared. To each sample, a volume of TCA (corresponding to 10% of total volume) was added and samples were incubated at 4°C for 2h in a spinning wheel. Pellets were collected by multiple rounds of centrifugation (20,000*g* for 15min, 4°C), pooled into a single eppendorf tube for each sample treatment, and washed twice with 500µL of ice-cold acetone. Supernatants were discarded and pellets were dried on a hot plate at 85°C to remove any residual acetone. Each pellet was re-suspended in 25-30µL of 1x NuPAGE® lithium dodecyl sulphate sample buffer (Life Technologies) containing a 1/25 dilution of 1M DTT. Samples were heated at 85°C for 5min, vortexed, and re-heated for 5min. If gel electrophoresis was not performed immediately, then samples were stored at -20°C until used.

5.2.1.3.2. Gel Electrophoresis

Samples (precipitated proteins and cell lysates) were centrifuged (16100*g* for 5min). Pre-stained Protein Standards-See Blue® Plus 2 (Life Technologies; 8µL) and samples (≤18µL per well) were loaded on NuPAGE® Novex® 4-12% Bis-Tris mini gels (Life Technologies), and run using NuPAGE® MES SDS running buffer (Life Technologies), diluted from 20x to 1x in ddH_2O, for 30min at 200 V.

5.2.1.3.3. Western Blotting

Protein transfer was performed using an iBlot and nitrocellulose transfer stacks (Life Technologies), following the manufacturer's instructions. Protein transfer was confirmed by staining the membranes with 0.1% Ponceau S/5% acetic acid (up to 10min or until protein bands were visible). Membranes were destained with ddH_2O, and blocked for 30min/RT in blocking solution (1% BSA/0.1% Tween/1x TBS) with rocking. This was followed by incubation (O/N at 4°C) with primary antibodies: anti-actin antibody (1/100, 1h) (Sigma) for lysate samples and anti-IL-1β (1/500, 3h) (Biovision), or anti-caspase-1 p10 (1/200, O/N used for pro-caspase-1 and active

caspase-1 detection) (Santa Cruz) for supernatant precipitated proteins. Membranes were then washed twice using 0.1% Tween 20/1x Tris Buffer Saline (TBS) followed by incubation with anti-rabbit IgG-whole molecule-peroxidase secondary antibody (diluted 1/10000 in blocking solution, 45min, RT) (Sigma). Membranes were incubated with peroxidase substrate-1 solution (Sigma) for 1min before excess solution was removed, and membranes were then imaged using a Chemidoc (Bio-Rad).

5.2.2. ASC SPECK FORMATION

ASC cells (kindly donated by Dr Hornung, University of Bonn, Germany), which stably express high levels of cerulean-tagged ASC and NLRP3-Flag, were seeded at a density of $2.5x10^5$ per well into 4 well culture slides (In Vitro Technologies, Lane Cove West, Australia), and allowed to adhere O/N. Appropriate samples were incubated with FhHDM-1 (15µM; equivalent to 120µg/mL) for 1h at 37 °C/5% CO_2. Cells were washed twice with PBS (RT), and then incubated with Nano-SiO_2 (200µg/mL) for 1, 2 or 3h. Samples were washed twice with PBS (RT), fixed for 30min with 4% w/v PFA, washed, and chambers were then removed. Slides were mounted with progold antifade and coverslipped, following the manufacturer's recommendations (Life Technologies). Dr Mansell and Ms Pinar (Monash University, Australia) completed the microscopic determination of speck formation in a blinded analysis. Ten fields of view were collected per sample treatment, with each field of view containing approximately 100 cells.

5.2.3. FHHDM-1 EFFECTS ON LYSOSOMAL INTEGRITY

5.2.3.1. LYSOSOMAL STABILITY

5.2.3.1.1. DQ Ova compartmentalisation

The method used was modified from Hornung, *et al.*[210]. BMDMs from BALB/c mice were plated into 35mm fluoro-microscopy dishes ($1x10^6$ cells per dish) and allowed to adhere O/N at 37°C/5% CO_2. Each sample treatment was staggered to allow immediate live cell imaging, thereby minimising times for cell damage and/or loss of fluorescence to occur. Appropriate samples were incubated with FhHDM-1 (15µM) at 37°C/5% CO_2 for 1h. Cells were washed twice with PBS (RT) and 10µg/mL DQ Ovalbumin (Life Technologies) alone, or DQ Ovalbumin in combination with ALUM (500µg/mL) were added, when appropriate, and cells were incubated for 1h at 37°C/5%

CO_2. Cells were washed twice with PBS (RT) and 1mL of RPMI phenol free media (Gibco® Life Technologies) was added prior to imaging using a Nikon A1 confocal microscope.

5.2.3.2. CATHEPSIN B ACTIVITY

BMDMs from BALB/c mice were plated into 35mm fluoro-microscopy dishes ($1x10^6$ cells per dish), and allowed to adhere O/N at 37°C/5% CO_2. Each sample treatment was staggered to allow immediate live cell imaging to minimise cell damage and/or loss of fluorescence. Appropriate samples were incubated with FhHDM-1 (15µM) for 1h at 37°C/5% CO_2. Cells were washed twice with PBS (RT), ALUM (500µg/mL in media) was added to appropriate samples, and cells were incubated for 3h at 37°C/5% CO_2. Cells were washed twice with PBS (RT) and stained using the CV-Cathepsin B detection kit (Enzo Life Sciences, Farmingdale, USA). Briefly, macrophages were incubated with 1xCV-(RR_2) reagent in media for 1h at 37°C/5% CO_2 for detection of cathepsin B activity, following the manufacturer's recommendations. Cells were then washed three times with PBS (RT) and incubated with 0.5% v/v Hoechst dye (37°C/5% CO_2 for 10min) to enable detection of the nucleus. Samples were then washed twice with PBS (RT) and 1mL of RPMI phenol free media was added (Gibco® Life Technologies) prior to imaging with a Nikon A1 confocal microscope.

5.3. Results

5.3.1. FhHDM-1 INHIBITS LYSOSOMAL-DEPENDENT NLRP3 ACTIVATION

5.3.1.1. FhHDM-1 REDUCES NLRP3 INFLAMMASOME ACTIVATION BY ALUM

The activation of the NLRP3 inflammasome by particulate signals is dependent upon the acidification of lysosomes. FhHDM-1 was shown to exert a direct impact upon the lysosomal-related functions of macrophages (Chapter 4). Therefore, the effects of FhHDM-1 on the activation of lysosomal associated NLRP3 within primary murine macrophages (BALB/c BMDMs) was investigated. Firstly, macrophages were primed with LPS (500ng/mL) for a period of 3h[210]. Subsequently, cells were treated with increasing concentrations of FhHDM-1 (2.5-25μM) for 1h prior to NLRP3 inflammasome activation using ALUM in an O/N incubation. ALUM was chosen as an activating signal as these crystals induce lysosomal disruption, leading to subsequent leakage of the active luminal contents, which causes NLRP3 inflammasome activation[210].

Initially, to assess NLRP3 activation, the secretion of IL-1β from cells was quantified by ELISA (Figure 5.2 A). Treatment of LPS primed macrophages with FhHDM-1, prior to exposure of cells to ALUM, significantly decreased ($p \leq 0.0001$) the secretion of IL-1β, in a concentration-dependent manner. However, the use of an ELISA for the detection of IL-1β does not distinguish between the presence of active and precursor forms of the cytokine. This distinction is important as NLRP3 activation induces the formation of active IL-1β from its inactive pro-form through cleavage by caspase-1[241, 248]. Therefore, the total proteins present in the culture supernatants were precipitated and analysed by western blotting using antibodies specific for the active form of IL-1β (17kDa) (Figure 5.2 D). Western blotting also allowed the detection of both precursor (45kDa) and active (10kDa) forms of caspase-1 within the cell lysates. The use of an actin-specific antibody confirmed that equal quantities of proteins were both extracted from the cells and supernatants, and loaded onto gels, therefore allowing direct comparison of protein expression levels between different treatments. Using this methodology, it was found that treatment of BMDMs with FhHDM-1 resulted in a concentration-dependent reduction in the secretion of active IL-1β, which corroborated the ELISA data. In addition, treatment of BMDMs with FhHDM-1 also reduced the

activation of caspase-1, which correlated with the observed decrease in the levels of active IL-1β detected, and suggested that inhibition of the NLRP3 inflammasome had occurred.

Co-incubation of primary human macrophages with the combination of LPS and ALUM induced the secretion of IL-1β, as detected by ELISA (Figure 5.2 C). LPS priming alone was not sufficient to induce IL-1β secretion, which confirms that its secretion is specific to the activation of the NLRP3 inflammasome. In agreement with the studies using murine BMDMs, the concentration of IL-1β in culture supernatants was significantly reduced ($p \leq 0.001$) for primary human macrophages that were primed with LPS and treated with FhHDM-1 prior to ALUM stimulation.

5.3.1.2. FhHDM-1 reduces NLRP3 inflammasome activation by Nano-SiO_2

To further confirm that FhHDM-1 was inhibiting lysosomal-associated activation of NLRP3, an alternative lysosomal destabilising agent was used to activate the NLRP3 inflammasome. The same experimental approach was applied, but in this instance Nano-SiO_2, as opposed to ALUM, was used as the second activation trigger. BMDMs from BALB/c mice were primed and exposed to increasing concentrations of FhHDM-1, prior to incubation with Nano-SiO_2 (500μg/mL) for 6h (the incubation time used was shorter due to the stronger potency of Nano-SiO_2 as compared to ALUM[210]). Again, the secretion of IL-1β was quantified using ELISA (Figure 5.2 B), and levels of activated IL-1β and caspase-1 were analysed by western blotting (Figure 5.2 E). Similar to the results obtained for the cellular activation of BMDMs using ALUM, FhHDM-1 treatment of macrophages significantly reduced the activation and secretion of IL-1β ($p \leq 0.05$) as well as caspase-1 cleavage, in a concentration-dependent manner, suggesting that FhHDM-1 reduced NLRP3 inflammasome activation normally induced by Nano-SiO_2.

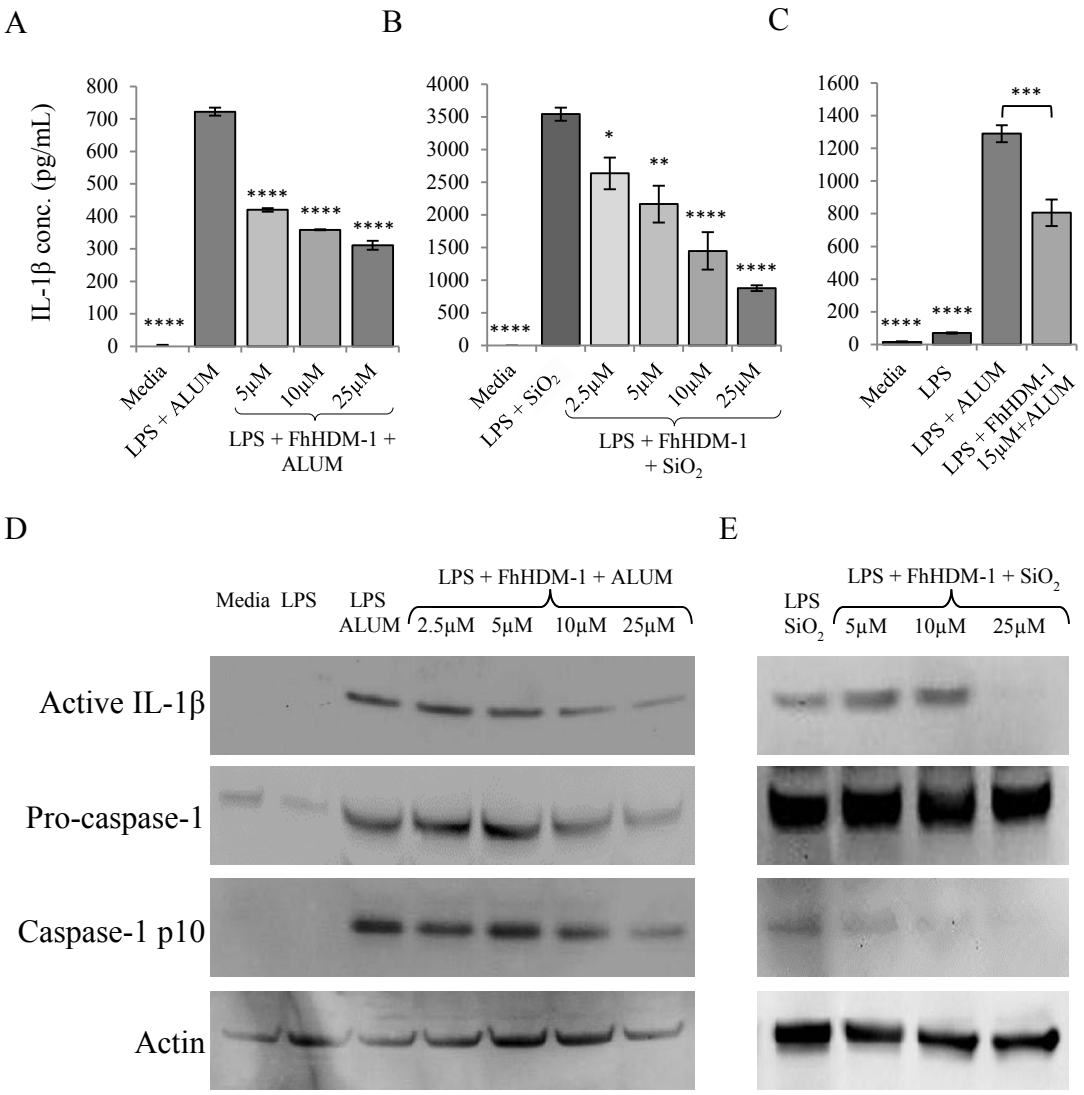

Figure 5.2 FhHDM-1 reduced NLRP3 inflammasome activation induced by lysosomal destabilising agents. BALB/c BMDMs (A, B, D & E) or human primary macrophages (C), were primed with LPS and incubated with FhHDM-1 (at increasing concentrations) prior to ALUM (A, C & D) or Nano-SiO_2, denoted as SiO_2, (B & E) induced NLRP3 inflammasome activation. Supernatants were assayed for IL-1β by ELISA (A-C). Statistically significant differences were determined by ANOVA followed by Dunnett's test, using the respective LPS + destabilising agent samples as control (*, $p \leq 0.05$; **, $p \leq 0.01$; ***, $p \leq 0.001$; ****, $p \leq 0.0001$). Supernatants of BALB/c BMDMs were also subjected to protein precipitation and cleaved (active) IL-1β, pro-caspase-1, or active caspase-1 (p10) were detected by western blotting (D & E). Actin was used as the protein loading quantification control. The presented data is representative of two individual experiments and for the ELISAs (A-C), IL-1β concentrations are expressed as the means of triplicate samples +/- SEM.

5.3.2. FhHDM-1 PREVENTS NLRP3 DEPENDENT ASC OLIGOMERISATION

NLRP3 activation results in the recruitment of ASC proteins and subsequent NLRP3 oligomerisation. This, in conjunction with ASC self-induced recruitment amplification, stimulates the aggregation of all the ASC proteins within the cell to a single subcellular location, a process that is referred to as 'ASC speck' formation. ASC proteins can then act as adaptors for inflammasome/pro-caspase-1 interactions, thus enabling the activation of the latter to occur by autocatalysis (Figure 5.1 E)[247]. Therefore, to confirm that FhHDM-1 was inhibiting the formation of inflammasome complexes, and preventing the generation of active capase-1 as a consequence, ASC recruitment was assessed[241, 248]. For these experiments, a macrophage cell line, which stably expresses a cerulean-tagged ASC was utilised. These cells can be used to analyse the formation of ASC oligomers, or 'specks', by microscopy, as a parameter that directly reflects the capacity of cells to respond to the activation signal[243, 256]. In addition, this cell line has been engineered to express high levels of the nlrp3 gene, which negates the need to include an agent to deliver a priming signal[256]. Therefore, in this system, any effect induced by FhHDM-1 would be attributed directly to the activation of NLRP3 inflammasome, as a consequence of lysosomal destabilisation events.

ASC cells were incubated with FhHDM-1 (15µM) for 1h prior to activation with Nano-SiO_2 (200µg/mL) for periods of 1, 2 or 3h. Activation using ALUM could not be tested since it is not potent enough to drive visible formation of specks in this cell line. Different time points, for Nano-SiO_2 induced activation were used to determine an optimal time period for speck formation and detection, whilst maintaining cell viability. An incubation period of 3h allowed for optimal speck formation in positive controls (Figure 5.3 D). Longer incubation times and increased Nano-SiO_2 concentrations induced unacceptable levels of cellular damage and/or pyroptosis (caspase-1 mediated cell death) which resulted in extensive cell loss, thus preventing further analysis by microscopy. In the absence of inflammasome activation, evenly distributed, low intensity cytoplasmic fluorescence was observed. In contrast, cells that were treated with Nano-SiO_2, and developed ASC specks as a result, possessed foci of intense fluorescence that, at the presented resolution, appeared as very bright cells (distinguished by red arrows in Figure 5.3 A-C). The abundance of cells with specks

was significantly reduced in samples that were pre-treated with FhHDM-1, followed by a 3h incubation period with Nano-SiO_2 ($p \leq 0.001$). These data suggest that FhHDM-1 interfered with NLRP3 oligomerisation and ASC recruitment, thereby exerting an inhibitory effect on NLRP3 activation events that occurred downstream of priming.

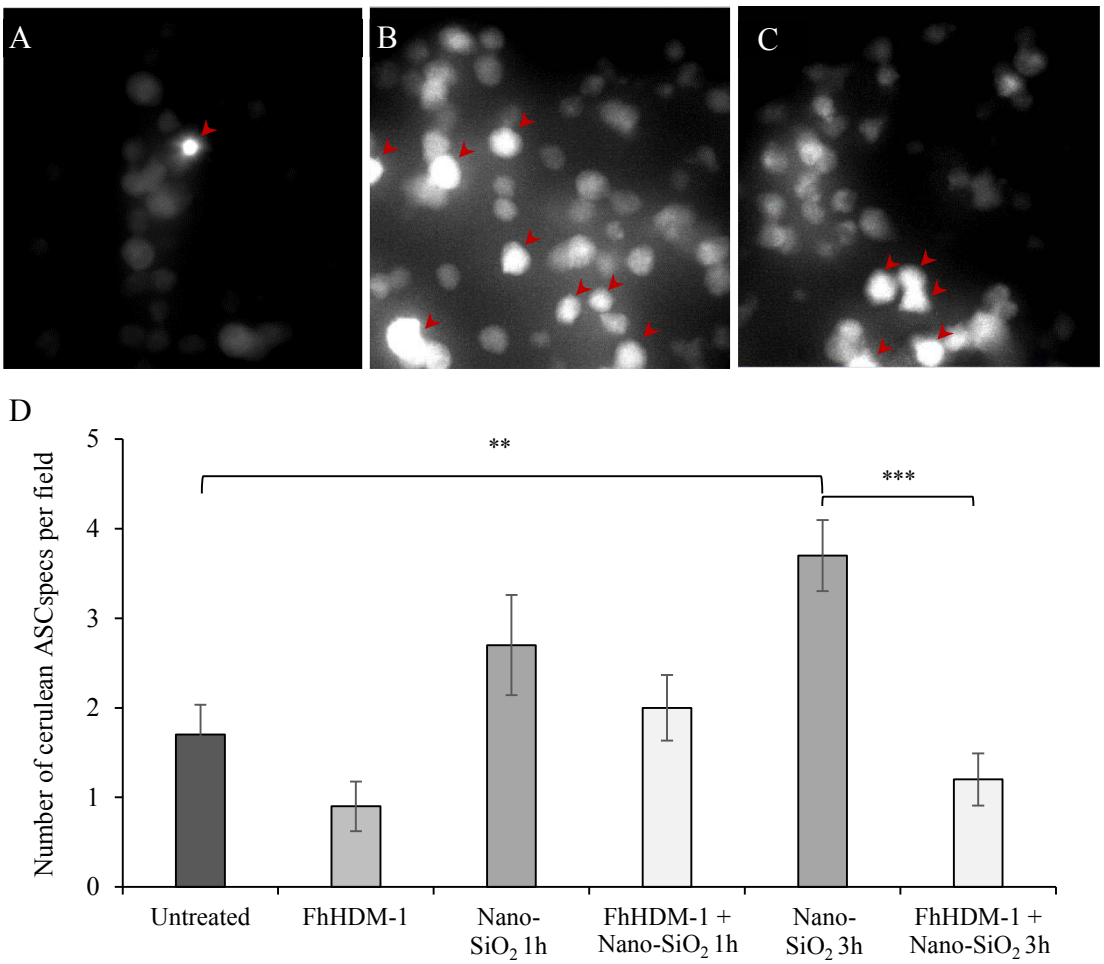

Figure 5.3 FhHDM-1 reduced ASC speck formation. BMDMs from BALB/c mice were pre-treated with FhHDM-1 (15µM) for 1h prior to NLRP3 inflammasome activation, via incubation with Nano-SiO_2 (200µg/mL) for 3h. Representative images (black and white versions) of speck formation, as detected by fluorescent microscopy, of untreated control (A), Nano-SiO_2 treated (positive control) (B), or pre FhHDM-1 incubated cells (test sample) (C). Graphic representation is provided (D) for the number of specks detected per field of view (total 10 fields per sample treatment) and statistically significant differences were determined by t-tests (**, $p \leq 0.01$; ***, $p \leq 0.001$). The presented data reflects the results of three individual experiments.

5.3.3. EFFECTS OF FHHDM-1 ON LYSOSOMAL INTEGRITY AND STABILITY AFTER ALUM-INDUCED INFLAMMASOME ACTIVATION

Both ALUM and Nano-SiO_2 activate the NLRP3 inflammasome in a process that is characterised by initial lysosomal swelling, followed by disruption of this organelle, which leads to leakage of lysosomal contents into the cytoplasmic region[210]. Given that all the data thus far indicated that FhHDM-1 was preventing lysosomal-dependent activation of NLRP3, the association between FhHDM-1 inhibition of lysosomal acidification and NLRP3 activation was further investigated. To assess lysosomal integrity, BMDMs from BALB/c mice were either untreated or pre-incubated with FhHDM-1 (15μM) for 1h prior to incubation with DQ Ovalbumin (DQOva; 10μg/mL), alone or in combination with ALUM (500μg/mL), for 1h. In this case, ALUM was selected as the activating signal because its effects are sufficiently mild to induce lysosomal swelling without disruption, when short incubation times are employed. Levels of processed DQOva, detected as green fluorescence, were decreased after pre-incubation with FhHDM-1 (Figure 5.4 C), but the dispersed, finely punctate distribution of the DQOva only control was maintained (Figure 5.4 B), indicative of vesicular containment of the processed molecule. In contrast, incubation of macrophages with DQOva/ALUM (Figure 5.4 D) caused lysosomal swelling, observed as enlarged foci of fluorescence. Pre-incubation of macrophages with FhHDM-1, prior to DQOva/ALUM treatment, did not prevent lysosomal enlargement/damage resulting from ALUM accumulation in this organelle, but the intensity of the overall detected fluorescence was reduced (Figure 5.4 E).

The observed changes in fluorescence intensity could be a consequence of decreased acidification in lysosomes, induced by FhHDM-1 treatment, which modulated the ability of macrophages to process DQOva (Chapter 4). Since NLRP3 activation induced by ALUM has been attributed to the lysosomal leakage of cathepsin B in particular, these changes in acidification may have prevented cathepsin B activation. To assess this, levels of cathepsin B activity were assessed using the CV-cathepsin B detection kit, which contains the highly permeable reagent, CV-RR_2, which consists of two arginine-arginine moieties that are conjugated to the fluorophore, cresyl violet. This double linkage to arginine (the substrate for cathepsin B) renders the fluorophore non-fluorescent. However, upon cathepsin B mediated cleavage, the

removal of a single or both arginine residues results in the emission of fluorescence by the liberated cresyl violet, which is directly proportional to cathepsin B activity[257]. Accordingly, BMDMs from BALB/c mice were left untreated or pre-treated with FhHDM-1 (15μM) for 1h, prior to incubation with ALUM (500μg/mL) for 3h, to allow lysosomal destabilisation to occur, prior to staining with CV-RR_2 (for 1h) and live cell confocal microscopy analyses. The emitted signal (green fluorescence in Figure 5.5) decreased in intensity upon pre-incubation with FhHDM-1 (Figure 5.5 C), as compared to control levels observed in untreated cells (Figure 5.5 B). Incubation with ALUM alone (Figure 5.5 D) caused a more profound decrease in fluorescence intensity. This observation was likely attributable to the leakage of lysosomal contents into the cytosol, which would not only distribute the fluorescence across a larger surface area (thereby dispersing fluorescence foci, and thus reducing the intensity per unit area), but would also expose cathepsin B to a neutral cytoplasmic pH, which would decrease its enzymatic activity. Pre-incubation with FhHDM-1 prior to ALUM treatment (Figure 5.5 E) further reduced cytosolic fluorescence to almost undetectable levels, which is likely reflecting a combination of reduced cathepsin B activity and its leakage into the cytosol. Collectively, this data suggested that FhHDM-1 did not protect lysosomes from becoming destabilised by ALUM treatment, but it did induce a reduction in cathepsin B activity.

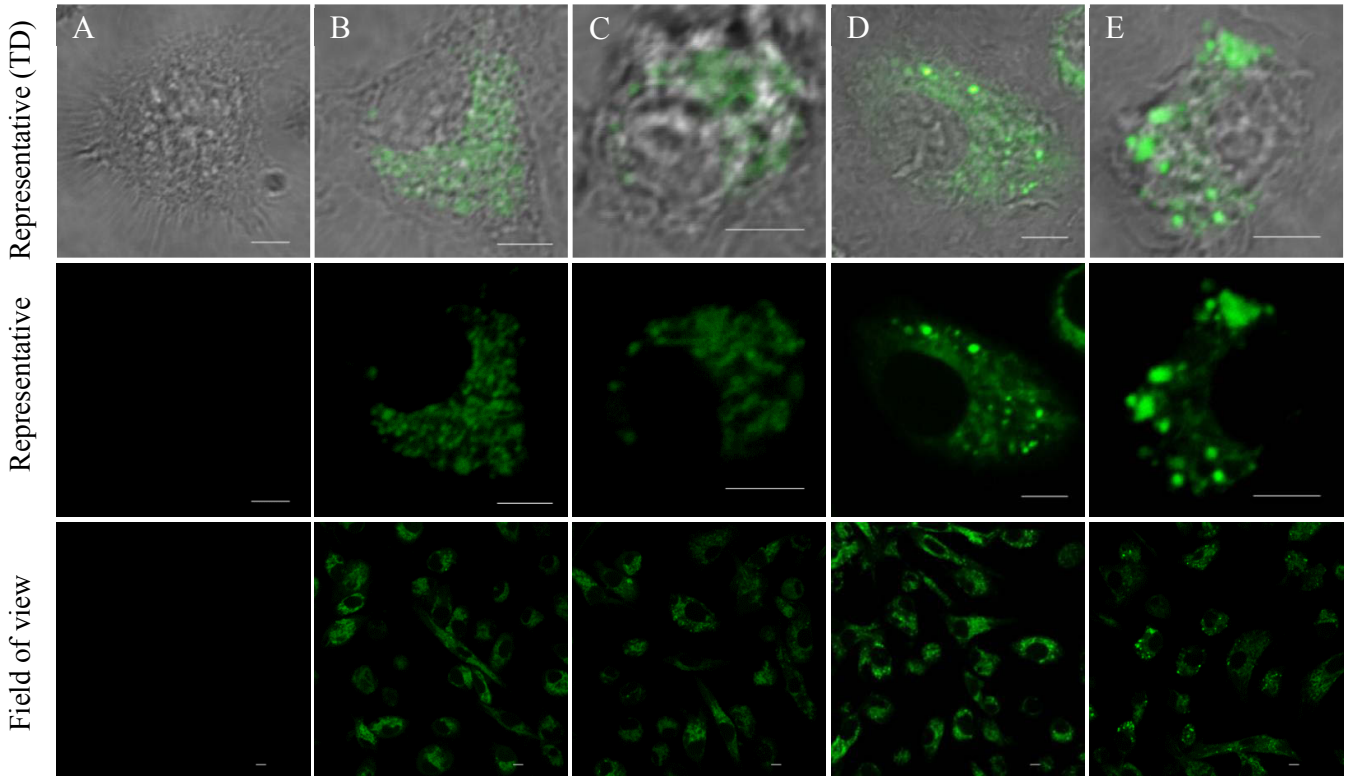

Figure 5.4 FhHDM-1 does not prevent the lysosomal destabilisation induced by ALUM. Live cell confocal microscopy images of BMDMs from BALB/c mice that were: untreated (A), incubated with 10µg/mL DQ Ovalbumin (DQOva) (B) as positive control of intact lysosomes, pre-incubated with FhHDM-1 (C & E) at 15µM for 1h followed by incubation with 10µg/mL DQ Ovalbumin alone (C), or in combination with 500µg/mL ALUM (E) for 1h. Samples where cells were incubated with DQOva/ALUM (D) were also included. Detection of DQOva processing, observed as green fluorescence, was utilised to assess lysosomal integrity (Scale bar: 5µm). Images are representative of four fields of view per sample treatment and the experiment was performed twice.

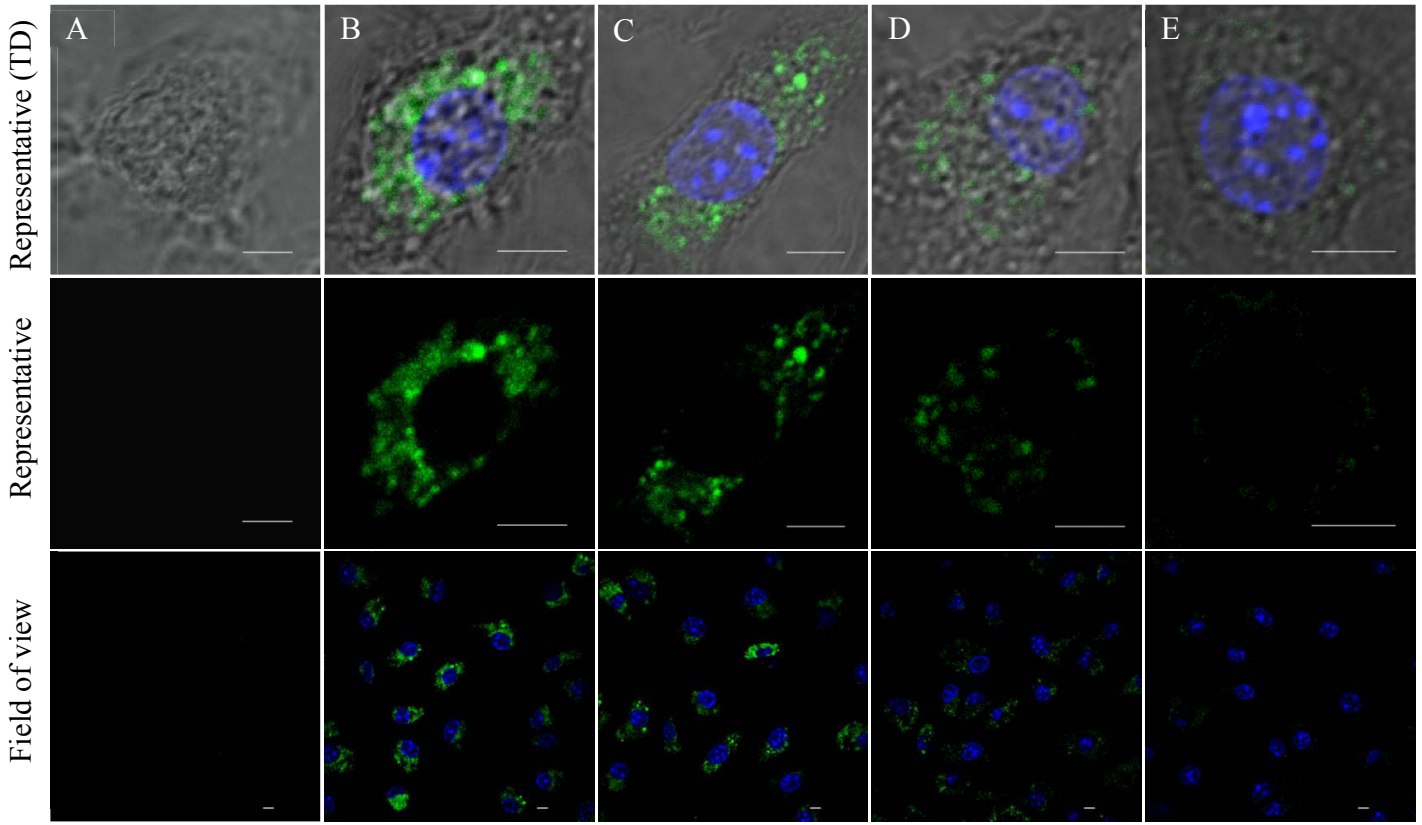

Figure 5.5 FhHDM-1 treatment of macrophages reduced cathepsin B activity. Live cell confocal microscopy images of BMDMs from BALB/c mice that were: untreated (A & B), or pre-incubated with FhHDM-1 (C & E) at 15µM for 1h followed by incubation with 500µg/mL ALUM (D & E) for 3h. Levels of cathepsin B activity were detected by staining cells (B-E) with the reagent CV-RR_2, which was observed as green fluorescence. Cell nuclei were detected by Hoechst staining and can be observed as blue fluorescence. (A) Corresponds to unstained control. (Scale bar: 5µm). Images are representative of four fields of view per sample treatment and the experiment was performed twice.

5.3.4. EFFECTS OF FHHDM-1 ON LPS PRIMING

Thus far, the presented NLRP3 inflammasome regulation data is consistent with the lysosomal localisation of FhHDM-1, and its ability to inhibit the acidification of this organelle. However, to further confirm the specific action of FhHDM-1, its effect on the LPS priming event (Signal I) was assessed. The hypothesis being that inhibition of lysosomal acidification is secondary to the priming of cells, and, therefore, FhHDM-1, if specifically targeted to the lysosome, would exert no effect on the LPS activation of macrophages. To investigate this, the cell supernatants collected from macrophages previously exposed to ALUM or Nano-SiO_2 were analysed for TNF secretion by ELISA. Production of this cytokine occurs as a direct response to TLR4 signalling by LPS and is independent of alterations to, or deletion of, nlrp3 gene expression or inflammasome activation[258-260]. As expected, priming of macrophages with LPS (positive controls) led to increased TNF secretion (LPS plus destabilising agent-treated samples in Figure 5.6). However, the addition of FhHDM-1 resulted in a significant reduction in the levels of secreted TNF, as compared to the positive controls, in a concentration dependent manner (at the lowest concentrations of FhHDM-1 used $p \leq 0.05$ for ALUM and Nano-SiO_2 samples) and independent of the lysosomal destabilising agent employed. These data indicate that FhHDM-1 may also be preventing the optimal priming of macrophages, and therefore inhibiting the activation and secretion of IL-1β by two regulatory mechanisms.

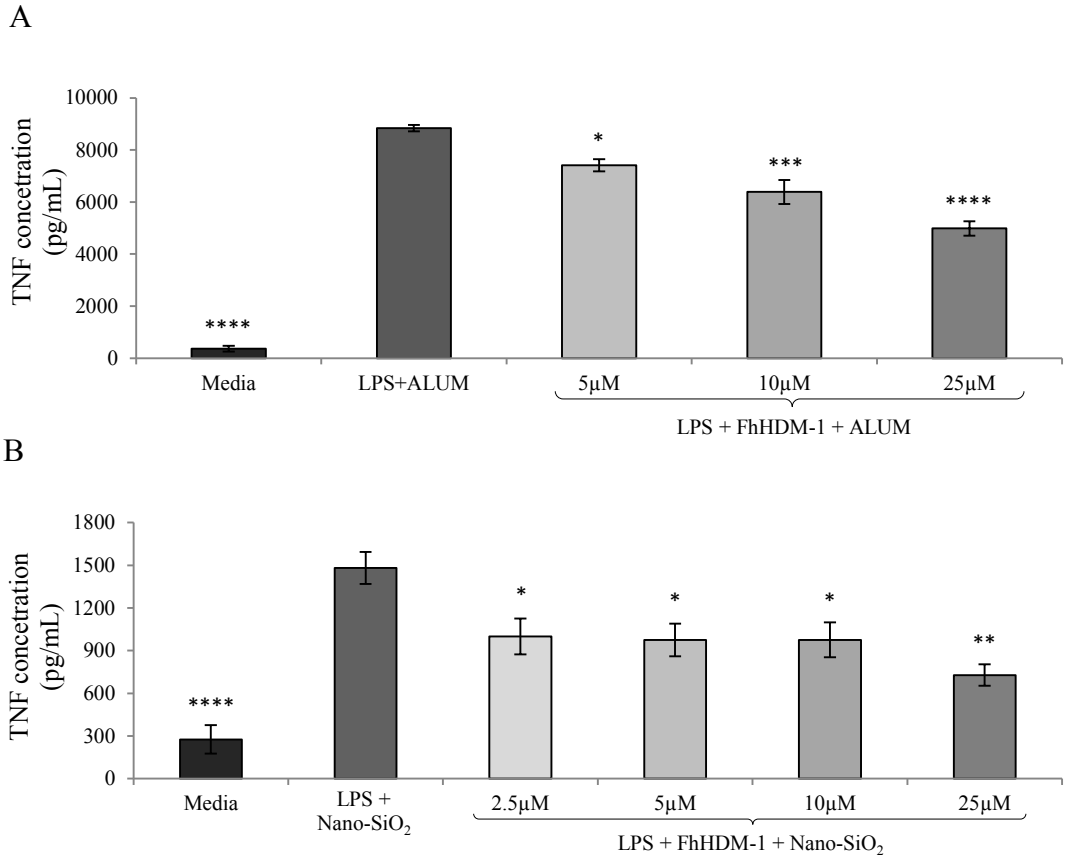

Figure 5.6 FhHDM-1 reduced LPS priming efficiency in macrophages. Supernatants of BMDMs from BALB/c mice primed with LPS and incubated with FhHDM-1 (at increasing concentrations) prior to ALUM (A) or Nano-SiO_2 (B) induced NLRP3 inflammasome activation were analysed for TNF secretion by ELISA. The presented data is representative of two individual experiments. TNF concentrations are expressed as the means of triplicate samples +/- SEM. Statistically significant differences were determined by ANOVA followed by Dunnett's test, using the respective LPS + destabilising agent samples as control (*, $p \leq 0.05$; **, $p \leq 0.01$; ***, $p \leq 0.001$; ****, $p \leq 0.0001$).

5.4. Discussion

Taken together, the presented data provides further evidence that FhHDM-1 targets the macrophage lysosome and impairs the functionality of this organelle. The net result is that lysosomal proteases are prevented from becoming fully activated, due to an inability to maintain optimal acidification within the lysosomal lumen. When released into the cytosol, following lysosomal rupture (induced by ALUM and Nano-SiO_2), these inactive proteases fail to stimulate the recruitment of ASC, and consequently, oligomerisation of NLRP3 is prevented. This, in turn, reduces the activation of caspase-1, and thus prevents the activation and secretion of the pro-inflammatory cytokine, IL-1β. This finding is in agreement with other reports that vATPase inhibitors (such as bafilomycin A) or cathepsin B inhibitors (such as CA-074-Me) prevent NLRP3 inflammasome activation, stimulated by the presence of lysosomal disruptive agents (such as Nano-SiO_2)[210, 248, 254].

However, the demonstration that FhHDM-1 also inhibited the priming event required for NLRP3 activation was an unexpected finding. Previous studies have reported that FhHDM-1 can bind to LPS and prevent its interaction with TLR4, thereby reducing its ability to stimulate macrophages[115]. Also, it has been shown that pre-incubation of macrophages with FhHDM-1, and other cathelicidin peptides, prior to LPS challenge, significantly reduced the secretion of TNF by macrophages[135, 136]. However, neither of these effects is likely to be the mode of action in this case, as FhHDM-1 exerted a significant inhibitory effect when co-incubated with macrophages 3h after LPS exposure (a time point at which LPS would have already been incorporated and removed).

It has been reported that the mammalian cathelicidin peptide, LL-37, inhibited the production of TNF when murine macrophages were stimulated simultaneously with a combination of LPS and IFNγ[261]. Of relevance to the current study, this inhibitory effect was also observed when LL-37 was added 3h after LPS/IFNγ treatment, albeit the inhibitory effects were less pronounced than those observed after concurrent exposure. In addition, it was found that the presence of LL-37 significantly decreased the transcriptional expression levels of TNF (by 87%), although the specific mechanism(s) of this inhibition was not investigated[261]. While the priming signal in this case is

different to the one used in the current study, the observed reduction in TNF transcription levels correlates with the decrease in quantities of TNF detected by ELISA in cells treated with FhHDM-1 3h after exposure to LPS.

Studies using THP-1 monocytes have shown that after LPS stimulation, LL-37 inhibited the translocation of NF-kB (p50/p65) to the nucleus, which would negatively impact the transcription of TNF[133]. In addition, simultaneous, as well as pre-incubation with the murine cathelicidin peptide, CRAMP, reportedly inhibited the expression levels of TNF induced by TLR agonists in murine macrophages. CRAMP prevents the phosphorylation of p38 and ERK mitogen-activated protein kinases (MAPKs)[262], which ultimately decreases the stability of TNF mRNA transcripts[263]. Furthermore, treatment of macrophages with CRAMP prevented the ability of LPS to induce increased expression levels of the TLR4 adaptor protein, MyD88, and thus inhibited the downstream signalling pathway[262].

It has been recently reported that inhibition of lysosomal acidification suppressed NLRP3-mediated release of IL-1β from macrophages, and the levels of pro-IL-1β (following LPS priming) were significantly reduced after treatment with either bafilomycin A or NH_4Cl (both inducers of lysosomal alkalisation)[264]. It was proposed that macrophage acidic calcium stores are dependent upon the acidification of lysosomes. Therefore, by depleting these stores, the transcripts for IL-1β were unstable, and, as a result, the levels of pro-cytokine were reduced; although in this case TNF and NLRP3 mRNA levels remained unaltered[264]. These data suggest that the reduction in IL-1β secretion observed in response to FhHDM-1 treatment may be attributable to a reduction in the levels of pro-IL-1β, due to the induced inhibition of lysosomal acidification. However, the additional reduction in TNF secretion indicates that FhHDM-1 is likely also acting to regulate the TLR4 signalling pathway, and thus inhibit the induction of pro-IL-1β expression normally stimulated by LPS.

All inflammasomes share some commonalities with NLRP3, including ASC aggregation (although not essential for NLRC4[241, 242]), caspase-1 activation, and subsequent release of active IL-1β and IL-18[241, 247, 248, 265]. The lack of constitutive pro-IL-β expression in most cell types ensures that the inflammasome-mediated maturation of IL-1β is dependent upon the priming event, which induces transcription of pro-IL-β[248, 260, 266]. Therefore, if FhHDM-1 is inhibiting the priming event required for the

induction of IL-1β precursor transcription, it would be expected that FhHDM-1 would be able to globally inhibit the full range of inflammasome complexes and signalling factors. It would be valuable to further assess the impact of FhHDM-1 on other inflammasome types and to determine if FhHDM-1 alters expression levels of TNF, proIL1-β, and NLRP3 by performing expression analyses at mRNA and protein levels, since their transcription is regulated by priming[246, 248]. If changes in the expression levels of these transcripts were identified, then it would be relevant to investigate the TLR signalling pathways in more depth in order to identify the specific targets of FhHDM-1. Additionally, inducing priming events with the use of other TLR4 ligands, such as TNF, CpG or IL-1β[246], would indicate if the effects observed for FhHDM-1 are specific to LPS priming of macrophages or if instead FhHDM-1 targets a common downstream molecule irrespective of the priming ligand used.

Despite commonalities in the suppression of LPS-mediated inflammatory responses, there are conflicting reports on the impact of cathelicidin-like peptides on the inflammasome complexes. For example, it has been reported that LL-37 alone acts as the second signal for inflammasome activation, via its interaction with $P2X_7$ receptors (involved in ATP-induced NLRP3 inflammasome activation), thus stimulating the secretion of mature IL-1β[144]. Similarly, protegrins (porcine cathelicidins) have also been reported to stimulate IL-1β posttranslational processing, via the $P2X_7$ receptor[267]. However, contrary to these observations, incubation of primed macrophages with the porcine cathelicidins, PR-26 and PR-39, does not cause IL-1β secretion, that is, they do not act on their own as inflammasome activating (Signal II) agents[267]. Similar results were found for FhHDM-1, where ELISA analysis of peptide treated macrophage supernatants resulted in undetectable levels (0pg/mL) of secreted mature IL-1β, regardless of the concentration of FhHDM-1 used. Structural characteristics do not seem to be associated with this property, given that, unlike LL-37 and FhHDM-1, which both adopt α-helical structures in solution, protegrins are characterised by β-sheet conformations. Furthermore, in the case of both PR-26 and PR-39, these cathelicidins lack both α-helical and β-sheet structural conformations[267]. Therefore, it is likely that the downstream effect of these cathelicidins may be associated with their cellular localisation and/or interactions with their ligands.

NLRP3 activation, associated with lysosomal disruptive agents, contributes to the development of several pathologies, including atherosclerosis[254, 268], Alzheimer's disease[234], gout/pseudogout[210, 240, 255], and silicosis[210]. Enhanced NLRP3 activity has also been associated with multiple inflammatory disorders, including contact hypersensitivity[269], and the cryopyrin-associated periodic syndromes (CAPS)[245]. Furthermore, although autoimmune diseases are not directly caused by inflammasome activity, their progression might be indirectly dependent upon these complexes, due to the roles for IL-1β and IL-18 in the development of Th1 and Th17 immune responses[245], which underpin the development of autoimmune/inflammatory disorders. This premise is supported by observations that a deficiency of NLRP3 results in reduced IL-18 secretion and delayed progression of experimental autoimmune encephalitis (a murine model of MS)[270]. During progression of Type II diabetes (a disease with an inflammatory profile), there is an accumulation of human islet amyloid polypeptide (IAPP) aggregates within the pancreatic islets, which are internalised by resident macrophages (the priming of which is suggested to be regulated by glucose metabolism), causing activation of NLRP3 inflammasomes. This activation is dependent upon phagolysosomal internalisation, cathepsin B activity, vATPase and caspase-1 function[271]. The resultant IL-1β secretion has been recognised to drive pancreatic beta cells to undergo apoptosis[272, 273]. Therefore, the ability of FhHDM-1 to inhibit the NLRP3 (and potentially other) inflammasomes suggests that it may hold great promise as an immune modulatory therapeutic.

CHAPTER 6 GENERAL DISCUSSION

The current study investigated the mechanisms by which a peptide secreted by the helminth parasite, *Fasciola hepatica*, modulated the biological activity of macrophages. This peptide, termed FhHDM-1, shares both structural and biochemical similarities with the cathelicidins, which are a major subset of host defence peptides (HDPs), naturally expressed in mammals. FhHDM-1 was found to exert its regulatory functions by modulating lysosomal-mediated activity in macrophages. The initial interaction between FhHDM-1 and the lipid raft subdomains on the plasma membrane of these cells, made it possible for the peptide to be actively endocytosed, which culminated in its delivery to endolysosomes. Within these vesicles, FhHDM-1 prevented optimal luminal acidification, which resulted in a negative impact upon lysosomal dependent macrophage functions, including their ability to process and subsequently present antigen to T cells, as well as causing a decrease in cathepsin B-mediated NLRP3 inflammasome activation.

The current study is the first to report that cathelicidin-like peptides are internalised by macrophages, via an active process, and are targeted to endolysosomal vesicles. After localisation of FhHDM-1 to this subcellular region, a reduction in endolysosomal acidification was observed. Again, this effect had not been previously attributed to the mechanism(s) of action of a cathelicidin-like peptide. Although the mechanism of this inhibition was not fully determined, the data obtained suggested that the immune modulatory effects of FhHDM-1 were attributable to either a direct inhibition of vATPases, or an inhibition of the maturation of acidified vesicles. Interestingly, macrophages exposed to the secreted products of the cercariae of the helminth parasite, *S. mansoni*, reportedly displayed a retarded rate of phagosome maturation, as compared to that observed for macrophages that internalised *E. coli*[274]. Therefore, it is possible that a component of the *S. mansoni* secretions could have an analogous function to that of FhHDM-1, which would explain the described retarded rate of phagosome maturation. Previous proteomic analysis of the secreted products of *S. mansoni* cercariae had identified a peptide, termed Sm16, which has more recently been defined as a structural homologue to FhHDM-1[135, 275, 276]. Altogether, these observations support the hypothesis that HDM-like peptides inhibit the acidification of

lysosomes, and thus restrict the lysosomal dependent functions of macrophages. It would be of significant interest to determine if this is indeed a function shared by trematode HDM-like peptides, and whether this activity is also characteristic of mammalian cathelicidin peptides.

Both, the prevention of lysosomal acidification and the inhibition of NLRP3 inflammasome activation, would be important for the establishment and persistence of *F. hepatica* within its mammalian host. Indeed, protection against infection by this parasite is associated with the development of a parasite-specific Th1 type immune response[26, 122]. Yet this parasite possesses the remarkable ability to switch the host's protective Th1 type immune responses towards a Th2 response[32, 107]. It has been recently reported that the NLRP3-dependent production of IL-1β from innate immune cells, inhibits the development of Th2 immune responses[277]. Thus, the data produced in the current study, suggests that, by inhibiting the activation of NLRP3, FhHDM-1 may be contributing to the potent immune-modulatory effect observed after infection with *F. hepatica.* Furthermore, hepatocyte cell death, associated with liver inflammatory conditions and fibrosis, has been characterised with excessive myeloid cell NLRP3 inflammasome activity, culminating in pyroptosis and abundant IL-1β secretion, which activates additional pro-inflammatory mechanisms, such as TNF-induced cell death[278]. Given that *Fasciola* juvenile worms migrate through the liver tissue to reach their final niche in the bile duct, the subsequent activation of host alarm/inflammatory signals within this tissue site (including NLRP3 activation) would further amplify any tissue damage[32, 52]. Therefore, by preventing host NLRP3 inflammasome activity, and its resultant pro-inflammatory outcomes, FhHDM-1 may be minimising the extent of host response to the collateral tissue damage. Similarly, the secretion of Sm16 from the egg stage of *S. mansoni* might also regulate the inflammatory processes leading to the formation and/or resolution of granulomas in liver tissue, where *S. mansoni* eggs are deposited[19, 32].

Importantly, the discovery here that FhHDM-1 inhibits lysosomal acidification has implications beyond contributing to our understanding of the biology of the parasite. Macrophages also play a central role in the pathogenesis of autoimmune disease. For example, macrophages with a pro-inflammatory phenotype have been suggested to be the driving force for the initiation and perpetuation of autoimmunity in several diseases,

including Type I diabetes (T1D) and multiple sclerosis (MS)[273, 279-281]. In such autoimmune disorders, the enzymatic activity of lysosomal proteases, which is regulated by luminal acidification, is largely responsible for the autoimmune sequalae[199, 240, 272, 282-285]. As a result, the current study suggests that FhHDM-1 and plausibly FhHDM-1-like peptides, through their ability to modulate macrophage function, represent a unique class of molecules, with potential therapeutic applications for the treatment of autoimmune/inflammatory disorders, in which excessive Th1/Th17 pro-inflammatory immune responses are predominant.

The potential of utilising HDPs as a new generation of immune regulatory therapeutics has been proposed and is currently being pursued[125, 130]. However, further investigations to elucidate the specific mechanisms by which these peptides modulate immune responses is still required before their clinical potential as immune regulators can be realised. Although promising discoveries have been made, the duality of action of certain HDPs according to their environment, can either result in exacerbation or prevention of inflammation, making it difficult to clarify their direct functions/mechanisms[125, 130, 286]. Furthermore, the adverse effects of HDPs including cytotoxicity, as well as their induced stimulation of histamine release and degranulation of mast cells[286], present important limitations towards their application as potential therapeutics, making the production of modified and thus safer synthetic analogues indispensable. Therefore, FhHDM-1 and its homologues may prove to be safer therapeutic alternatives to HDPs, given that they preserve some of the immune modulatory roles of cathelicidins without the negative aspect of being cytotoxic[135].

This study has elucidated a novel immune modulatory mechanism of action of FhHDM-1 on macrophage function. Such information not only expands our understanding of the impact that FhHDM-1, and putatively other cathelicidin-like peptides, have on macrophages and how such effects serve to benefit both parasites and their host, but also opens a wide range of potential therapeutic applications against pathologies associated with excessive inflammation, driven by macrophage lysosomal-dependent mechanisms.

REFERENCES

1. David, T., Thomas, C., Zaccone, P., Dunne, D.W. & Cooke, A., 2004; The impact of infection on the incidence of autoimmune disease. Curr Top Med Chem. 4, 521-529.

2. Carvalho, L., Sun, J., Kane, C., Marshall, F., Krawczyk, C. & Pearce, E.J., 2009; Review series on helminths, immune modulation and the hygiene hypothesis: mechanisms underlying helminth modulation of dendritic cell function. Immunology. 126, 28-34.

3. Mosser, D.M. & Edwards, J.P., 2008; Exploring the full spectrum of macrophage activation. Nat Rev Immunol. 8, 958-969.

4. Zanoni, I. & Granucci, F., 2010; Regulation of antigen uptake, migration, and lifespan of dendritic cell by Toll-like receptors. Journal of Molecular Medicine. 88, 873-880.

5. Mills, C.D. & Ley, K., 2014; M1 and M2 macrophages: the chicken and the egg of immunity. J Innate Immun. 6, 716-726.

6. Geginat, J., Paroni, M., Facciotti, F., Gruarin, P., Kastirr, I., Caprioli, F., Pagani, M. & Abrignani, S., 2013; The CD4-centered universe of human T cell subsets. Seminars in Immunology. 25, 252-262.

7. Fietta, P. & Delsante, G., 2009; The Effector T Helper Cell Triade. Rivista Di Biologia-Biology Forum. 102, 61-74.

8. Peters, A., Lee, Y. & Kuchroo, V.K., 2011; The many faces of Th17 cells. Curr Opin Immunol. 23, 702-706.

9. Korn, T., Oukka, M., Kuchroo, V. & Bettelli, E., 2007; Th17 cells: Effector T cells with inflammatory properties. Seminars in Immunology. 19, 362-371.

10. Hirota, K., Duarte, J.H., Veldhoen, M., Hornsby, E., Li, Y., Cua, D.J., Ahlfors, H., Wilhelm, C., Tolaini, M., Menzel, U., Garefalaki, A., Potocnik, A.J. & Stockinger, B., 2011; Fate mapping of IL-17-producing T cells in inflammatory responses. Nat Immunol. 12, 255-263.

11. Romagnani, S., 1994; Regulation of the development of type 2 T-helper cells in allergy. Curr Opin Immunol. 6, 838-846.

12. Wick, G., Grundtman, C., Mayerl, C., Wimpissinger, T.F., Feichtinger, J., Zelger, B., Sgonc, R. & Wolfram, D., 2013; The Immunology of Fibrosis. Annual Review of Immunology, Vol 31. 31, 107-135.

13. Diaz, A. & Allen, J.E., 2007; Mapping immune response profiles: the emerging scenario from helminth immunology. European Journal of Immunology. 37, 3319-3326.

14. Murray, P.J. & Wynn, T.A., 2011; Protective and pathogenic functions of macrophage subsets. Nature Reviews Immunology. 11, 723-737.

15. Barros, M.H.M., Hauck, F., Dreyer, J.H., Kempkes, B. & Niedobitek, G., 2013; Macrophage Polarisation: an Immunohistochemical Approach for Identifying M1 and M2 Macrophages. Plos One. 8.

16. Mantovani, A., Sica, A. & Locati, M., 2005; Macrophage polarization comes of age. Immunity. 23, 344-346.

17. Martinez, F.O., Helming, L. & Gordon, S., 2009; Alternative activation of macrophages: an immunologic functional perspective. Annual Review of Immunology. 27, 451-483.

18. Gause, W.C., Wynn, T.A. & Allen, J.E., 2013; Type 2 immunity and wound healing: evolutionary refinement of adaptive immunity by helminths. Nature Reviews Immunology. 13, 607-614.

19. McSorley, H.J. & Maizels, R.M., 2012; Helminth infections and host immune regulation. Clin Microbiol Rev. 25, 585-608.

20. Maizels, R.M., Pearce, E.J., Artis, D., Yazdanbakhsh, M. & Wynn, T.A., 2009; Regulation of pathogenesis and immunity in helminth infections. J Exp Med. 206, 2059-2066.

21. Allen, J.E. & Maizels, R.M., 2011; Diversity and dialogue in immunity to helminths. Nat Rev Immunol. 11, 375-388.

22. Hasnain, S.Z., Evans, C.M., Roy, M., Gallagher, A.L., Kindrachuk, K.N., Barron, L., Dickey, B.F., Wilson, M.S., Wynn, T.A., Grencis, R.K. & Thornton, D.J., 2011; Muc5ac: a critical component mediating the rejection of enteric nematodes. J Exp Med. 208, 893-900.

23. Herbert, D.R., Yang, J.Q., Hogan, S.P., Groschwitz, K., Khodoun, M., Munitz, A., Orekov, T., Perkins, C., Wang, Q., Brombacher, F., Urban, J.F., Jr., Rothenberg, M.E. & Finkelman, F.D., 2009; Intestinal epithelial cell secretion of RELM-beta protects against gastrointestinal worm infection. J Exp Med. 206, 2947-2957.

24. Akiho, H., Blennerhassett, P., Deng, Y. & Collins, S.M., 2002; Role of IL-4, IL-13, and STAT6 in inflammation-induced hypercontractility of murine smooth muscle cells. Am J Physiol Gastrointest Liver Physiol. 282, G226-232.

25. Cliffe, L.J., Humphreys, N.E., Lane, T.E., Potten, C.S., Booth, C. & Grencis, R.K., 2005; Accelerated intestinal epithelial cell turnover: a new mechanism of parasite expulsion. Science. 308, 1463-1465.

26. Mulcahy, G., O'Connor, F., Clery, D., Hogan, S.F., Dowd, A.J., Andrews, S.J. & Dalton, J.P., 1999; Immune responses of cattle to experimental anti-*Fasciola hepatica* vaccines. Research in Veterinary Science. 67, 27-33.

27. Mulcahy, G., O'Connor, F., McGonigle, S., Dowd, A., Clery, D.G., Andrews, S.J. & Dalton, J.P., 1998; Correlation of specific antibody titre and avidity with protection in cattle immunized against *Fasciola hepatica*. Vaccine. 16, 932-939.

28. Hoffmann, K.F., James, S.L., Cheever, A.W. & Wynn, T.A., 1999; Studies with double cytokine-deficient mice reveal that highly polarized Th1- and Th2-type cytokine and antibody responses contribute equally to vaccine-induced immunity to *Schistosoma mansoni*. Journal of Immunology. 163, 927-938.

29. Zhang, W.Y., Moreau, E., Hope, J.C., Howard, C.J., Huang, W.Y. & Chauvin, A., 2005; *Fasciola hepatica* and *Fasciola gigantica*: comparison of cellular response to experimental infection in sheep. Exp Parasitol. 111, 154-159.

30. WHO, 2012; WHO/TDR in Technical Report Series 196, Italy.

31. Maizels, R.M. & Yazdanbakhsh, M., 2003; Immune regulation by helminth parasites: cellular and molecular mechanisms. Nat Rev Immunol. 3, 733-744.

32. Moreau, E. & Chauvin, A., 2009; Immunity against Helminths: Interactions with the Host and the Intercurrent Infections. Journal of Biomedicine and Biotechnology, 9.

33. Hewitson, J.P., Grainger, J.R. & Maizels, R.M., 2009; Helminth immunoregulation: The role of parasite secreted proteins in modulating host immunity. Molecular and Biochemical Parasitology. 167, 1-11.

34. Finlay, C.M., Walsh, K.P. & Mills, K.H.G., 2014; Induction of regulatory cells by helminth parasites: exploitation for the treatment of inflammatory diseases. Immunol Rev. 259, 206-230.

35. Falcone, F.H., Loukas, A., Quinnell, R.J. & Pritchard, D.I., 2004; The innate allergenicity of helminth parasites. Clinical Reviews in Allergy & Immunology. 26, 61-72.

36. Johnston, C.J., McSorley, H.J., Anderton, S.M., Wigmore, S.J. & Maizels, R.M., 2014; Helminths and immunological tolerance. Transplantation. 97, 127-132.

37. Donnelly, S., O'Neill, S.M., Sekiya, M., Mulcahy, G. & Dalton, J.P., 2005; Thioredoxin peroxidase secreted by *Fasciola hepatica* induces the alternative activation of macrophages. Infection and Immunity. 73, 166-173.

38. Pineda, M.A., Lumb, F., Harnett, M.M. & Harnett, W., 2014; ES-62, a therapeutic anti-inflammatory agent evolved by the filarial nematode *Acanthocheilonema viteae*. Molecular and Biochemical Parasitology. 194, 1-8.

39. Robinson, M.W., Dalton, J.P., O'Brien, B.A. & Donnelly, S., 2013; *Fasciola hepatica*: the therapeutic potential of a worm secretome. Int J Parasitol. 43, 283-291.

40. Holland, M.J., Harcus, Y.M., Riches, P.L. & Maizels, R.M., 2000; Proteins secreted by the parasitic nematode *Nippostrongylus brasiliensis* act as adjuvants for Th2 responses. Eur J Immunol. 30, 1977-1987.

41. Pritchard, D.I., Hewitt, C. & Moqbel, R., 1997; The relationship between immunological responsiveness controlled by T-helper 2 lymphocytes and infections with parasitic helminths. Parasitology. 115 Suppl, S33-44.

42. Maizels, R.M., McSorley, H.J. & Smyth, D.J., 2014; Helminths in the Hygiene Hypothesis - Sooner or Later ? Clin Exp Immunol.

43. Okada, H., Kuhn, C., Feillet, H. & Bach, J.F., 2010; The 'hygiene hypothesis' for autoimmune and allergic diseases: an update. Clin Exp Immunol. 160, 1-9.

44. Correale, J. & Farez, M., 2007; Association between parasite infection and immune responses in multiple sclerosis. Ann Neurol. 61, 97-108.

45. Correale, J., Farez, M. & Razzitte, G., 2008; Helminth infections associated with multiple sclerosis induce regulatory B cells. Ann Neurol. 64, 187-199.

46. McSorley, H.J., Hewitson, J.P. & Maizels, R.M., 2013; Immunomodulation by helminth parasites: defining mechanisms and mediators. Int J Parasitol. 43, 301-310.

47. Sajid, M. & McKerrow, J.H., 2002; Cysteine proteases of parasitic organisms. Mol Biochem Parasitol. 120, 1-21.

48. Phillips, C., Coward, W.R., Pritchard, D.I. & Hewitt, C.R., 2003; Basophils express a type 2 cytokine profile on exposure to proteases from helminths and house dust mites. J Leukoc Biol. 73, 165-171.

49. Fraga, L.A.D., Lamb, E.W., Moreno, E.C., Chatterjee, M., Dvorak, J., Delcroix, M., Sajid, M., Caffrey, C.R. & Davies, S.J., 2010; Rapid induction of IgE responses to a worm cysteine protease during murine pre-patent schistosome infection. Bmc Immunology. 11.

50. Alexander, J., Coombs, G.H. & Mottram, J.C., 1998; *Leishmania mexicana* cysteine proteinase-deficient mutants have attenuated virulence for mice and potentiate a Th1 response. Journal of Immunology. 161, 6794-6801.

51. Chua, K.Y., Stewart, G.A., Thomas, W.R., Simpson, R.J., Dilworth, R.J., Plozza, T.M. & Turner, K.J., 1988; Sequence analysis of cDNA coding for a major house dust mite allergen, Der p 1. Homology with cysteine proteases. J Exp Med. 167, 175-182.

52. Piedrafita, D., Raadsma, H.W., Prowse, R. & Spithill, T.W., 2004; Immunology of the host-parasite relationship in fasciolosis (*Fasciola hepatica* and *Fasciola gigantica*). Canadian Journal of Zoology-Revue Canadienne De Zoologie. 82, 233-250.

53. Smith, A.M., Dowd, A.J., Heffernan, M., Robertson, C.D. & Dalton, J.P., 1993; *Fasciola hepatica*: a secreted cathepsin L-like proteinase cleaves host immunoglobulin. Int J Parasitol. 23, 977-983.

54. Alderete, J.F., Provenzano, D. & Lehker, M.W., 1995; Iron mediates *Trichomonas vaginalis* resistance to complement lysis. Microb Pathog. 19, 93-103.

55. Culley, F.J., Brown, A., Conroy, D.M., Sabroe, I., Pritchard, D.I. & Williams, T.J., 2000; Eotaxin is specifically cleaved by hookworm metalloproteases preventing its action in vitro and in vivo. Journal of Immunology. 165, 6447-6453.

56. Gregory, W.F. & Maizels, R.M., 2008; Cystatins from filarial parasites: Evolution, adaptation and function in the host-parasite relationship. International Journal of Biochemistry & Cell Biology. 40, 1389-1398.

57. Manoury, B., Gregory, W.F., Maizels, R.M. & Watts, C., 2001; Bm-CPI-2, a cystatin homolog secreted by the filarial parasite *Brugia malayi*, inhibits class II MHC-restricted antigen processing. Curr Biol. 11, 447-451.

58. Pfaff, A.W., Schulz-Key, H., Soboslay, P.T., Taylor, D.W., MacLennan, K. & Hoffmann, W.H., 2002; *Litomosoides sigmodontis* cystatin acts as an immunomodulator during experimental filariasis. Int J Parasitol. 32, 171-178.

59. Schonemeyer, A., Lucius, R., Sonnenburg, B., Brattig, N., Sabat, R., Schilling, K., Bradley, J. & Hartmann, S., 2001; Modulation of human T cell responses and macrophage functions by onchocystatin, a secreted protein of the filarial nematode *Onchocerca volvulus*. Journal of Immunology. 167, 3207-3215.

60. Sansom, D.M., Manzotti, C.N. & Zheng, Y., 2003; What's the difference between CD80 and CD86? Trends Immunol. 24, 314-319.

61. Klotz, C., Ziegler, T., Figueiredo, A.S., Rausch, S., Hepworth, M.R., Obsivac, N., Sers, C., Lang, R., Hammerstein, P., Lucius, R. & Hartmann, S., 2011; A helminth immunomodulator exploits host signaling events to regulate cytokine production in macrophages. PLoS Pathog. 7, e1001248.

62. Vray, B., Hartmann, S. & Hoebeke, J., 2002; Immunomodulatory properties of cystatins. Cellular and Molecular Life Sciences. 59, 1503-1512.

63. Miller, S., Schreuer, D. & Hammerberg, B., 1991; Inhibition of antigen-driven proliferative responses and enhancement of antibody production during infection with *Brugia pahangi*. Journal of Immunology. 147, 1007-1013.

64. Schramm, G., Mohrs, K., Wodrich, M., Doenhoff, M.J., Pearce, E.J., Haas, H. & Mohrs, M., 2007; Cutting edge: IPSE/alpha-1, a glycoprotein from *Schistosoma mansoni* eggs, induces IgE-dependent, antigen-independent IL-4 production by murine basophils in vivo. Journal of Immunology. 178, 6023-6027.

65. Steinfelder, S., Andersen, J.F., Cannons, J.L., Feng, C.G., Joshi, M., Dwyer, D., Caspar, P., Schwartzberg, P.L., Sher, A. & Jankovic, D., 2009; The major component in schistosome eggs responsible for conditioning dendritic cells for Th2 polarization is a T2 ribonuclease (omega-1). J Exp Med. 206, 1681-1690.

66. Abdulla, M.H., Lim, K.C., McKerrow, J.H. & Caffrey, C.R., 2011; Proteomic identification of IPSE/alpha-1 as a major hepatotoxin secreted by *Schistosoma mansoni* eggs. PLoS Negl Trop Dis. 5, e1368.

67. Tundup, S., Srivastava, L., Harn, D.A. & Annals, N.Y.A.S., 2012; Polarization of host immune responses by helminth-expressed glycans. Glycobiology of the Immune Response. 1253, E1-E13.

68. Everts, B., Perona-Wright, G., Smits, H.H., Hokke, C.H., van der Ham, A.J., Fitzsimmons, C.M., Doenhoff, M.J., van der Bosch, J., Mohrs, K., Haas, H., Mohrs, M., Yazdanbakhsh, M. & Schramm, G., 2009; Omega-1, a glycoprotein secreted by *Schistosoma mansoni* eggs, drives Th2 responses. J Exp Med. 206, 1673-1680.

69. Zaccone, P., Burton, O.T., Gibbs, S.E., Miller, N., Jones, F.M., Schramm, G., Haas, H., Doenhoff, M.J., Dunne, D.W. & Cooke, A., 2011; The *S. mansoni*

glycoprotein omega-1 induces Foxp3 expression in NOD mouse CD4(+) T cells. Eur J Immunol. 41, 2709-2718.

70. Panda, S.K., Kumar, S., Tupperwar, N.C., Vaidya, T., George, A., Rath, S., Bal, V. & Ravindran, B., 2012; Chitohexaose activates macrophages by alternate pathway through TLR4 and blocks endotoxemia. PLoS Pathog. 8, e1002717.

71. Thomas, P.G., Carter, M.R., Atochina, O., Da'Dara, A.A., Piskorska, D., McGuire, E. & Harn, D.A., 2003; Maturation of dendritic cell 2 phenotype by a helminth glycan uses a Toll-like receptor 4-dependent mechanism. Journal of Immunology. 171, 5837-5841.

72. Harn, D.A., McDonald, J., Atochina, O. & Da'dara, A.A., 2009; Modulation of host immune responses by helminth glycans. Immunol Rev. 230, 247-257.

73. Bhargava, P., Li, C., Stanya, K.J., Jacobi, D., Dai, L., Liu, S., Gangl, M.R., Harn, D.A. & Lee, C.H., 2012; Immunomodulatory glycan LNFPIII alleviates hepatosteatosis and insulin resistance through direct and indirect control of metabolic pathways. Nat Med. 18, 1665-1672.

74. Atochina, O., Da'dara, A.A., Walker, M. & Harn, D.A., 2008; The immunomodulatory glycan LNFPIII initiates alternative activation of murine macrophages in vivo. Immunology. 125, 111-121.

75. Harnett, W. & Harnett, M.M., 2010; Helminth-derived immunomodulators: can understanding the worm produce the pill? Nat Rev Immunol. 10, 278-284.

76. Kreider, T., Anthony, R.M., Urban, J.F., Jr. & Gause, W.C., 2007; Alternatively activated macrophages in helminth infections. Curr Opin Immunol. 19, 448-453.

77. Maizels, R.M., Balic, A., Gomez-Escobar, N., Nair, M., Taylor, M.D. & Allen, J.E., 2004; Helminth parasites--masters of regulation. Immunol Rev. 201, 89-116.

78. Vermeire, J.J., Cho, Y., Lolis, E., Bucala, R. & Cappello, M., 2008; Orthologs of macrophage migration inhibitory factor from parasitic nematodes. Trends Parasitol. 24, 355-363.

79. Chiumiento, L. & Bruschi, F., 2009; Enzymatic antioxidant systems in helminth parasites. Parasitology Research. 105, 593-603.

80. Robinson, M.W., Hutchinson, A.T., Dalton, J.P. & Donnelly, S., 2010; Peroxiredoxin: a central player in immune modulation. Parasite Immunol. 32, 305-313.

81. Carta, S., Castellani, P., Delfino, L., Tassi, S., Vene, R. & Rubartelli, A., 2009; DAMPs and inflammatory processes: the role of redox in the different outcomes. J Leukoc Biol. 86, 549-555.

82. Henkle-Duhrsen, K. & Kampkotter, A., 2001; Antioxidant enzyme families in parasitic nematodes. Molecular and Biochemical Parasitology. 114, 129-142.

83. Dzik, J.M., 2006; Molecules released by helminth parasites involved in host colonization. Acta Biochimica Polonica. 53, 33-64.

84. Salazar-Calderon, M., Martin-Alonso, J.M., Ruiz de Eguino, A.D., Casais, R., Marin, M.S. & Parra, F., 2000; *Fasciola hepatica*: heterologous expression and functional characterization of a thioredoxin peroxidase. Exp Parasitol. 95, 63-70.

85. Alger, H.M., Sayed, A.A., Stadecker, M.J. & Williams, D.L., 2002; Molecular and enzymatic characterisation of *Schistosoma mansoni* thioredoxin. Int J Parasitol. 32, 1285-1292.

86. Donnelly, S., Stack, C.M., O'Neill, S.M., Sayed, A.A., Williams, D.L. & Dalton, J.P., 2008; Helminth 2-Cys peroxiredoxin drives Th2 responses through a mechanism involving alternatively activated macrophages. FASEB J. 22, 4022-4032.

87. Al-Riyami, L. & Harnett, W., 2012; Immunomodulatory properties of ES-62, a phosphorylcholine-containing glycoprotein secreted by *Acanthocheilonema viteae*. Endocrine, metabolic & immune disorders drug targets. 12.

88. Deehan, M.R., Frame, M.J., Parkhouse, R.M.E., Seatter, S.D., Reid, S.D., Harnett, M.M. & Harnett, W., 1998; A phosphorylcholine-containing filarial nematode-secreted product disrupts B lymphocyte activation by targeting key proliferative signaling pathways. Journal of Immunology. 160, 2692-2699.

89. Houston, K.M., Wilson, E.H., Eyres, L., Brombacher, F., Harnett, M.M., Alexander, J. & Harnett, W., 2000; Presence of phosphorylcholine on a filarial nematode protein influences immunoglobulin G subclass response to the molecule by an interleukin-10-dependent mechanism. Infection and Immunity. 68, 5466-5468.

90. Harnett, M.M., Deehan, M.R., Williams, D.M. & Harnett, W., 1998; Induction of signalling anergy via the T-cell receptor in cultured Jurkat T cells by pre-exposure to a filarial nematode secreted product. Parasite Immunol. 20, 551-563.

91. Goodridge, H.S., Marshall, F.A., Else, K.J., Houston, K.M., Egan, C., Al-Riyami, L., Liew, F.Y., Harnett, W. & Harnett, M.M., 2005; Immunomodulation via novel use of TLR4 by the filarial nematode phosphorylcholine-containing secreted product, ES-62. Journal of Immunology. 174, 284-293.

92. Kim, J.Y., Cho, M.K., Choi, S.H., Lee, K.H., Ahn, S.C., Kim, D.H. & Yu, H.S., 2010; Inhibition of dextran sulfate sodium (DSS)-induced intestinal inflammation via enhanced IL-10 and TGF-beta production by galectin-9 homologues isolated from intestinal parasites. Mol Biochem Parasitol. 174, 53-61.

93. Turner, D.G., Wildblood, L.A., Inglis, N.F. & Jones, D.G., 2008; Characterization of a galectin-like activity from the parasitic nematode, *Haemonchus contortus*, which modulates ovine eosinophil migration in vitro. Vet Immunol Immunopathol. 122, 138-145.

94. Bower, M.A., Constant, S.L. & Mendez, S., 2008; *Necator americanus*: the Na-ASP-2 protein secreted by the infective larvae induces neutrophil recruitment in vivo and in vitro. Exp Parasitol. 118, 569-575.

95. Asojo, O.A., Goud, G., Dhar, K., Loukas, A., Zhan, B., Deumic, V., Liu, S., Borgstahl, G.E. & Hotez, P.J., 2005; X-ray structure of Na-ASP-2, a pathogenesis-related-1 protein from the nematode parasite, *Necator americanus*, and a vaccine antigen for human hookworm infection. J Mol Biol. 346, 801-814.

96. Moyle, M., Foster, D.L., McGrath, D.E., Brown, S.M., Laroche, Y., De Meutter, J., Stanssens, P., Bogowitz, C.A., Fried, V.A., Ely, J.A. & et al., 1994; A hookworm glycoprotein that inhibits neutrophil function is a ligand of the integrin CD11b/CD18. J Biol Chem. 269, 10008-10015.

97. Rieu, P., Sugimori, T., Griffith, D.L. & Arnaout, M.A., 1996; Solvent-accessible residues on the metal ion-dependent adhesion site face of integrin CR3 mediate its binding to the neutrophil inhibitory factor. J Biol Chem. 271, 15858-15861.

98. Younis, A.E., Geisinger, F., Ajonina-Ekoti, I., Soblik, H., Steen, H., Mitreva, M., Erttmann, K.D., Perbandt, M., Liebau, E. & Brattig, N.W., 2011; Stage-specific excretory-secretory small heat shock proteins from the parasitic nematode *Strongyloides* ratti--putative links to host's intestinal mucosal defense system. FEBS J. 278, 3319-3336.

99. Rzepecka, J., Rausch, S., Klotz, C., Schnoller, C., Kornprobst, T., Hagen, J., Ignatius, R., Lucius, R. & Hartmann, S., 2009; Calreticulin from the intestinal nematode *Heligmosomoides polygyrus* is a Th2-skewing protein and interacts with murine scavenger receptor-A. Mol Immunol. 46, 1109-1119.

100. van der Kleij, D., Latz, E., Brouwers, J.F., Kruize, Y.C., Schmitz, M., Kurt-Jones, E.A., Espevik, T., de Jong, E.C., Kapsenberg, M.L., Golenbock, D.T., Tielens, A.G. & Yazdanbakhsh, M., 2002; A novel host-parasite lipid cross-talk. *Schistosomal* lyso-phosphatidylserine activates toll-like receptor 2 and affects immune polarization. J Biol Chem. 277, 48122-48129.

101. Gomez-Escobar, N., Gregory, W.F. & Maizels, R.M., 2000; Identification of tgh-2, a filarial nematode homolog of *Caenorhabditis elegans* daf-7 and human transforming growth factor beta, expressed in microfilarial and adult stages of *Brugia malayi*. Infection and Immunity. 68, 6402-6410.

102. Maizels, R.M., Hewitson, J.P., Murray, J., Harcus, Y.M., Dayer, B., Filbey, K.J., Grainger, J.R., McSorley, H.J., Reynolds, L.A. & Smith, K.A., 2012; Immune modulation and modulators in *Heligmosomoides polygyrus* infection. Exp Parasitol. 132, 76-89.

103. Harnett, W., Worms, M.J., Kapil, A., Grainger, M. & Parkhouse, R.M., 1989; Origin, kinetics of circulation and fate in vivo of the major excretory-secretory product of *Acanthocheilonema viteae*. Parasitology. 99 Pt 2, 229-239.

104. Houston, K.M. & Harnett, W., 2004; Structure and synthesis of nematode phosphorylcholine-containing glycoconjugates. Parasitology. 129, 655-661.

105. Donnelly, S., O'Neill, S.M., Stack, C.M., Robinson, M.W., Turnbull, L., Whitchurch, C. & Dalton, J.P., 2010; Helminth Cysteine Proteases Inhibit TRIF-dependent Activation of Macrophages via Degradation of TLR3. Journal of Biological Chemistry. 285, 3383-3392.

106. O'Neill, S.M., Brady, M.T., Callanan, J.J., Mulcahy, G., Joyce, P., Mills, K.H.G. & Dalton, J.P., 2000; *Fasciola hepatica* infection downregulates Th1 responses in mice. Parasite Immunol. 22, 147-155.

107. Brady, M.T., O'Neill, S.M., Dalton, J.P. & Mills, K.H.G., 1999; Fasciola hepatica suppresses a protective Th1 response against *Bordetella pertussis*. Infection and Immunity. 67, 5372-5378.

108. Robinson, M.W., Menon, R., Donnelly, S.M., Dalton, J.P. & Ranganathan, S., 2009; An integrated transcriptomics and proteomics analysis of the secretome of the helminth pathogen *Fasciola hepatica*: proteins associated with invasion and infection of the mammalian host. Mol Cell Proteomics. 8, 1891-1907.

109. Clery, D., Torgerson, P. & Mulcahy, G., 1996; Immune responses of chronically infected adult cattle to *Fasciola hepatica*. Vet Parasitol. 62, 71-82.

110. Flynn, R.J., Irwin, J.A., Olivier, M., Sekiya, M., Dalton, J.P. & Mulcah, G., 2007; Alternative activation of ruminant macrophages by *Fasciola hepatica*. Vet Immunol Immunopathol. 120, 31-40.

111. Walsh, K.P., Brady, M.T., Finlay, C.M., Boon, L. & Mills, K.H., 2009; Infection with a helminth parasite attenuates autoimmunity through TGF-beta-mediated suppression of Th17 and Th1 responses. Journal of Immunology. 183, 1577-1586.

112. O'Neill, S.M., Mills, K.H. & Dalton, J.P., 2001; *Fasciola hepatica* cathepsin L cysteine proteinase suppresses *Bordetella pertussis*-specific interferon-gamma production in vivo. Parasite Immunol. 23, 541-547.

113. Cantacessi, C., Young, N.D., Nejsum, P., Jex, A.R., Campbell, B.E., Hall, R.S., Thamsborg, S.M., Scheerlinck, J.P. & Gasser, R.B., 2011; The transcriptome of *Trichuris suis*--first molecular insights into a parasite with curative properties for key immune diseases of humans. Plos One. 6, e23590.

114. Robinson, M.W., Alvarado, R., To, J., Hutchinson, A.T., Dowdell, S.N., Lund, M., Turnbull, L., Whitchurch, C.B., O'Brien, B.A., Dalton, J.P. & Donnelly, S., 2012; A helminth cathelicidin-like protein suppresses antigen processing and presentation in macrophages via inhibition of lysosomal vATPase. Faseb Journal. 26, 4614-4627.

115. Robinson, M.W., Donnelly, S., Hutchinson, A.T., To, J., Taylor, N.L., Norton, R.S., Perugini, M.A. & Dalton, J.P., 2011; A Family of Helminth Molecules that Modulate Innate Cell Responses via Molecular Mimicry of Host Antimicrobial Peptides. Plos Pathogens. 7.

116. Robinson, M.W., Dalton, J.P. & Donnelly, S., 2008; Helminth pathogen cathepsin proteases: it's a family affair. Trends in Biochemical Sciences. 33, 601-608.

117. Joshi, A.D., Schaller, M.A., Lukacs, N.W., Kunkel, S.L. & Hogaboam, C.M., 2008; TLR3 modulates immunopathology during a *Schistosoma mansoni* egg-driven Th2 response in the lung. European Journal of Immunology. 38, 3436-3449.

118. Xu, J., Zhang, H., Chen, L., Zhang, D., Ji, M., Wu, H. & Wu, G., 2014; *Schistosoma japonicum* infection induces macrophage polarization. Journal of biomedical research. 28.

119. Tundup, S., Srivastava, L., Nagy, T. & Harn, D., 2013; CD14/TRIF pathway regulates macrophage polarization and Th2 immune responses. Journal of Immunology. 190.

120. Golden, O., Flynn, R.J., Read, C., Sekiya, M., Donnelly, S.M., Stack, C., Dalton, J.P. & Mulcahy, G., 2010; Protection of cattle against a natural infection of *Fasciola hepatica* by vaccination with recombinant cathepsin L1 (rFhCL1). Vaccine. 28, 5551-5557.

121. Dalton, J.P., Robinson, M.W., Mulcahy, G., O'Neill, S.M. & Donnelly, S., 2013; Immunomodulatory molecules of *Fasciola hepatica*: Candidates for both vaccine and immunotherapeutic development. Vet Parasitol. 195, 272-285.

122. Dalton, J.P., Neill, S.O., Stack, C., Collins, P., Walshe, A., Sekiya, M., Doyle, S., Mulcahy, G., Hoyle, D., Khaznadji, E., Moire, N., Brennan, G., Mousley, A., Kreshchenko, N., Maule, A.G. & Donnelly, S.M., 2003; *Fasciola hepatica* cathepsin L-like proteases: biology, function, and potential in the development of first generation liver fluke vaccines. Int J Parasitol. 33, 1173-1181.

123. Martinez-Sernandez, V., Mezo, M., Gonzalez-Warleta, M., Perteguer, M.J., Muino, L., Guitian, E., Garate, T. & Ubeira, F.M., 2014; The MF6p/FhHDM-1

major antigen secreted by the trematode parasite *Fasciola hepatica* is a heme-binding protein. J Biol Chem. 289, 1441-1456.

124. Cotton, S., Donnelly, S., Robinson, M.W., Dalton, J.P. & Thivierge, K., 2012; Defense peptides secreted by helminth pathogens: antimicrobial and/or immunomodulator molecules? Front Immunol. 3, 269.

125. Jenssen, H. & Hancock, R.E., 2010; Therapeutic potential of HDPs as immunomodulatory agents. Methods in Molecular Biology. 618, 329-347.

126. Fjell, C.D., Hancock, R.E.W. & Cherkasov, A., 2007; AMPer: a database and an automated discovery tool for antimicrobial peptides. Bioinformatics. 23, 1148-1155.

127. Hancock, R.E. & Chapple, D.S., 1999; Peptide antibiotics. Antimicrob Agents Chemother. 43, 1317-1323.

128. Oppenheim, J.J. & Yang, D., 2005; Alarmins: chemotactic activators of immune responses. Current Opinion in Immunology. 17, 359-365.

129. Peters, B.M., Shirtliff, M.E. & Jabra-Rizk, M.A., 2010; Antimicrobial peptides: primeval molecules or future drugs? PLoS Pathog. 6, e1001067.

130. Zhang, L. & Falla, T.J., 2010; Potential therapeutic application of host defense peptides. Methods in Molecular Biology. 618, 303-327.

131. Durr, U.H.N., Sudheendra, U.S. & Ramamoorthy, A., 2006; LL-37, the only human member of the cathelicidin family of antimicrobial peptides. Biochimica Et Biophysica Acta-Biomembranes. 1758, 1408-1425.

132. Hirsch, T., Metzig, M., Niederbichler, A., Steinau, H.U., Eriksson, E. & Steinstraesser, L., 2008; Role of host defense peptides of the innate immune response in sepsis. Shock. 30, 117-126.

133. Mookherjee, N., Brown, K.L., Bowdish, D.M., Doria, S., Falsafi, R., Hokamp, K., Roche, F.M., Mu, R., Doho, G.H., Pistolic, J., Powers, J.P., Bryan, J., Brinkman, F.S. & Hancock, R.E., 2006; Modulation of the TLR-mediated inflammatory response by the endogenous human host defense peptide LL-37. Journal of Immunology. 176, 2455-2464.

134. Di Nardo, A., Braff, M.H., Taylor, K.R., Na, C., Granstein, R.D., McInturff, J.E., Krutzik, S., Modlin, R.L. & Gallo, R.L., 2007; Cathelicidin antimicrobial peptides block dendritic cell TLR4 activation and allergic contact sensitization. Journal of Immunology. 178, 1829-1834.

135. Thivierge, K., Cotton, S., Schaefer, D.A., Riggs, M.W., To, J., Lund, M.E., Robinson, M.W., Dalton, J.P. & Donnelly, S.M., 2013; Cathelicidin-like helminth defence molecules (HDMs): absence of cytotoxic, anti-microbial and anti-protozoan activities imply a specific adaptation to immune modulation. PLoS Negl Trop Dis. 7, e2307.

136. Vandamme, D., Landuyt, B., Luyten, W. & Schoofs, L., 2012; A comprehensive summary of LL-37, the factotum human cathelicidin peptide. Cellular Immunology. 280, 22-35.

137. Burton, M.F. & Steel, P.G., 2009; The chemistry and biology of LL-37. Natural Product Reports. 26, 1572-1584.

138. Sorensen, O.E., Follin, P., Johnsen, A.H., Calafat, J., Tjabringa, G.S., Hiemstra, P.S. & Borregaard, N., 2001; Human cathelicidin, hCAP-18, is processed to the antimicrobial peptide LL-37 by extracellular cleavage with proteinase 3. Blood. 97, 3951-3959.

139. Reinhardt, R.L., Kang, S.J., Liang, H.E. & Locksley, R.M., 2006; T helper cell effector fates--who, how and where? Curr Opin Immunol. 18, 271-277.

140. Mosser, D.M., 2003; The many faces of macrophage activation. J Leukoc Biol. 73, 209-212.

141. Harding, C.V., Canaday, D. & Ramachandra, L., 2010; Choosing and preparing antigen-presenting cells. Curr Protoc Immunol. Chapter 16, Unit 16 11.

142. Alvarado, R., 2010; Modulation of the Macrophage Proteome by Novel Parasite Derived Molecules. Bachelor of Science (Honours) in Biomedical Science Thesis-UTS, Sydney.

143. Mookherjee, N., Lippert, D.N.D., Hamill, P., Falsafi, R., Nijnik, A., Kindrachuk, J., Pistolic, J., Gardy, J., Miri, P., Naseer, M., Foster, L.J. & Hancock, R.E.W., 2009; Intracellular Receptor for Human Host Defense Peptide LL-37 in Monocytes. Journal of Immunology. 183, 2688-2696.

144. Elssner, A., Duncan, M., Gavrilin, M. & Wewers, M.D., 2004; A novel P2X(7) receptor activator, the human cathelicidin-derived peptide LL37, induces IL-1 beta processing and release. Journal of Immunology. 172, 4987-4994.

145. Bowdish, D.M.E., Davidson, D.J., Lau, Y.E., Lee, K., Scott, M.G. & Hancock, R.E.W., 2005; Impact of LL-37 on anti-infective immunity. Journal of Leukocyte Biology. 77, 451-459.

146. Bowdish, D.M.E., Davidson, D.J. & Hancock, R.E.W., 2005; A re-evaluation of the role of host defence peptides in mammalian immunity. Current Protein & Peptide Science. 6, 35-51.

147. Hancock, R.E. & Sahl, H.G., 2006; Antimicrobial and host-defense peptides as new anti-infective therapeutic strategies. Nat Biotechnol. 24, 1551-1557.

148. Lau, Y.E., Rozek, A., Scott, M.G., Goosney, D.L., Davidson, D.J. & Hancock, R.E., 2005; Interaction and cellular localization of the human host defense peptide LL-37 with lung epithelial cells. Infection and Immunity. 73, 583-591.

149. De, Y., Chen, Q., Schmidt, A.P., Anderson, G.M., Wang, J.M., Wooters, J., Oppenheim, J.J. & Chertov, O., 2000; LL-37, the neutrophil granule- and epithelial cell-derived cathelicidin, utilizes formyl peptide receptor-like 1

(FPRL1) as a receptor to chemoattract human peripheral blood neutrophils, monocytes, and T cells. J Exp Med. 192, 1069-1074.

150. Sandgren, S., Wittrup, A., Cheng, F., Jonsson, M., Eklund, E., Busch, S. & Belting, M., 2004; The human antimicrobial peptide LL-37 transfers extracellular DNA plasmid to the nuclear compartment of mammalian cells via lipid rafts and proteoglycan-dependent endocytosis. The Journal of Biological Chemistry. 279, 17951-17956.

151. Grdisa, M., 2011; The Delivery of Biologically Active (Therapeutic) Peptides and Proteins into Cells. Current Medicinal Chemistry. 18, 1373-1379.

152. Lo, S.L. & Wang, S., 2010; Intracellular Protein Delivery Systems Formed by Noncovalent Bonding Interactions between Amphipathic Peptide Carriers and Protein Cargos. Macromolecular Rapid Communications. 31, 1134-1141.

153. Alberts B, J.A., Lewis J, et al., 2002; Molecular Biology of the Cell, Edn. 4th Garland Science, New York.

154. Nykjaer, A., Fyfe, J.C., Kozyraki, R., Leheste, J.R., Jacobsen, C., Nielsen, M.S., Verroust, P.J., Aminoff, M., de la Chapelle, A., Moestrup, S.K., Ray, R., Gliemann, J., Willnow, T.E. & Christensen, E.I., 2001; Cubilin dysfunction causes abnormal metabolism of the steroid hormone 25(OH) vitamin D-3. Proceedings of the National Academy of Sciences of the United States of America. 98, 13895-13900.

155. Hutchinson, A.T., Ramsland, P.A., Jones, D.R., Agostino, M., Lund, M.E., Jennings, C.V., Bockhorni, V., Yuriev, E., Edmundson, A.B. & Raison, R.L., 2010; Free Ig light chains interact with sphingomyelin and are found on the surface of myeloma plasma cells in an aggregated form. J Immunol. 185, 4179-4188.

156. McGowan, E.M., Alling, N., Jackson, E.A., Yagoub, D., Haass, N.K., Allen, J.D. & Martinello-Wilks, R., 2011; Evaluation of cell cycle arrest in estrogen

responsive MCF-7 breast cancer cells: pitfalls of the MTS assay. Plos One. 6, e20623.

157. Pike, L.J., 2003; Lipid rafts: bringing order to chaos. Journal of Lipid Research. 44, 655-667.

158. Lajoie, P. & Nabi, I.R., 2010; LIPID RAFTS, CAVEOLAE, AND THEIR ENDOCYTOSIS, International Review of Cell and Molecular Biology, Vol. 282, ed. K.W. Jeon, 135-163, Elsevier Academic Press Inc, San Diego.

159. Janes, P.W., Ley, S.C. & Magee, A.I., 1999; Aggregation of lipid rafts accompanies signaling via the T cell antigen receptor. The Journal of Cell Biology. 147, 447-461.

160. Doherty, G.J. & McMahon, H.T., 2009; Mechanisms of Endocytosis. Annual Review of Biochemistry. 78, 857-902.

161. Djaldetti, M., Salman, H., Bergman, M., Djaldetti, R. & Bessler, H., 2002; Phagocytosis - The mighty weapon of the silent warriors. Microscopy Research and Technique. 57, 421-431.

162. Kirkham, M. & Parton, R.G., 2005; Clathrin-independent endocytosis: new insights into caveolae and non-caveolar lipid raft carriers. Biochim Biophys Acta. 1746, 349-363.

163. Lakadamyali, M., Rust, M.J. & Zhuang, X.W., 2006; Ligands for clathrin-mediated endocytosis are differentially sorted into distinct populations of early endosomes. Cell. 124, 997-1009.

164. Rodal, S.K., Skretting, G., Garred, O., Vilhardt, F., van Deurs, B. & Sandvig, K., 1999; Extraction of cholesterol with methyl-beta-cyclodextrin perturbs formation of clathrin-coated endocytic vesicles. Molecular Biology of the Cell. 10, 961-974.

165. Dubinsky, W.P., Mayorga-Wark, O. & Schultz, S.G., 1999; Volume regulatory responses of basolateral membrane vesicles from Necturus enterocytes: Role of the cytoskeleton. Proceedings of the National Academy of Sciences of the United States of America. 96, 9421-9426.

166. Mohrmann, K. & van der Sluijs, P., 1999; Regulation of membrane transport through the endocytic pathway by rabGTPases. Mol Membr Biol. 16, 81-87.

167. Clague, M.J. & Urbe, S., 2001; The interface of receptor trafficking and signalling. J Cell Sci. 114, 3075-3081.

168. Chavrier, P., Parton, R.G., Hauri, H.P., Simons, K. & Zerial, M., 1990; Localization of low molecular weight GTP binding proteins to exocytic and endocytic compartments. Cell. 62, 317-329.

169. Platta, H.W. & Stenmark, H., 2011; Endocytosis and signaling. Curr Opin Cell Biol. 23, 393-403.

170. D'Hondt, K., Heese-Peck, A. & Riezman, H., 2000; Protein and lipid requirements for endocytosis. Annu Rev Genet. 34, 255-295.

171. Repnik, U., Stoka, V., Turk, V. & Turk, B., 2012; Lysosomes and lysosomal cathepsins in cell death. Biochim Biophys Acta. 1824, 22-33.

172. Torgersen, M.L., Skretting, G., van Deurs, B. & Sandvig, K., 2001; Internalization of cholera toxin by different endocytic mechanisms. J Cell Sci. 114, 3737-3747.

173. Mallard, F., Antony, C., Tenza, D., Salamero, J., Goud, B. & Johannes, L., 1998; Direct pathway from early/recycling endosomes to the Golgi apparatus revealed through the study of shiga toxin B-fragment transport. J Cell Biol. 143, 973-990.

174. Emanuelsson, O. & von Heijne, G., 2001; Prediction of organellar targeting signals. Biochim Biophys Acta. 1541, 114-119.

175. Helmerhorst, E.J., Breeuwer, P., van't Hof, W., Walgreen-Weterings, E., Oomen, L.C., Veerman, E.C., Amerongen, A.V. & Abee, T., 1999; The cellular target of histatin 5 on *Candida albicans* is the energized mitochondrion. J Biol Chem. 274, 7286-7291.

176. Lande, R., Gregorio, J., Facchinetti, V., Chatterjee, B., Wang, Y.H., Homey, B., Cao, W., Wang, Y.H., Su, B., Nestle, F.O., Zal, T., Mellman, I., Schroder, J.M., Liu, Y.J. & Gilliet, M., 2007; Plasmacytoid dendritic cells sense self-DNA coupled with antimicrobial peptide. Nature. 449, 564-U566.

177. Drin, G. & Antonny, B., 2010; Amphipathic helices and membrane curvature. Febs Letters. 584, 1840-1847.

178. Ford, M.G.J., Mills, I.G., Peter, B.J., Vallis, Y., Praefcke, G.J.K., Evans, P.R. & McMahon, H.T., 2002; Curvature of clathrin-coated pits driven by epsin. Nature. 419, 361-366.

179. Min, C.K., Bang, S.Y., Cho, B.A., Choi, Y.H., Yang, J.S., Lee, S.H., Seong, S.Y., Kim, K.W., Kim, S., Jung, J.U., Choi, M.S., Kim, I.S. & Cho, N.H., 2008; Role of amphipathic helix of a herpesviral protein in membrane deformation and T cell receptor downregulation. PLoS Pathog. 4, e1000209.

180. Kubo, S., Nemani, V.M., Chalkley, R.J., Anthony, M.D., Hattori, N., Mizuno, Y., Edwards, R.H. & Fortin, D.L., 2005; A combinatorial code for the interaction of alpha-synuclein with membranes. J Biol Chem. 280, 31664-31672.

181. Park, J., Lee, B.S., Choi, J.K., Means, R.E., Choe, J. & Jung, J.U., 2002; Herpesviral protein targets a cellular WD repeat endosomal protein to downregulate T lymphocyte receptor expression. Immunity. 17, 221-233.

182. Park, J., Cho, N.H., Choi, J.K., Feng, P., Choe, J. & Jung, J.U., 2003; Distinct roles of cellular Lck and p80 proteins in herpesvirus saimiri Tip function on lipid rafts. Journal of Virology. 77, 9041-9051.

183. Katzmann, D.J., Odorizzi, G. & Emr, S.D., 2002; Receptor downregulation and multivesicular-body sorting. Nature Reviews Molecular Cell Biology. 3, 893-905.

184. Sorensen, O., Cowland, J.B., Askaa, J. & Borregaard, N., 1997; An ELISA for hCAP-18, the cathelicidin present in human neutrophils and plasma. Journal of Immunological Methods. 206, 53-59.

185. Bulow, E., Bengtsson, N., Calafat, J., Gullberg, U. & Olsson, I., 2002; Sorting of neutrophil-specific granule protein human cathelicidin, hCAP-18, when constitutively expressed in myeloid cells. Journal of Leukocyte Biology. 72, 147-153.

186. Sorensen, O.E., Follin, P., Johnsen, A.H., Calafat, J., Tjabringa, G.S., Hiemstra, P.S. & Borregaard, N., 2001; Human cathelicidin, hCAP-18, is processed to the antimicrobial peptide LL-37 by extracellular cleavage with proteinase 3. Blood. 97, 3951-3959.

187. Shaykhiev, R., Sierigk, J., Herr, C., Krasteva, G., Kummer, W. & Bals, R., 2010; The antimicrobial peptide cathelicidin enhances activation of lung epithelial cells by LPS. Faseb Journal. 24, 4756-4766.

188. Mosser, D.M. & Zhang, X., 2008; Activation of murine macrophages. Curr Protoc Immunol. Chapter 14, Unit 14 12.

189. Harding, C.V. & Ramachandra, L., 2010; Presenting exogenous antigen to T cells. Curr Protoc Immunol. Chapter 16, Unit 16 12.

190. Rodriguez, A., Webster, P., Ortego, J. & Andrews, N.W., 1997; Lysosomes behave as Ca2+-regulated exocytic vesicles in fibroblasts and epithelial cells. Journal of Cell Biology. 137, 93-104.

191. Andrews, N.W., 2005; Membrane repair and immunological danger. Embo Reports. 6, 826-830.

192. Andrews, N.W., 2000; Regulated secretion of conventional lysosomes. Trends in Cell Biology. 10, 316-321.

193. Luzio, J.P., Pryor, P.R. & Bright, N.A., 2007; Lysosomes: fusion and function. Nature Reviews Molecular Cell Biology. 8, 622-632.

194. Appelqvist, H., Waster, P., Kagedal, K. & Ollinger, K., 2013; The lysosome: from waste bag to potential therapeutic target. J Mol Cell Biol. 5, 214-226.

195. Schroder, B.A., Wrocklage, C., Hasilik, A. & Saftig, P., 2010; The proteome of lysosomes. Proteomics. 10, 4053-4076.

196. Saftig, P., Schroder, B. & Blanz, J., 2010; Lysosomal membrane proteins: life between acid and neutral conditions. Biochemical Society Transactions. 38, 1420-1423.

197. Braulke, T. & Bonifacino, J.S., 2009; Sorting of lysosomal proteins. Biochim Biophys Acta. 1793, 605-614.

198. Mindell, J.A., 2012; Lysosomal Acidification Mechanisms. Annual Review of Physiology. 74, 69-86.

199. Turk, V., Stoka, V., Vasiljeva, O., Renko, M., Sun, T., Turk, B. & Turk, D., 2012; Cysteine cathepsins: From structure, function and regulation to new frontiers. Biochimica Et Biophysica Acta-Proteins and Proteomics. 1824, 68-88.

200. Ohkuma, S. & Poole, B., 1978; Fluorescence probe measurement of the intralysosomal pH in living cells and the perturbation of pH by various agents. Proc Natl Acad Sci U S A. 75, 3327-3331.

201. Ohkuma, S., Moriyama, Y. & Takano, T., 1982; Identification and characterization of a proton pump on lysosomes by fluorescein-isothiocyanate-dextran fluorescence. Proc Natl Acad Sci U S A. 79, 2758-2762.

202. Luzio, J.P., Parkinson, M.D., Gray, S.R. & Bright, N.A., 2009; The delivery of endocytosed cargo to lysosomes. Biochem Soc Trans. 37, 1019-1021.

203. Luzio, J.P., Gray, S.R. & Bright, N.A., 2010; Endosome-lysosome fusion. Biochem Soc Trans. 38, 1413-1416.

204. Huotari, J. & Helenius, A., 2011; Endosome maturation. EMBO J. 30, 3481-3500.

205. Bright, N.A., Gratian, M.J. & Luzio, J.P., 2005; Endocytic delivery to lysosomes mediated by concurrent fusion and kissing events in living cells. Current Biology. 15, 360-365.

206. Apostolopoulos, V., Yuriev, E., Lazoura, E., Yu, M. & Ramsland, P.A., 2008; MHC and MHC-like molecules: structural perspectives on the design of molecular vaccines. Hum Vaccin. 4, 400-409.

207. Watts, C., 2012; The endosome-lysosome pathway and information generation in the immune system. Biochimica Et Biophysica Acta-Proteins and Proteomics. 1824, 14-21.

208. Watts, C., 2001; Antigen processing in the endocytic compartment. Current Opinion in Immunology. 13, 26-31.

209. Shimonkevitz, R., Kappler, J., Marrack, P. & Grey, H., 1983; Antigen recognition by H-2-restricted T cells. I. Cell-free antigen processing. J Exp Med. 158, 303-316.

210. Hornung, V., Bauernfeind, F., Halle, A., Samstad, E.O., Kono, H., Rock, K.L., Fitzgerald, K.A. & Latz, E., 2008; Silica crystals and aluminum salts activate the NALP3 inflammasome through phagosomal destabilization. Nature Immunology. 9, 847-856.

211. Thilo, L., Stroud, E. & Haylett, T., 1995; Maturation of early endosomes and vesicular traffic to lysosomes in relation to membrane recycling. J Cell Sci. 108 (Pt 4), 1791-1803.

212. Dolman, N.J., Kilgore, J.A. & Davidson, M.W., 2013; A review of reagents for fluorescence microscopy of cellular compartments and structures, part I: BacMam labeling and reagents for vesicular structures. Curr Protoc Cytom. Chapter 12, Unit 12 30.

213. Huss, M., Ingenhorst, G., Konig, S., Gassel, M., Drose, S., Zeeck, A., Altendorf, K. & Wieczorek, H., 2002; Concanamycin A, the specific inhibitor of V-ATPases, binds to the V(o) subunit c. J Biol Chem. 277, 40544-40548.

214. Johnson, I.D., 2010; The Molecular Probes® Handbook—A Guide to Fluorescent Probes and Labeling Technologies, Edn. 11th, Life Technologies Corporation.

215. Makrigiorgos, G.M., 1997; Detection of lipid peroxidation on erythrocytes using the excimer-forming property of a lipophilic BODIPY fluorescent dye. Journal of Biochemical and Biophysical Methods. 35, 23-35.

216. Jones, L.J., Upson, R.H., Haugland, R.P., Panchuk-Voloshina, N., Zhou, M. & Haugland, R.P., 1997; Quenched BODIPY dye-labeled casein substrates for the assay of protease activity by direct fluorescence measurement. Anal Biochem. 251, 144-152.

217. Barnden, M.J., Allison, J., Heath, W.R. & Carbone, F.R., 1998; Defective TCR expression in transgenic mice constructed using cDNA-based alpha- and beta-chain genes under the control of heterologous regulatory elements. Immunol Cell Biol. 76, 34-40.

218. Schroder, K., Hertzog, P.J., Ravasi, T. & Hume, D.A., 2004; Interferon-gamma: an overview of signals, mechanisms and functions. J Leukoc Biol. 75, 163-189.

219. Laughlin, T.F. & Ahmad, Z., 2010; Inhibition of *Escherichia coli* ATP synthase by amphibian antimicrobial peptides. Int J Biol Macromol. 46, 367-374.

220. Hong, S. & Pedersen, P.L., 2008; ATP synthase and the actions of inhibitors utilized to study its roles in human health, disease, and other scientific areas. Microbiol Mol Biol Rev. 72, 590-641.

221. Bullough, D.A., Ceccarelli, E.A., Roise, D. & Allison, W.S., 1989; Inhibition of the bovine-heart mitochondrial F1-ATPase by cationic dyes and amphipathic peptides. Biochim Biophys Acta. 975, 377-383.

222. Marshansky, V. & Futai, M., 2008; The V-type H+-ATPase in vesicular trafficking: targeting, regulation and function. Curr Opin Cell Biol. 20, 415-426.

223. Hurtado-Lorenzo, A., Skinner, M., El Annan, J., Futai, M., Sun-Wada, G.H., Bourgoin, S., Casanova, J., Wildeman, A., Bechoua, S., Ausiello, D.A., Brown, D. & Marshansky, V., 2006; V-ATPase interacts with ARNO and Arf6 in early endosomes and regulates the protein degradative pathway. Nature Cell Biology. 8, 124-U128.

224. Forgac, M., 2007; Vacuolar ATPases: rotary proton pumps in physiology and pathophysiology. Nat Rev Mol Cell Biol. 8, 917-929.

225. Toyomura, T., Murata, Y., Yamamoto, A., Oka, T., Sun-Wada, G.H., Wada, Y. & Futai, M., 2003; From lysosomes to the plasma membrane: localization of vacuolar-type H+ -ATPase with the a3 isoform during osteoclast differentiation. J Biol Chem. 278, 22023-22030.

226. Sun-Wada, G.H., Tabata, H., Kuhara, M., Kitahara, I., Takashima, Y. & Wada, Y., 2011; Generation of Chicken Monoclonal Antibodies Against the a1, a2, and a3 Subunit Isoforms of Vacuolar-type Proton ATPase. Hybridoma. 30, 199-203.

227. Duffield, A., Kamsteeg, E.J., Brown, A.N., Pagel, P. & Caplan, M.J., 2003; The tetraspanin CD63 enhances the internalization of the H,K-ATPase beta-subunit. Proc Natl Acad Sci U S A. 100, 15560-15565.

228. Huynh, K.K., Eskelinen, E.L., Scott, C.C., Malevanets, A., Saftig, P. & Grinstein, S., 2007; LAMP proteins are required for fusion of lysosomes with phagosomes. EMBO J. 26, 313-324.

229. Desjardins, M., Nzala, N.N., Corsini, R. & Rondeau, C., 1997; Maturation of phagosomes is accompanied by changes in their fusion properties and size-selective acquisition of solute materials from endosomes. J Cell Sci. 110 (Pt 18), 2303-2314.

230. Shui, W., Sheu, L., Liu, J., Smart, B., Petzold, C.J., Hsieh, T.Y., Pitcher, A., Keasling, J.D. & Bertozzi, C.R., 2008; Membrane proteomics of phagosomes suggests a connection to autophagy. Proceedings of the National Academy of Sciences U S A. 105, 16952-16957.

231. Ewald, S.E., Lee, B.L., Lau, L., Wickliffe, K.E., Shi, G.P., Chapman, H.A. & Barton, G.M., 2008; The ectodomain of Toll-like receptor 9 is cleaved to generate a functional receptor. Nature. 456, 658-662.

232. Gangloff, M., 2012; Different dimerisation mode for TLR4 upon endosomal acidification? Trends Biochem Sci. 37, 92-98.

233. Takeda, K. & Akira, S., 2005; Toll-like receptors in innate immunity. Int Immunol. 17, 1-14.

234. Halle, A., Hornung, V., Petzold, G.C., Stewart, C.R., Monks, B.G., Reinheckel, T., Fitzgerald, K.A., Latz, E., Moore, K.J. & Golenbock, D.T., 2008; The NALP3 inflammasome is involved in the innate immune response to amyloid-beta. Nature Immunology. 9, 857-865.

235. Tschopp, J. & Schroder, K., 2010; NLRP3 inflammasome activation: The convergence of multiple signalling pathways on ROS production? Nat Rev Immunol. 10, 210-215.

236. Broker, L.E., Huisman, C., Span, S.W., Rodriguez, J.A., Kruyt, F.A. & Giaccone, G., 2004; Cathepsin B mediates caspase-independent cell death induced by microtubule stabilizing agents in non-small cell lung cancer cells. Cancer Res. 64, 27-30.

237. Roberg, K., Kagedal, K. & Ollinger, K., 2002; Microinjection of cathepsin d induces caspase-dependent apoptosis in fibroblasts. Am J Pathol. 161, 89-96.

238. Bivik, C.A., Larsson, P.K., Kagedal, K.M., Rosdahl, I.K. & Ollinger, K.M., 2006; UVA/B-induced apoptosis in human melanocytes involves translocation of cathepsins and Bcl-2 family members. J Invest Dermatol. 126, 1119-1127.

239. Rathinam, V.A., Vanaja, S.K. & Fitzgerald, K.A., 2012; Regulation of inflammasome signaling. Nat Immunol. 13, 333-332.

240. Martinon, F., Petrilli, V., Mayor, A., Tardivel, A. & Tschopp, J., 2006; Gout-associated uric acid crystals activate the NALP3 inflammasome. Nature. 440, 237-241.

241. Gaide, O. & Hoffman, H.M., 2008; Insight into the inflammasome and caspase-activating mechanisms. Expert Rev Clin Immunol. 4, 61-77.

242. Miao, E.A., Alpuche-Aranda, C.M., Dors, M., Clark, A.E., Bader, M.W., Miller, S.I. & Aderem, A., 2006; Cytoplasmic flagellin activates caspase-1 and secretion of interleukin 1 beta via Ipaf. Nature Immunology. 7, 569-575.

243. Martinon, F., Mayor, A. & Tschopp, J., 2009; The inflammasomes: guardians of the body. Annu Rev Immunol. 27, 229-265.

244. Chen, M., Wang, H., Chen, W. & Meng, G., 2011; Regulation of adaptive immunity by the NLRP3 inflammasome. International Immunopharmacology. 11, 549-554.

245. Ciraci, C., Janczy, J.R., Sutterwala, F.S. & Cassel, S.L., 2012; Control of innate and adaptive immunity by the inflammasome. Microbes and Infection. 14, 1263-1270.

246. Yin, Y., Pastrana, J.L., Li, X., Huang, X., Mallilankaraman, K., Choi, E.T., Madesh, M., Wang, H. & Yang, X.F., 2013; Inflammasomes: sensors of metabolic stresses for vascular inflammation. Front Biosci (Landmark Ed). 18, 638-649.

247. Miao, E.A., Rajan, J.V. & Aderem, A., 2011; Caspase-1-induced pyroptotic cell death. Immunol Rev. 243, 206-214.

248. Hornung, V. & Latz, E., 2010; Critical functions of priming and lysosomal damage for NLRP3 activation. Eur J Immunol. 40, 620-623.

249. Bauernfeind, F.G., Horvath, G., Stutz, A., Alnemri, E.S., MacDonald, K., Speert, D., Fernandes-Alnemri, T., Wu, J., Monks, B.G., Fitzgerald, K.A., Hornung, V. & Latz, E., 2009; Cutting edge: NF-kappaB activating pattern recognition and cytokine receptors license NLRP3 inflammasome activation by regulating NLRP3 expression. Journal of Immunology. 183, 787-791.

250. Lamkanfi, M. & Dixit, V.M., 2014; Mechanisms and Functions of Inflammasomes. Cell. 157, 1013-1022.

251. Shirasu, K., 2009; The HSP90-SGT1 chaperone complex for NLR immune sensors. Annu Rev Plant Biol. 60, 139-164.

252. Kadota, Y., Shirasu, K. & Guerois, R., 2010; NLR sensors meet at the SGT1–HSP90 crossroad. Trends in Biochemical Sciences. 35, 199-207.

253. Petrilli, V., Papin, S., Dostert, C., Mayor, A., Martinon, F. & Tschopp, J., 2007; Activation of the NALP3 inflammasome is triggered by low intracellular potassium concentration. Cell Death Differ. 14, 1583-1589.

254. Rajamaki, K., Lappalainen, J., Oorni, K., Valimaki, E., Matikainen, S., Kovanen, P.T. & Eklund, K.K., 2010; Cholesterol crystals activate the NLRP3 inflammasome in human macrophages: a novel link between cholesterol metabolism and inflammation. Plos One. 5, e11765.

255. Kingsbury, S.R., Conaghan, P.G. & McDermott, M.F., 2011; The role of the NLRP3 inflammasome in gout. Journal of inflammation research. 4.

256. McAuley, J.L., Tate, M.D., MacKenzie-Kludas, C.J., Pinar, A., Zeng, W., Stutz, A., Latz, E., Brown, L.E. & Mansell, A., 2013; Activation of the NLRP3 inflammasome by IAV virulence protein PB1-F2 contributes to severe pathophysiology and disease. PLoS Pathog. 9, e1003392.

257. Van Noorden, C.J., Boonacker, E., Bissell, E.R., Meijer, A.J., van Marle, J. & Smith, R.E., 1997; Ala-Pro-cresyl violet, a synthetic fluorogenic substrate for the analysis of kinetic parameters of dipeptidyl peptidase IV (CD26) in individual living rat hepatocytes. Anal Biochem. 252, 71-77.

258. Martinon, F., Agostini, L., Meylan, E. & Tschopp, J., 2004; Identification of Bacterial Muramyl Dipeptide as Activator of the NALP3/Cryopyrin Inflammasome. Current Biology. 14, 1929-1934.

259. Flach, T.L., Ng, G., Hari, A., Desrosiers, M.D., Zhang, P., Ward, S.M., Seamone, M.E., Vilaysane, A., Mucsi, A.D., Fong, Y., Prenner, E., Ling, C.C., Tschopp, J., Muruve, D.A., Amrein, M.W. & Shi, Y., 2011; Alum interaction with dendritic cell membrane lipids is essential for its adjuvanticity. Nat Med. 17, 479-487.

260. Schroder, K., Sagulenko, V., Zamoshnikova, A., Richards, A.A., Cridland, J.A., Irvine, K.M., Stacey, K.J. & Sweet, M.J., 2012; Acute lipopolysaccharide

priming boosts inflammasome activation independently of inflammasome sensor induction. Immunobiology. 217, 1325-1329.

261. Brown, K.L., Poon, G.F., Birkenhead, D., Pena, O.M., Falsafi, R., Dahlgren, C., Karlsson, A., Bylund, J., Hancock, R.E. & Johnson, P., 2011; Host defense peptide LL-37 selectively reduces proinflammatory macrophage responses. Journal of Immunology. 186, 5497-5505.

262. Pinheiro da Silva, F., Gallo, R.L. & Nizet, V., 2009; Differing effects of exogenous or endogenous cathelicidin on macrophage toll-like receptor signaling. Immunol Cell Biol. 87, 496-500.

263. Rutault, K., Hazzalin, C.A. & Mahadevan, L.C., 2001; Combinations of ERK and p38 MAPK inhibitors ablate tumor necrosis factor-alpha (TNF-alpha) mRNA induction. Evidence for selective destabilization of TNF-alpha transcripts. J Biol Chem. 276, 6666-6674.

264. Weber, K. & Schilling, J.D., 2014; Lysosomes Integrate Metabolic-Inflammatory Cross-talk in Primary Macrophage Inflammasome Activation. J Biol Chem. 289, 9158-9171.

265. Hornung, V. & Latz, E., 2010; Intracellular DNA recognition. Nat Rev Immunol. 10, 123-130.

266. Bauernfeind, F., Ablasser, A., Bartok, E., Kim, S., Schmid-Burgk, J., Cavlar, T. & Hornung, V., 2011; Inflammasomes: current understanding and open questions. Cell Mol Life Sci. 68, 765-783.

267. Perregaux, D.G., Bhavsar, K., Contillo, L., Shi, J. & Gabel, C.A., 2002; Antimicrobial peptides initiate IL-1 beta posttranslational processing: a novel role beyond innate immunity. Journal of Immunology. 168, 3024-3032.

268. Grebe, A. & Latz, E., 2013; Cholesterol crystals and inflammation. Curr Rheumatol Rep. 15, 313.

269. Watanabe, H., Gaide, O., Petrilli, V., Martinon, F., Contassot, E., Roques, S., Kummer, J.A., Tschopp, J. & French, L.E., 2007; Activation of the IL-1beta-processing inflammasome is involved in contact hypersensitivity. J Invest Dermatol. 127, 1956-1963.

270. Gris, D., Ye, Z., Iocca, H.A., Wen, H., Craven, R.R., Gris, P., Huang, M., Schneider, M., Miller, S.D. & Ting, J.P., 2010; NLRP3 plays a critical role in the development of experimental autoimmune encephalomyelitis by mediating Th1 and Th17 responses. Journal of Immunology. 185, 974-981.

271. Lamkanfi, M., Mueller, J.L., Vitari, A.C., Misaghi, S., Fedorova, A., Deshayes, K., Lee, W.P., Hoffman, H.M. & Dixit, V.M., 2009; Glyburide inhibits the Cryopyrin/Nalp3 inflammasome. J Cell Biol. 187, 61-70.

272. Masters, S.L., Dunne, A., Subramanian, S.L., Hull, R.L., Tannahill, G.M., Sharp, F.A., Becker, C., Franchi, L., Yoshihara, E., Chen, Z., Mullooly, N., Mielke, L.A., Harris, J., Coll, R.C., Mills, K.H., Mok, K.H., Newsholme, P., Nunez, G., Yodoi, J., Kahn, S.E., Lavelle, E.C. & O'Neill, L.A., 2010; Activation of the NLRP3 inflammasome by islet amyloid polypeptide provides a mechanism for enhanced IL-1beta in type 2 diabetes. Nat Immunol. 11, 897-904.

273. Mathis, D., Vence, L. & Benoist, C., 2001; beta-Cell death during progression to diabetes. Nature. 414, 792-798.

274. Paveley, R.A., Aynsley, S.A., Cook, P.C., Turner, J.D. & Mountford, A.P., 2009; Fluorescent imaging of antigen released by a skin-invading helminth reveals differential uptake and activation profiles by antigen presenting cells. PLoS Negl Trop Dis. 3, e528.

275. Curwen, R.S., Ashton, P.D., Sundaralingam, S. & Wilson, R.A., 2006; Identification of novel proteases and immunomodulators in the secretions of schistosome cercariae that facilitate host entry. Mol Cell Proteomics. 5, 835-844.

276. Rao, K.V. & Ramaswamy, K., 2000; Cloning and expression of a gene encoding Sm16, an anti-inflammatory protein from *Schistosoma mansoni*. Mol Biochem Parasitol. 108, 101-108.

277. Zaiss, M.M., Maslowski, K.M., Mosconi, I., Guenat, N., Marsland, B.J. & Harris, N.L., 2013; IL-1beta suppresses innate IL-25 and IL-33 production and maintains helminth chronicity. PLoS Pathog. 9, e1003531.

278. Wree, A., Eguchi, A., McGeough, M.D., Pena, C.A., Johnson, C.D., Canbay, A., Hoffman, H.M. & Feldstein, A.E., 2014; NLRP3 Inflammasome Activation Results in Hepatocyte Pyroptosis, Liver Inflammation, and Fibrosis in Mice. Hepatology. 59, 898-910.

279. Calderon, B., Carrero, J.A. & Unanue, E.R., 2014; The central role of antigen presentation in islets of Langerhans in autoimmune diabetes. Curr Opin Immunol. 26, 32-40.

280. Bogie, J.F., Stinissen, P. & Hendriks, J.J., 2014; Macrophage subsets and microglia in multiple sclerosis. Acta Neuropathol.

281. Vogel, D.Y.S., Vereyken, E.J.F., Glim, J.E., Heijnen, P., Moeton, M., van der Valk, P., Amor, S., Teunissen, C.E., van Horssen, J. & Dijkstra, C.D., 2013; Macrophages in inflammatory multiple sclerosis lesions have an intermediate activation status. Journal of Neuroinflammation. 10.

282. Yamada, A., Ishimaru, N., Arakaki, R., Katunuma, N. & Hayashi, Y., 2010; Cathepsin L inhibition prevents murine autoimmune diabetes via suppression of CD8(+) T cell activity. Plos One. 5, e12894.

283. Maehr, R., Mintern, J.D., Herman, A.E., Lennon-Dumenil, A.M., Mathis, D., Benoist, C. & Ploegh, H.L., 2005; Cathepsin L is essential for onset of autoimmune diabetes in NOD mice. J Clin Invest. 115, 2934-2943.

284. Bever, C.T., Jr. & Garver, D.W., 1995; Increased cathepsin B activity in multiple sclerosis brain. J Neurol Sci. 131, 71-73.

285. Amorini, A.M., Petzold, A., Tavazzi, B., Eikelenboom, J., Keir, G., Belli, A., Giovannoni, G., Di Pietro, V., Polman, C., D'Urso, S., Vagnozzi, R., Uitdehaag, B. & Lazzarino, G., 2009; Increase of uric acid and purine compounds in biological fluids of multiple sclerosis patients. Clin Biochem. 42, 1001-1006.

286. Mookherjee, N., Rehaume, L.M. & Hancock, R.E.W., 2007; Cathelicidins and functional analogues as antisepsis molecules. Expert Opinion on Therapeutic Targets. 11, 993-1004.